SURFACE MODIFICATION FOR IMPROVED BLOOD COMPATIBILITY

SURFACE MODIFICATION WITH POLYETHYLENE GLYCOL-PROTEIN CONJUGATES FOR IMPROVED BLOOD COMPATIBILITY

By

SARA ALIBEIK, BEng., MESc.

A Thesis
Submitted to the School of Graduate Studies
In Partial Fulfillment of the Requirements
For the Degree
Doctor of Philosophy

McMaster University

DOCTOR OF PHILOSOPHY (2011) McMaster University
(Biomedical Engineering) Hamilton, Ontario

TITLE: SURFACE MODIFICATION WITH POLYETHYLENE GLYCOL-PROTEIN CONJUGATES FOR IMPROVED BLOOD COMPATIBILITY

AUTHOR: Sara Alibeik
B.Eng. (University of Tehran)
M.E.Sc. (University of Western Ontario)

SUPERVISORS: Professor John L. Brash
Professor Shiping Zhu

NUMBER OF PAGES: xiii, 193

ABSTRACT

The work presented in this thesis was focused on the surface modification of biomaterials with combinations of polyethylene glycol (PEG) and bioactive molecules (protein anticoagulants) for improved blood compatibility. Since the fate of biomaterials in contact with blood depends significantly on plasma protein-surface interactions, the objective of this work was to reduce non-specific protein adsorption using PEG and to promote specific protein interactions that could inhibit clot formation using protein anticoagulants as modifiers.

Two anticoagulant molecules were used in this work: hirudin, a specific inhibitor of thrombin and corn trypsin inhibitor (CTI), a specific inhibitor of clotting factor XIIa. Gold, used as a model substrate, was modified with PEG and anticoagulant molecules using two methods referred to as sequential and direct. In the sequential method PEG was first immobilized on the surface and then the bioactive molecule was attached (conjugated) to the PEG. In the direct method, a PEG-bioactive molecule conjugate was first formed and then immobilized on the surface. Surfaces were characterized by contact angle, ellipsometry and x-ray photoelectron spectroscopy (XPS). Uptake of the bioactive molecules was measured by radiolabeling. Biointeraction studies included plasma protein adsorption, bioactivity assays using chromogenic substrates and clotting time assays. For PEG-hirudin and PEG-CTI surfaces (both direct and sequential) the protein resistance was similar to that of the PEG-alone surfaces. Despite having a lower density of bioactive molecule (both hirudin and CTI), the sequential surfaces showed superior bioactivity compared to the direct ones.

To determine the optimal ratio of free PEG and bioactive molecule-PEG conjugate on the surface (best combination of protein resistance and bioactivity), PEG-CTI was immobilized on gold substrate with varying ratio of conjugated to free PEG using both direct and sequential methods. As the ratio increased, protein resistance was maintained while specific interactions (bioactivity) increased. The optimal composition appeared to be where all PEG molecules are conjugated to a CTI molecule.

In the final part of this project, PEG and CTI were immobilized on polyurethane as a material with applicability to medical device construction. A sequential method was developed for this substrate. Comparison of the PEG-CTI surface with PEG only or CTI only surfaces indicated that the combination of PEG-CTI was effective both in reducing non-specific protein adsorption and promoting the specific interactions of CTI with its target plasma protein, factor XIIa. In fact, the presence of PEG improved CTI interactions with FXIIa compared with CTI only surfaces. Thus, sequential attachment of PEG and CTI may be effective for modifying polyurethane surfaces used in blood-contacting medical devices.

ACKNOWLEDGEMENTS

First and foremost, I would like to express my profound thanks and appreciation to my supervisors. I am vastly grateful to Dr. John L. Brash for always being there with great guidance and encouragement. I would like to express my gratitude to Dr. Shiping Zhu for his constant support all through my journey to complete this work. Having two great researchers in the field of biomaterials and polymers as my supervisors enabled me to learn a lot not only about the field but also how to tackle research problems in general. My sincere gratitude is also extended to my other supervisory committee member, Dr. William P. Sheffield, for his valuable suggestions on my research.

I would like to continue by acknowledging the researchers of Brash/Zhu labs. Many thanks to Rena M. Cornelius and Glenn McClung for their valuable assistance in the lab. I would also like to thank all my colleagues in Brash/Zhu labs, especially Kyla Sask for her friendship and helpful discussions on research work.

Last but not least, I am grateful to my family: To my parents, Minou and Mahmoud, for their continuous support all through my life, to my brothers, Rouzbeh and Amin, and my sister-in-law, Delnavaz, for always being there for me. Finally, I would like to thank my husband, Suhaib, for his patience, encouragement and steadfast support. Without him, I would not have been able to persevere and accomplish this work. I would like to dedicate this thesis to my parents and my husband.

TABLE OF CONTENTS

LIST OF FIGURES

LIST OF TABLES

LIST OF ABBREVIATIONS

ADP	Adenosine Diphosphate
ATH	Antithrombin-Heparin Complex
ATP	Adenosine Triphosphate
CTI	Corn Trypsin Inhibitor
F	Factor
Fg	Fibrinogen
Fn	Fibronectin
GP	Glycoprotein
HEMA	Hydroxyethyl Methacrylate
HMWK	High Molecular Weight Kininogen
HV	Hirudin Variant
IgG	Immunogammaglobulin
LMWH	Low Molecular Weight Heparin
OEGMA	Oligoethylene Glycol Monomethacrylate
PEG	Polyethylene Glycol
PEO	Polyethylene Oxide
PLL	Poly L-lysine
PPACK	D-phenylalanyl-L-prolyl-L-arginine Chloromethyl Ketone
PU	Polyurethane
PUU	Polyurethaneurea
SAMs	Self-Assembled Monolayers

TF	Tissue Factor
t-PA	Tissue Plasminogen Activator
Vn	Vitronectin
vWF	von Willebrand Factor
XPS	X-Ray Photoelectron Spectroscopy

CHAPTER 1. INTRODUCTION AND LITERATURE REVIEW

Biomaterials may be defined as materials used in applications where they interact with the biological environment. Recently, Williams described a biomaterial as ‘‘ a substance that has been engineered to take a form which, alone or as part of a complex system, is used to direct, by control of interactions with components of living systems, the course of any therapeutic or diagnostic procedure, in human or veterinary medicine [1].’’ Biomaterials are used in applications related to gene therapy, tissue engineering, biosensors, drug delivery, medically related nano- and bio-technologies and implantable medical devices [1, 2]. In all such applications, it is important to minimize unacceptable and unwanted biological interactions with the material. In other words, biomaterials need to be “biocompatible”. Biocompatibility is usually defined based on the application. For implantable medical devices, for example, biocompatibility is defined as the ability of the medical device to perform its intended function without any undesirable systemic or local host response [3].

The host response can take different forms depending on the application [4]; it usually starts with protein adsorption. Other reactions include complement activation, immune response, cell adhesion, coagulation and thrombosis (in the case of blood contacting materials), and tumor formation [3, 5, 6]. Biomaterials properties, both physical and chemical, influence the host response. These properties include surface chemistry, surface topography and morphology, surface energy, ion content, hydrophilicity and hydrophobicity, bulk properties and composition, water content, porosity, degradability and degradation product toxicity [2].

Biomaterials design has the aim of minimizing or, ideally, eliminating the complications associated with the host response. In this research, surface modification has been carried out to improve blood compatibility. Accordingly, this chapter will provide background information on blood-material interactions and biomaterials modification for blood compatibility.

1.1 Blood-Material Interactions

Many complications are associated with blood-contacting devices such as stents, catheters, left ventricular assist devices, heart valves, vascular grafts, etc. The interactions of the blood-contacting material can ultimately lead to the failure of the device. When blood contacts a foreign material, blood proteins adsorb to the surface and usually form a monolayer within seconds [7, 8]. This is usually followed by platelet adhesion and activation, leukocyte adhesion, activation of the complement system, activation of blood coagulation and thrombus formation [5, 6, 9]. Figure 1.1 shows a simplified view of blood-material interactions [10]. Coagulation (contact factor pathway) is activated by the adsorption and activation of contact factor pathway proteins. Furthermore, adsorbed proteins such as fibrinogen and fibronectin are known to influence platelet adhesion and activation (see platelet section of this chapter for more details). Erythrocyte and leukocyte interactions are also influenced by the nature of the adsorbed protein layer [11-13]. Leukocyte adhesion is linked to the inflammatory response to medical implants [14]. In blood contact complement activation often occurs and contributes to the inflammatory and immune responses [15]. Complement system is made of a number of proteins in blood that are involved in three pathways (classical, alternative and lectin binding

pathways), leading to complement activation. It is important to note that leukocyte and complement activation contribute to biomaterials-associated thrombosis [6] Activated leukocytes produce and release substances such as platelet activating factors [8]. Complement activation is also closely associated with platelet activation [16]. Due to the importance of protein adsorption as the initiating step of blood-material interactions, protein structure and protein adsorption phenomena are discussed in the following sections.

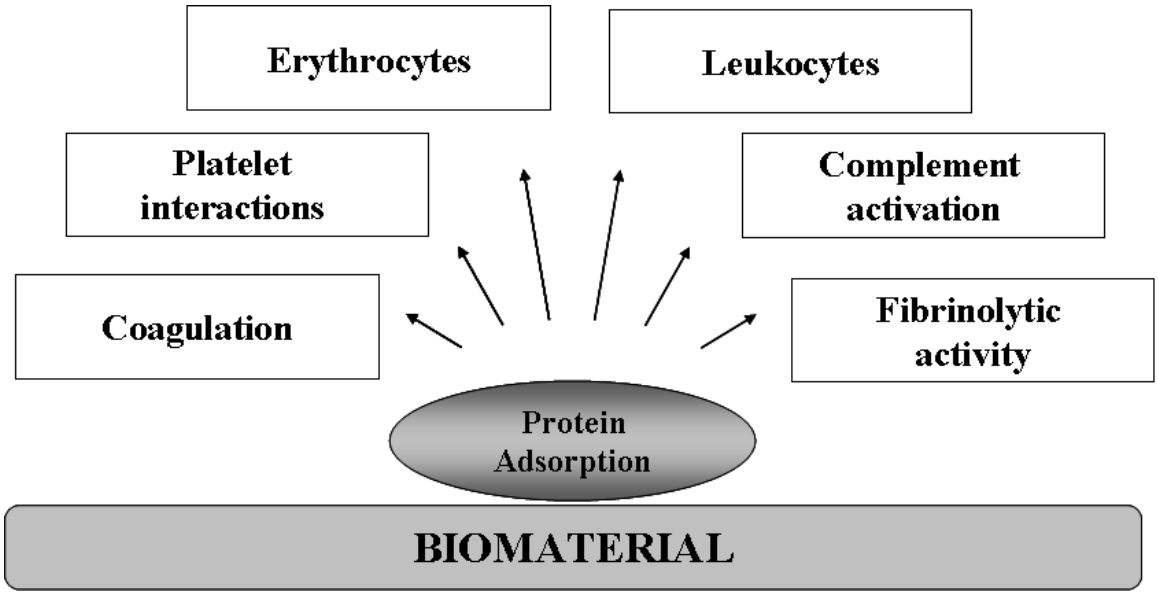

Figure 1. 1 Blood response to biomaterial (adapted from Ref # [10], Courtney et al, 1994) (with permission from publisher)

1.1.1 Protein Structure and Properties

Proteins are biopolymers in which amino acids are linked together in long chains by peptide bonds formed between the amino and carboxyl groups of adjacent residues.

Proteins are generally globally charged depending on the amino acid composition. The net charge can be positive, negative or zero depending on the pH of the solution and protein's isoelectric point (pH at which the protein's net charge is zero).

Protein structure has four levels: primary, secondary, tertiary and quaternary. The primary structure describes the amino acid sequence. The secondary structure refers to the chain conformation, e.g. α-helix and β-sheet. The tertiary structure describes the overall shape of the protein determined largely by chain folding. The quaternary structure refers to the spatial arrangement of individual polypeptide chains in multi-chain proteins such as hemoglobin [17]. In general, the three-dimensional structure of protein is determined by interactions such as hydrogen bonding, electrostatic interactions, disulfide bonds, van der Waals forces and hydrophobic interactions.

There are two main classes of proteins: fibrous and globular [18]. Fibrous proteins are long, rod-shaped proteins or aggregates that are typically insoluble in water. Most of the structural proteins such as collagen are fibrous proteins. Globular proteins have a quasi-spherical (globular) shape that is created by the tertiary and quaternary structure. Their non-polar residues are usually in the interior and the polar residues are on the periphery. Thus, they are generally soluble in water although to different extents depending on the molecular weight and surface composition. Most of the plasma proteins fall into this class.

In the presence of an interface such as a biomaterial, proteins have a tendency to adsorb to the surface due to their amphipathic nature (presence of polar and non-polar regions) and generally high molecular weight [19]. Several interactions are possible

between protein and surface [20]. Hydrophobic interactions leading to disordering of water associated with the material and the protein surface, and thus to a gain of entropy, are considered one of the main driving forces for protein adsorption. This is sometimes referred to as hydrophobic dehydration. Second, electrostatic interactions between opposite electrical charges on protein and surface can occur. Third, protein and surface can interact through van der Waals forces. Finally, depending on the surface chemistry and protein structure, covalent and hydrogen bonding between the protein and surface are possible [21]. Protein-surface interactions can lead to conformational changes, unfolding, reorientation and denaturation [22]. In denaturation, the native structure of the protein is changed and this can have a significant effect on biological functions, leading, for example, to blood coagulation and platelet adhesion.

1.1.2 Protein Adsorption

Protein adsorption refers to the "accumulation" of protein at an interface. Adsorbed quantity depends on protein concentration and protein-surface affinity [23]. The kinetics of adsorption is influenced by affinity and the rate of transport to the surface. Protein size influences the rate of the transport (diffusion), with smaller proteins diffusing faster that bigger ones. Protein properties such as charge, hydrophilicity, hydrophobicity and internal structure influence protein-surface affinity [20]. For example, larger "soft" proteins adsorb with higher affinity than smaller "hard" ones that have greater structural stability [19].

The properties of the adsorbing interface also play an important role in protein adsorption. Factors such as surface hydrophilicity/hydrophobicity, surface topography, surface charge and chemistry can influence protein adsorption [24, 25]. Hydrophilic surfaces tend to adsorb less protein than hydrophobic ones [26]. Rough surfaces provide more surface area for protein adsorption. Roughness can also influence the geometrical arrangement of protein on surfaces and thus can affect protein adsorption [27]. Surface chemistry strongly affects the protein-surface binding mechanism. Clearly adsorption will be influenced by the relative signs of the surface and protein charge.

Protein surface interactions start with the diffusion of protein from the bulk solution to the interface [28]. Protein-material interactions as such then occur including protein spreading, conformational change and denaturation [29, 30]. Once adsorbed, proteins can exchange with other proteins that have higher affinities [31]. Desorption per se, i.e release into pure buffer is generally not observed, especially on hydrophobic surfaces.

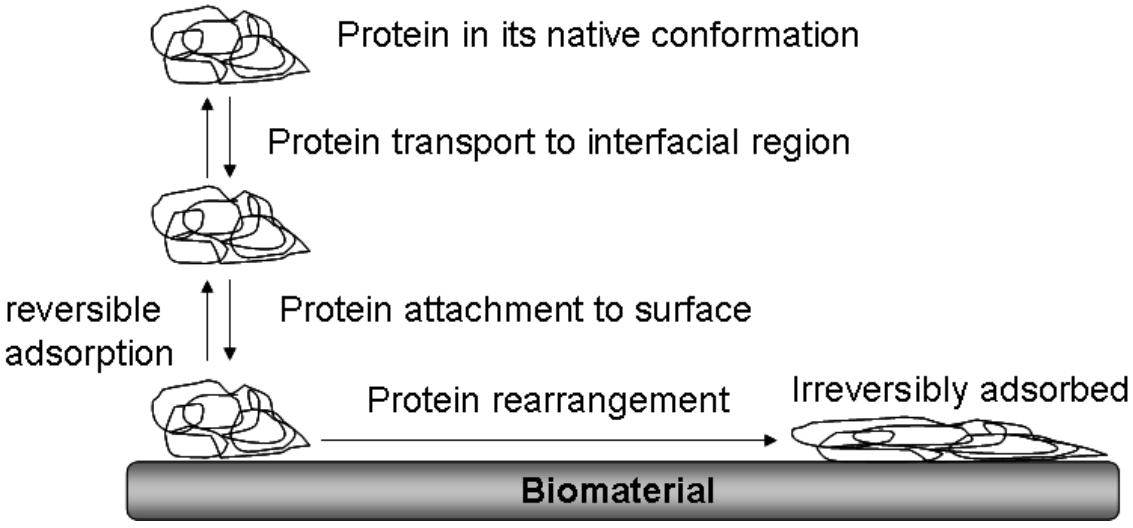

Figure 1. 2 Protein adsorption on biomaterials (adapted and redrawn from ref #[30])

Several models have been used to describe protein adsorption [29, 32]. The Langmuir model or isotherm describes adsorption from a single component system. It is based on the following assumptions: adsorption is reversible; the surface is energetically uniform and the heat of adsorption ΔH_a is independent of coverage; adsorption is restricted to a monolayer; the adsorption sites are independent of each other, i.e. adsorption of one molecule does not affect that of any other. The model is described by Equation 1.1 [32] derived by equating the rates of adsorption and desorption (dynamic equilibrium):

$$\theta = \frac{KC_p}{1 + KC_p} \qquad \text{Equation 1.1}$$

Where θ is the surface fractional coverage, C_p is the protein solution concentration at equilibrium, and K is the adsorption equilibrium constant (rate constant for adsorption, k_a, divided by rate constant for desorption, k_d). As a function of solution concentration, adsorption increases linearly at low concentrations ($KC_p<<1$; $\theta \sim KC_p$) and reaches a plateau at higher concentrations ($KC_p>>1$; $\theta \sim 1$). The plateau is interpreted as a monolayer.

Some of the assumptions in the Langmuir model do not generally reflect experimental observations in the case of protein adsorption. Thus protein adsorption is generally irreversible on a realistic time scale [33]. Also it is not true that the earlier adsorbed proteins do not affect the adsorption of later-arriving proteins.

The random sequential adsorption (RSA) model addresses the irreversibility and the excluded surface effect of protein adsorption. This model assumes that adsorption

happens on a homogeneous surface and that adsorption continues until no space is left on the surface. Eq1.2 describes the rate of adsorption based on RSA assumptions [34-37].

$$\frac{d\theta}{dt} = k_a C_p \Phi \qquad \text{Equation 1.2}$$

Where Φ is the fraction of the surface available for protein adsorption. C_p is the solution concentration of the protein. K_a is the rate constant of protein adsorption and θ is the fractional coverage of protein. The limitation of the RSA model as well as the Langmuir model is that they do not take into consideration the surface diffusion of protein [38].

The assumption that ΔH_a is independent of coverage is also generally not true for proteins. The Freundlich and Temkin models [39-41] account for this non-independence on a largely empirical basis. The Freundlich model assumes that ΔH_a decreases exponentially in magnitude with coverage leading to the isotherm Eq 1.3 [39]:

$$\theta = kC_p^{1/n} \qquad \text{Equation 1.3}$$

Where k is the equilibrium constant and n is an exponent related to the adsorption energy.

This model predicts that adsorption increases indefinitely with the increase of the solution concentration. The Temkin model assumes that ΔH_a decreases linearly in magnitude with coverage leading to the isotherm Eq 1.4 [42, 43]:

$$\theta = k \ln(nC_p) \qquad \text{Equation 1.4}$$

Where the symbols have the same meaning as in Equation 1.3.

In a multi-protein system such as blood or plasma, many proteins compete for the adsorption sites on the surface. Diffusion controls protein adsorption initially and thus, in

the early stages, concentration and protein size are critical [44-46]; smaller proteins present at higher concentration adsorb more than larger ones at lower concentration. At longer time as the surface fills, however, proteins of higher surface affinity will displace those of lower affinity independent of concentration and size. These exchange phenomena are known as the "Vroman effect" [45, 47]. The Vroman effect describes protein adsorption from plasma as an "adsorption-displacement" phenomenon. It has been observed for plasma proteins such as albumin, IgG and fibrinogen (Fg) [45, 48, 49]. For example, initially adsorbed Fg has been shown to be displaced at longer time by other higher affinity, low concentration proteins such as high molecular weight kininogen [7, 48].

One of the main consequences of protein adsorption on blood contacting biomaterials is the activation of the plasma coagulation cascade. Blood coagulation mechanisms are reviewed in the following sections.

1.1.3 Blood Coagulation

The blood coagulation cascade involves a series of reactions in which an inactive clotting factor (zymogen) becomes enzymatically active and can activate other (zymogen) clotting factors. The coagulation cascade is shown in Figure 1.3. It can be initiated intrinsically (contact factor pathway) or extrinsically (tissue factor (TF) pathway). Both pathways lead to the common coagulation pathway which results in the formation of thrombin and fibrin. The tissue factor (extrinsic) pathway is initiated by vascular injury for haemostatic control. The contact factor (intrinsic) pathway, on the other hand, is initiated when blood interacts with a foreign material.

The cascade model of coagulation was proposed in the 1960's. In a recent study, Monroe et al showed that coagulation not only involves a cascade of proteolytic reactions but also involves cells, and that cells play a major role in directing and controlling the coagulation process [50]. In their cell-based model of haemostasis, they described the three steps of initiation, amplification and propagation. In the initiation phase, the extrinsic pathway starts with TF-bearing cells. The thrombin generated in the initiation phase activates platelets (amplification). Finally, in the propagation phase, the intrinsic pathway takes place on the activated platelets [50].

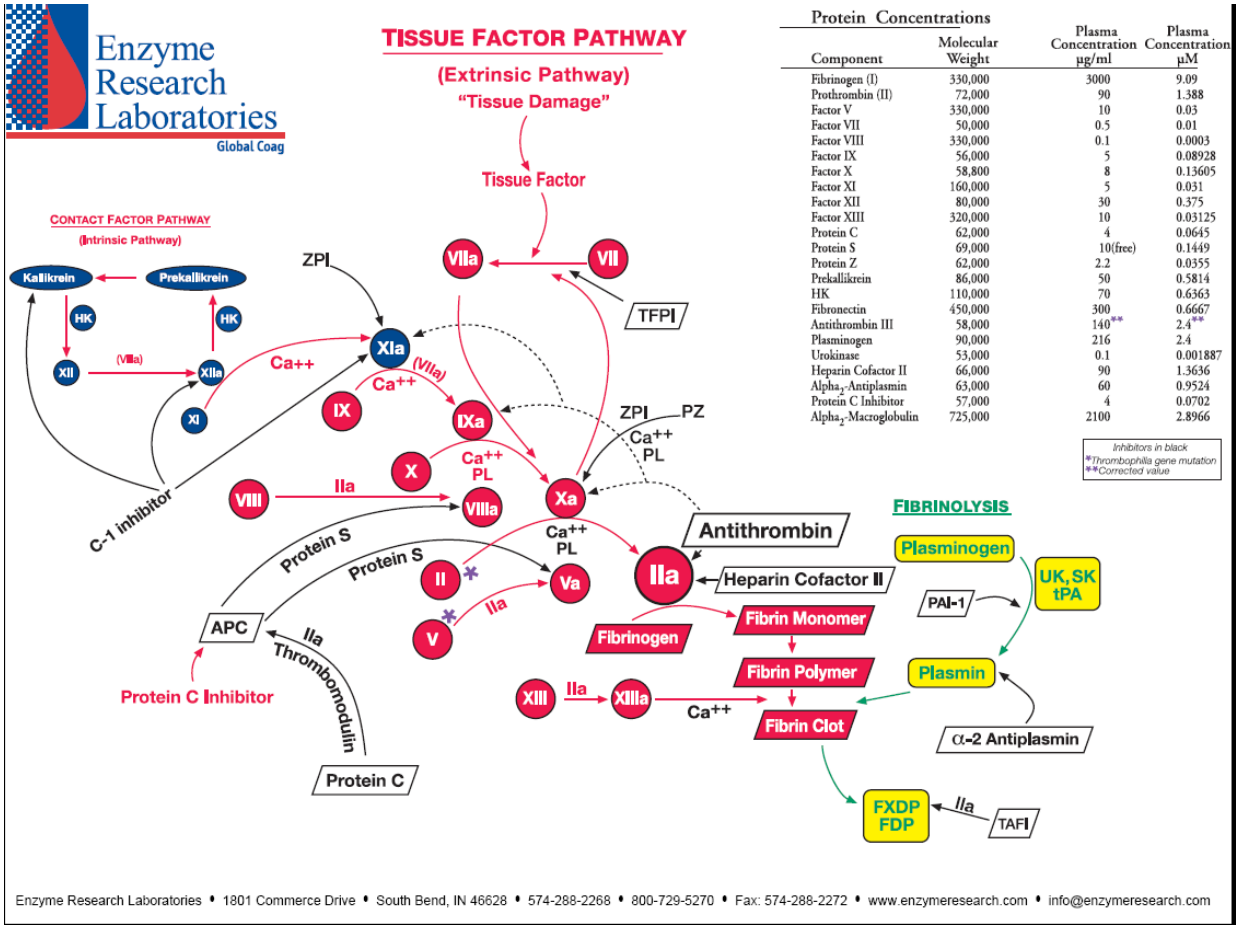

Figure 1. 3 Blood coagulation cascade. From: http://www.enzymeresearch.com/CASCADES_2004/images/CASCADE_erl_2007.pdf (reprinted with permission)

1.1.3.1 Contact Factor (Intrinsic) Pathway

The contact factor (intrinsic) pathway starts with the activation of clotting factor (F) XII (Hageman factor) to FXIIa (refer to Fig 1.2). FXIIa then converts prekallikrein to kallikrein. Kallikrein amplifies the activation of FXII to FXIIa. FXIIa then converts FXI to FXIa. The presence of high molecular weight kininogen (HMWK) is essential for the activation of kallikrein and FXI [51]. FXIa activates FIX. This is followed by the

activation of FX to FXa, FII (prothrombin) to FIIa (thrombin) and finally the conversion of fibrinogen to fibrin, the clot material.

It is generally understood that biomaterials-induced clot formation is caused by the activation of FXII. The mechanism of interaction of FXII with surfaces, however, is not well understood and has been the subject of continuing research [51-55]. Several studies have shown that FXII is mainly activated by contact with negatively charged surfaces [51-53, 56]. It was believed that the specific binding of FXII to negatively charged surfaces was responsible for the activation of FXII in contact with such surfaces. A recent study [54] showed that FXII was activated in buffer with the same efficiency at both anionic hydrophilic surfaces and hydrophobic surfaces while in plasma, FXII activation was attenuated on hydrophobic surfaces. This study concluded that the presence of plasma proteins affects surface activation of FXII. Due to the importance of FXII, thrombin and fibrinogen to the work reported in this thesis, the structure and function of these three proteins is discussed in the next sections.

1.1.3.1.1 Hageman Factor (FXII)

Hageman factor is an 80 kDa protein present in plasma at a concentration of ~30 μg/mL. It is activated by formation of a heavy chain and a light chain by cleavage within a disulfide loop. The heavy chain contains three surface binding regions and the light chain contains the catalytic domain [57, 58].

Upon surface contact, FXII undergoes a conformational change and cleavage of Arg353-Val354 by plasma proteinases; it is thus converted to FXIIa (αFXIIa) [59]. Heavy chain and light chain of FXIIa has molecular weights of 52 kDa and 28 kDa, respectively

[60]. The surface contact activation of FXII is referred to in the literature as autoactivation [56]. FXII can also be activated by kallikrein and FXIIa through a reciprocal self-amplification reaction [59].

1.1.3.2 Thrombin

Thrombin is a serine protease of 308 amino acid residues with a molecular weight of 37 kDa [61]. It is composed of an A chain with a molecular weight of 6 kDa and a B chain with a molecular weight of 31 kDa. The A and B chains are connected by a disulfide bond. The B chain contains the three active sites of thrombin at His57, Asp102, and Ser195 [62].

Thrombin plays a major role in coagulation by converting fibrinogen to fibrin and by activating FXIII which is involved in crosslinking fibrin [63]. Furthermore, thrombin amplifies its own production by activating FV, FVIII and FXI. Thrombin also activates protein C which is involved in the inactivation of FVa and FVIIIa to prevent further clot formation [64].

Besides its interaction with plasma proteins, thrombin also interacts with cells via receptors [65]. Thrombin interaction with platelets is a major thrombin-cell interaction and has an important role in clot formation. Thrombin induces platelet activation and aggregation. The surface of the activated platelets then becomes a catalyst for the activation of clotting factors. Other cells that can interact with thrombin include monocytes, leukocytes and endothelial cells. Thrombin can interact with damaged endothelial cells to stimulate the production of tissue factor [61].

1.1.3.3 Fibrinogen

Fibrinogen (Fg) is a globular protein with a molecular weight of 340 kDa and dimensions of 450 X 90 X 90 Å [66]. It is present in plasma at a concentration of about 3 mg/mL. It consists of two sets of α, β and γ polypeptide chains [67]. As the precursor of fibrin it plays a major role in coagulation. Thrombin cleaves Fg to allow polymerization and fibrin formation, and cross-linked fibrin forms a meshwork in which blood cells are trapped to form the mature clot. Fig 1.4 shows thrombin-Fg interactions.

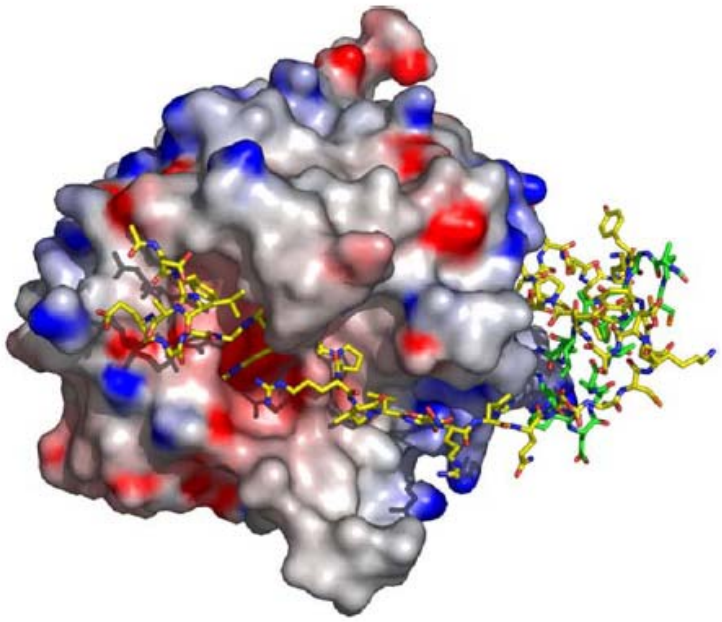

Figure 1. 4 Model of thrombin interacting with N-terminal fibrinogen Aα chain. (Ref # [62], with permission)

Fg adsorption on biomaterials has been studied extensively. Adsorbed Fg has been shown to bind to and activate platelets by interaction with the platelet glycoprotein IIb-IIIa integrin receptor [68-70]. The availability of RGD sequences in adsorbed fibrinogen, which interact with GPIIb-IIIa, is important for platelet adhesion [70]. Adsorbed Fg has

also been shown to stimulate activation of the inflammatory pathways by interaction with monocytes [71-73]. Indeed Fg is considered as a major adhesion or general cell-binding protein.

1.1.4 Inhibition of Blood Coagulation: Anticoagulants

Anticoagulants have been widely used for surface modification of biomaterials. Most anticoagulants used in biomaterials applications target thrombin to inhibit clot formation. These anticoagulants inhibit thrombin either directly or indirectly.

The most commonly used anticoagulant, which inhibits thrombin indirectly, is heparin. Heparin is a highly sulfated glycosaminoglycan [74] with average molecular weight 12,000 Da (range 5,000 to 40,000 Da). Heparin binds antithrombin and catalyzes the inhibition of thrombin and FXa by antithrombin. Heparin interacts with antithrombin through a specific pentasaccharide sequence [75]. Only one third of the molecules in unfractionated heparin (with average MW of 15,000) and one fifth of those in low molecular weight heparin (LMWH, with average MW of 5,000) contain this pentasaccharide sequence [75]. Fondaparinux (with average MW of 1,500) is a synthetic analog of the heparin pentasaccharide sequence [76]. The binding of the pentasaccharide unit of heparin to antithrombin results in a conformational change in antithrombin. The antithrombin reactive centre loop can then accelerate the interaction of antithrombin with FXa [74]. In order to catalyze antithrombin-thrombin interactions, however, heparin needs to bind to thrombin as well as antithrombin. To accomplish this, the pentasaccharide chain needs to be long enough to be able to interact with both thrombin and antithrombin [76]. Thus, compared with unfractionated heparin, LMWH is less

capable of inhibiting thrombin due to its shorter pentasaccharide chain length and fondaparinux is only capable of inhibiting FXa.

There are limitations and unwanted side effects associated with heparin. Platelet factor 4 and heparinases can inactivate heparin [77]. Furthermore, heparin is not able to inhibit clot-bound thrombin [78]. In contrast, direct thrombin inhibitors are able to inhibit both clot-bound and free thrombin.

Direct thrombin inhibitors include hirudin and its analogues as well as short peptides such as D-phenylalanyl-L-prolyl-L-arginine chloromethyl ketone (PPACK) [79, 80]. These inhibitors can bind directly to the active site or the anion-binding exosite or both active and anion-binding sites of thrombin.

1.1.4.1 Hirudin

Hirudin is a small protein containing 65 amino acid residues (including 3 lysines) and three disulfide bridges; its molecular weight is approximately 6.9 kDa. The N-terminal of hirudin binds to the apolar binding site of thrombin, and the C-terminal can interact with the anion-binding exosite of thrombin [81]. The Pro46-Lys47-Pro48 sequence of hirudin occupies the basic specificity pocket near the active site of thrombin. Thus, hirudin is able to inhibit both free and fibrin-bound thrombin. Hirudin also interferes with the site for interaction of thrombin with platelets [82, 83]. Fig 1.5 and Fig 1.6 show the amino acid sequence and crystal structure of hirudin, respectively [84, 85]. Hirudin has been used by a number of researchers as a surface modifier on biomaterials for improved blood compatibility. These studies are discussed in more detail in the section on research on surface modification with bioactive molecules (section 1.2.3.2).

Hirudin occurs naturally in leeches. It is also available in recombinant form. The main isoforms of hirudin isolated from leeches are HV1 and HV2. HV1 has a Val-Val sequence at its N-terminal. HV2 has an Ile-Thr sequence at its N-terminal. The HV3 isoform has the same sequence as the HV2 form except for an alanine residue adjacent to the sulfated tyrosine [86]. The hirudin used in the research reported in this thesis is the recombinant product lepirudin (Refludan®), derived from yeast cells. It is identical to HV2 except for the presence of leucine instead of isoleucine at the N-terminal and the absence of sulfate group on its tyrosine residue.

Two important recombinant hirudin types are hirugen and hirulog. Hirugen contains the C-terminal portion of hirudin (amino acid residues 53-64) and thus it can inhibit the fibrinogen binding site of thrombin but not the active site [87]. Hirulog, also known as bivalirudin, is a 20-amino acid polypeptide with a molecular weight of around 2.2 kDa. It contains the N-terminal residues and the C-terminal residues of hirudin. The termini are connected by four glycine residues [88]. Hirulog inhibits both the active site and the anionic binding site of thrombin. Unlike hirudin, hirulog inhibition of thrombin is reversible. Thrombin bound to hirulog retains partial activity by cleaving the Arg3-Pro4 bond of hirulog [89].

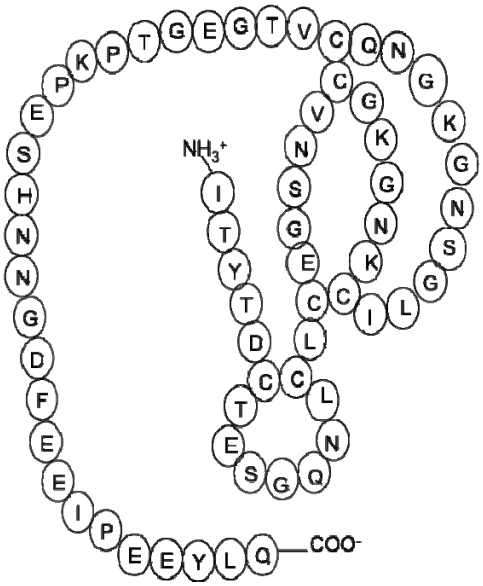

Figure 1. 5 Amino acid sequence of hirudin (HV2)(adapted and redrawn from ref #[84])

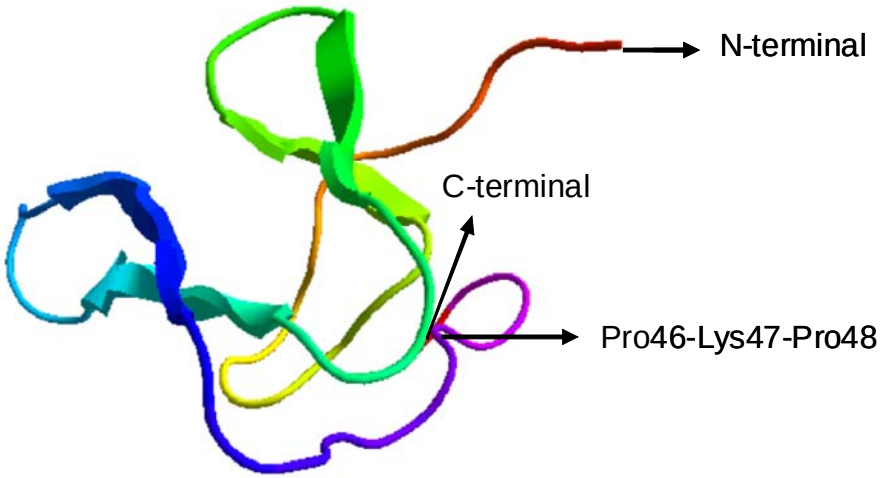

Figure 1. 6 Crystal structure of hirudin in ribbon format, prepared by CLC Main Workbench 6 software using Protein Data Base file 1HIC. The active sites of hirudin are N-terminal, C-terminal and Pro46-Lys47-Pro48.

1.1.4.2 Corn Trypsin Inhibitor (CTI)

Corn trypsin inhibitor (CTI) is a relatively small protein of molecular weight ~12.5 kDa (112 amino acids). The amino acid sequence of CTI and its crystal structure are shown in Fig 1.7 and Fig 1.8 respectively [90, 91]. The isoelectric point of CTI is around 4.5. The active site is at Arg^{36}-Leu^{37} [91]. One study has reported dimensions of 57 X 57 X 80.5 Å after crystallization [92].

CTI is isolated from kernels of corn. Recombinant CTI has also been prepared and used for studies of activity [93, 94]. CTI can bind specifically to and inhibit the catalytic activity of trypsin [95]. CTI also inhibits clotting factor XIIa by forming a 1:1 complex [93]. Since it specifically inhibits FXIIa and since activation of FXII to FXIIa is among the first reactions in the contact factor pathway, CTI has been widely used for the study of tissue factor (TF)-dependent coagulation reactions [96-98]. In such studies, CTI has been used to suppress the contact factor pathway. It has been shown to prolong plasma clotting time by ~4 fold [96, 97]. It may thus be seen a promising candidate for surface modification of biomaterials for improved blood compatibility, but other than the studies done by Weitz and coworkers [99, 100] as well as the studies conducted in our lab and reported in this thesis, CTI has not been used for the biomaterials surface modification. Weitz and coworkers modified commercial polymeric catheters with PEG-CTI conjugate using a methacrylic coating to which the PEG-CTI conjugate was attached via epoxy groups. They observed significantly higher FXIIa inhibition and longer clotting times on the modified catheters compared with the unmodified ones.

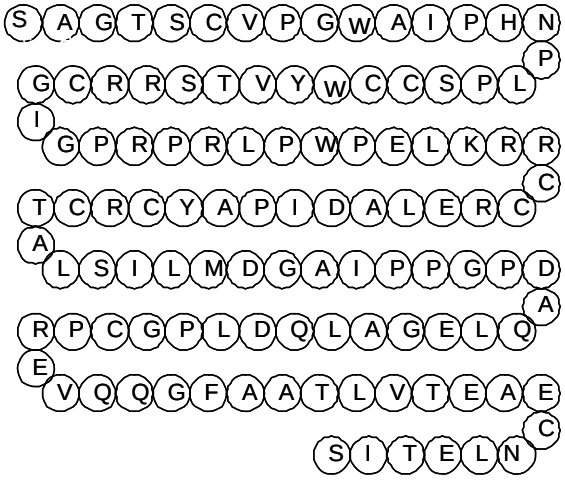

Figure 1. 7 Amino acid sequence of CTI (adapted and redrawn from Ref # [90])

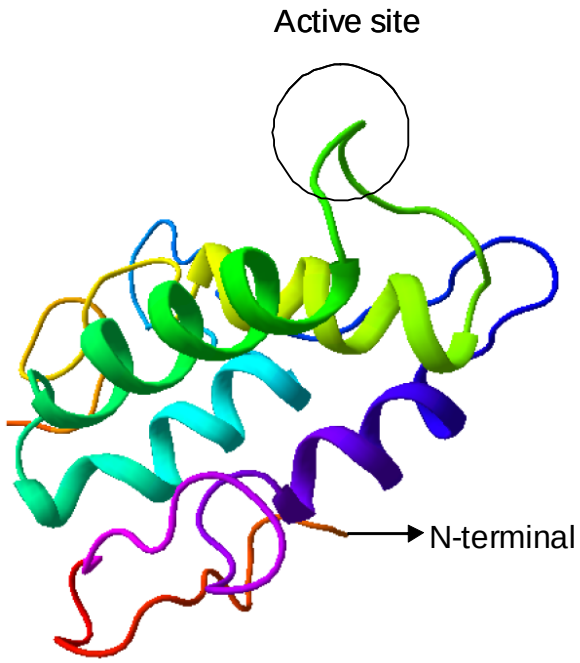

Figure 1. 8 Crystal structure of corn trypsin inhibitor in ribbon format, prepared by CLC Main Workbench 6 software using Protein Data Base file 1BFA. The active site of CTI is at Arg36-Leu37.

1.1.5 Platelets

Platelets are disc shaped anuclear granular blood cells with a diameter of 2-4 μm and with a concentration of 150,000 to 400,000 per microlitre of blood. They play an important role in haemostasis and thrombosis [101]. In haemostasis upon vascular injury, exposure of subendothelial matrix causes adhesion and morphological changes of platelets. This results in a change of platelet shape with the creation of pseudopodia. Collagen, von Willebrand factor (vWF), fibronectin and other adhesive proteins are the matrix components that mediate platelet adhesion [102, 103]. Collagen is probably the principal mediator of platelet adhesion [104]. The platelet membrane has several collagen receptors including integrin $\alpha_2\beta_1$, glycoprotein (GP) VI and GPIV [104]. Subendothelial vWF has also been shown to play an important role in platelet adhesion by interaction with the GPIb-IX receptor in platelets [103, 105]. Following platelet adhesion, intracellular granules release their contents including adenosine diphosphate (ADP), adenosine triphosphate (ATP), calcium ions and platelet factor 4. ADP release mediates the recruitment of additional platelets to the site of injury and results in platelet aggregation. Along with fibrin, platelets are a major component of the clot or thrombus formed at the site of injury [105].

In blood contact with biomaterials, platelets adhere to the surface. The interaction of platelet receptors with adsorbed protein layers is believed to be responsible mainly for platelet adhesion to biomaterials [106]. Similar to haemostasis, platelet adhesion on biomaterials results in the release of granule contents that can promote platelet aggregation. It has been shown that platelet receptors interact principally with the peptide

ligands of four proteins: fibrinogen (Fg), vitronectin (Vn), fibronectin (Fn) and von Willebrand factor (vWF) [106, 107]. Fg binds to GPIIb-IIIa in stimulated platelets. Vn binds to vitronectin receptor, Fn binds to GPIc-IIa and vWF binds to GPIb-IX. Tsai et al showed that Fg is the major adsorbed protein mediating platelet adhesion and aggregation on biomaterials [69, 108]. Platelet receptors are believed to recognize and bind to the RGD sequence in the Aα chains and a specific dodecapeptide sequence in the γ chains of Fg [109].

Thrombin generated in coagulation can also activate platelets by cleaving its platelet receptor [61, 110]. Furthermore, thrombin generation leads to fibrin formation and fibrin can cause further aggregation [111]. The surfaces of activated platelets also provide a site for interaction and activation of clotting factors of the intrinsic pathway [50].

1.2 Biomaterials Modification for Blood Compatibility

Four general classes of biomaterials may be recognized, namely, polymers, ceramics, metals and natural materials. Various combinations of these four classes, referred to as composites, have also been used to construct biomedical devices. In most of the applications, the biomaterials trigger biological responses that can lead to device failure as discussed above. Biomaterials modification has been widely practiced to create materials that are more biocompatible, or in the context of blood contacting devices, to improve blood compatibility. Numerous approaches have been used to modify biomaterials. These can be divided into two major categories: bulk modification and surface modification. Since the focus of this thesis is on surface modification, literature

related to this category will be discussed in detail in the next sections. The "base" materials for modification used in the work reported here were gold and a polyurethane. More details on these two materials are given in the following sections. A review of the literature is given on general approaches to surface modification for improved blood compatibility including modification for protein resistance, modification for bioactivity (attachment of bioactive molecules), and modification for both protein resistance and bioactivity.

1.2.1 Surface Modification using Gold-Thiol Chemistry

The general inertness of gold as well as its specific reactivity with thiol and disulfide containing molecules are major reasons for its use as a model material in biomaterials studies. Being relatively pure, optically reflective, and available in highly smooth form, it is also amenable to detailed physical characterization such as ellipsometry, surface plasmon resonance and others. Thiols and disulfides chemisorb to gold with a bond energy of 45 kcal/mol [112, 113]. On crystalline gold surface with 1,1,1 orientation, the sulfur atoms of adsorbing thiols reside in the three-fold hollows between the gold atoms (Fig 1.9) [114]. Oxidative interaction of S-H or S-S bonds with gold is believed to occur during chemisorption [115, 116]. The reactions may be represented as follows [117]:

$$RS\text{-}SR + Au^{0}_{n} \longrightarrow RS^{-}Au^{+}.\,Au^{0}_{n}$$

$$R\text{-}SH + Au^{0}_{n} \longrightarrow RS^{-}Au^{+}.\,Au^{0}_{n} + 1/2\ H_2$$

Gold-thiol chemistry has been used generally to create self-assembled monolayers (SAMs) for applications ranging from electronics to nanotechnology to biosensors and biomedical devices [118, 119]. Chemisorption of long chain alkanethiols (R-SH) or dialkyldisulfides (RS-SR) has been widely studied for the formation of SAMs [120-123]. When gold is exposed to a solution of an alkanethiol or dialkyldisulfide, 80-90% of the monolayer is achieved within a few minutes. It then takes several more hours for the monolayer to rearrange and achieve an ordered structure. The driving force for the formation of SAMs is van der Waals interactions between adjacent carbon chains.

Factors such as contamination of the gold, time of chemisorption, temperature, size and concentration of the thiol or disulfide containing molecule can influence chemisorption and the formation of SAMs [124-126]. Gold surfaces are prone to contamination [127] such that upon exposure to lab air, a hydrocarbon layer is readily formed. Although studies have shown that hydrocarbon contamination is displaced [121], when long chain alkanethiols are used to prepare SAMs, it is advisable to clean the gold thoroughly prior to the chemisorption reaction. It was shown that as the chain length of the chemisorbing molecule decreased (chain length less than 10 carbons), surface heterogeneity increased [125, 128]. SAMs are usually formed within a few minutes at 1 mM concentration. 100 minutes or more may be required when the concentration is decreased to 1μM [117].

When SAMs are formed on gold, the spacing between the neighboring sulfur atoms is 4.97Å (Fig 1.9). Thus if all the sites are occupied, the calculated area per molecule is 21.4 $Å^2$ (density 4.6 molecules/nm^2). On hydrocarbon SAMs, the carbon

chains are tilted to about 30º from the surface normal as shown in Fig 1.7 and sulfur atoms form a √3 x √3 R30º lattice on gold [116, 129] to optimize interchain interactions. Due to their well-defined chemistry and ease of characterization, SAMs are considered to be excellent model systems in the study of biomaterials [112, 130-133].

The surface properties of thiol-modified gold surfaces can be tailored by varying the head terminal group of the thiol or disulfide containing molecule. In this work, gold-thiol chemistry was used to attach polyethylene glycol (PEG) to gold to create model surfaces for the study of blood-material interactions. Other studies have shown that closely packed monolayers of PEG can be formed using thiol-gold chemistry [134-136]. The mechanism of formation of the PEG layer on gold in these cases is similar to that of hydrocarbon SAMs. There are, however, some differences between the two systems. For example, chemisorption of alkanethiol terminated PEG on gold was shown to reach saturation after about 2 h while for hydrocarbon SAMs saturation is achieved much quicker [134].

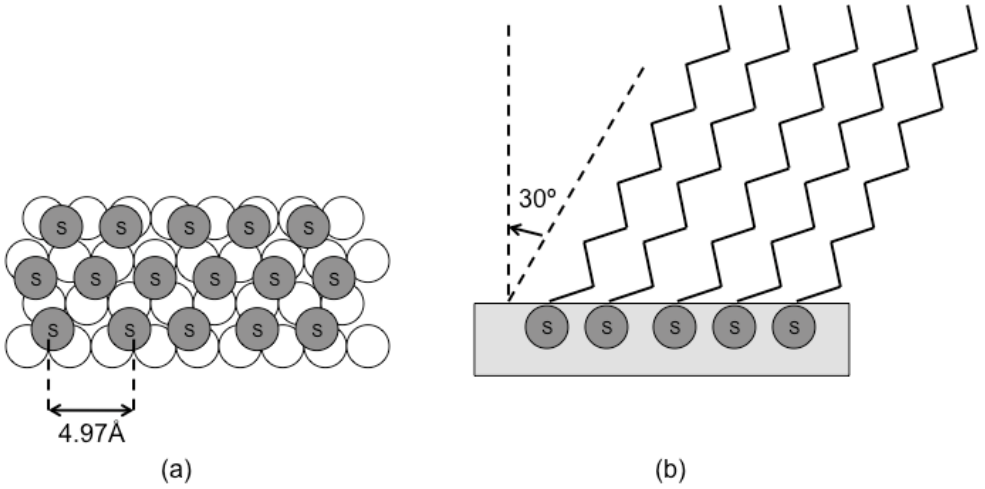

Figure 1. 9 SAMs on gold (a) Top view (b) side view

1.2.2 Segmented Polyurethanes as Biomaterials

Polyurethanes (PU) are block copolymers consisting of sequences of soft and hard segments or blocks. The soft segment types include polyester, polyether, polycarbonate, and polybutadiene. The hard segment components are a diisocyanate and a small molecule diol or diamine (the chain extender). Most of the biomedical grade polyurethanes, including the polyurethane used in the work reported here, are based on an aromatic diisocyanate and a polyether soft segment. In the solid state, the hard and soft segments segregate to form microdomains due to thermodynamic incompatibility. The hard segment domains are dispersed in the soft segment domains and act as virtual crosslinks giving the materials elastomeric properties overall (Fig 1.10).

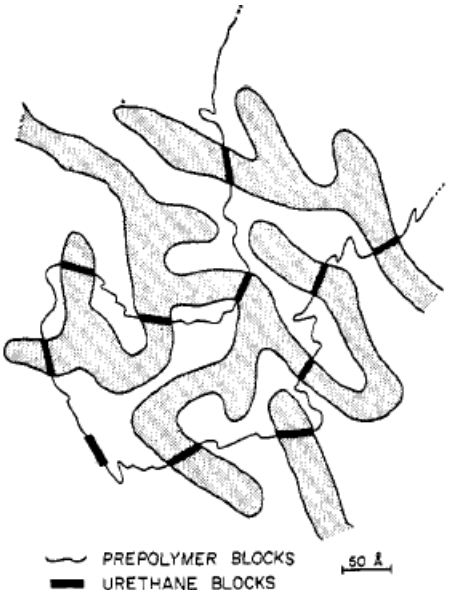

Figure 1. 10 Illustration of microphase separation of polyurethane (Reprinted with permission, from Ref #[137] Copyright © 1971, American Chemical Society)

The typical polymer forming reactions are shown in Fig 1.11. In the first step of the reaction, a diisocyanate reacts with a polyol to form the prepolymer. The second step involves the reaction of prepolymer with a diol or diamine (chain extension). If the chain extender is a diol, a urethane linkage will be formed. If it is a diamine, a urea linkage will be formed [138]. A wide range of mechanical and physical properties can be obtained based on the choice of soft and hard segment and the ratio of the two. This broad range of properties, as well as the finding that some polyurethanes have modest biocompatibility, has resulted in the wide use of these materials in biomedical devices [139]. Polyurethanes have been used in devices such as such as left ventricular assists, catheters, pace maker lead insulation and heart valves [140-143]. They have also been used in artificial organs, drug delivery systems and scaffolds for tissue engineering [144].

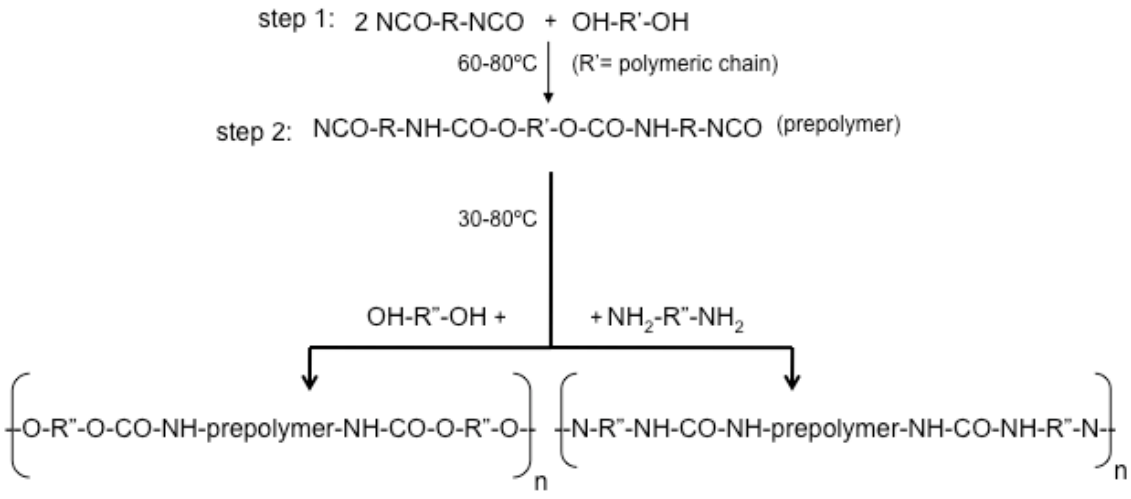

Figure 1. 11 Polyurethane forming reaction.

The widespread use of polyurethanes in biomedical applications is not only due to the versatility of their properties but also to their relatively good "biocompatibility"

compared with other materials [145-147]. Biocompatibility, however, needs to be further improved for applications such as small diameter vascular grafts and other long term blood-contacting devices since thrombosis and clot formation do occur. Bulk and surface modification of polyurethane has been extensively investigated. In bulk modification the composition of the polymer chains is varied to improve mechanical, physical and biological properties. Some of the bulk modification methods include varying the soft segment, diisocyanate or chain extender, incorporating ionic groups or other side chains in the soft or hard segment [148-154]. Surface modification methods include surface coating, surface treatment by various physical and chemical methods, and surface grafting of polymers [49, 155, 156]. These are discussed in the following sections.

1.2.3 Surface Modification for Blood Compatibility

Interactions between a material and the biological environment occur on the material's surface. Hence, many studies have been focused on surface modification of biomaterials for improved blood compatibility. These studies have used surface coating and physical adsorption, incorporation of surface active components and covalent attachment (e.g chemical grafting). In this work, covalent attachment was used. Three general strategies were pursued: modification with protein resistant molecules for reduction of non specific protein adsorption, modification with bioactive molecules to promote adsorption of specific proteins, and combinations of the two.

1.2.3.1 Surface Modification for Protein Resistance

Numerous studies have focused on surface modification with protein resistant molecules. Such surfaces are sometimes referred to in the literature as "non-fouling" surfaces. Reduction in non-specific protein adsorption is believed to prevent or at least minimize the adverse reactions caused by protein adsorption such as coagulation, complement activation, platelet adhesion, leukocyte adhesion and activation and the foreign body response [157-159].

Surface modification with hydrophilic polymers has been widely used to reduce non-specific protein adsorption. The mechanism of the protein resistant properties of hydrophilic molecules is not fully understood. Polyethylene glycol (PEG), also referred to as polyethylene oxide (PEO), is the most studied protein resistant molecule. Other protein resistant molecules used for surface modification include poly 2-hydroxyethylmethacrylate (PHEMA), poly sulfobetaine and poly carboxybetaine methacrylate, poly 2-methoxyethylacrylate (poly(MEA)), polyacrylic acid (PAA), polysaccharides, poly(methacrylates), and poly(2-methacryloyloxyethyl phosphorylcholine) (poly(MPC)) [160-167].

1.2.3.1.1 Surface Modification with Polyethylene Glycol

Polyethylene glycol (PEG) is a linear polymer with repeat unit $-CH_2-CH_2-O-$. PEG is crystalline and is soluble in water at room temperature. PEG (especially PEGs of molecular weight above 2000) comes out of the solution at a temperature known as the cloud point. The cloud point depends generally on solution conditions such as ionic strength and PEG concentration [168]. For example, under high ionic strength condition

(buffer containing 0.6 M K_2SO_4), cloud point of around 60°C was observed [169]. PEG is considered to be non-toxic and has been used for the modification of protein drugs by so-called PEGylation [170]. The covalent attachment of PEG to a protein drug leads to an increase in the molecular weight of the drug and thus a prolonged circulation life time. Also the shielding properties of the PEG diminish the immune response. PEGs used in this way are usually modified with a functional group that reacts with amino or thiol groups of the protein [171]. Attachment to thiol groups results in a more site specific PEGylation since proteins usually have only a few thiol groups [172].

Two mechanisms have been proposed to explain the protein resistant properties of PEG attached to a surface. The first mechanism involves the flexibility and mobility of PEG chains. Flexibility is due to the conformational freedom of the –C-C-O- backbone of PEG due to unrestricted rotation around the C-O bonds. This mechanism is usually referred to as "excluded volume- steric repulsion" (Fig 1.12). When the protein approaches the PEG modified surface, it compresses the flexible PEG chains. This implies an entropy loss generating a repulsive interaction, thus effectively pushing the protein away from the surface. The second mechanism is related to the low interfacial energy at the PEG-water interface and the ability of the PEG chains to bind water tightly (hydrogen bonding). Based on this mechanism the proteins are kept away from the surface by the water barrier, also referred to as "osmotic repulsion" [168].

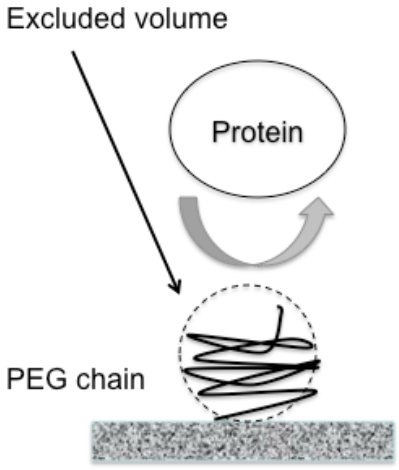

Figure 1. 12 Excluded volume-steric repulsion of proteins by PEG.

Different surface modification techniques have been used with PEG ranging from physical adsorption (coating) to covalent grafting to chemisorption. When PEG is covalently grafted or chemisorbed to the surface through its end group, three surface "regimes" may be distinguished depending on the PEG density [173]. If the density is low, the PEG will be in a random coil conformation giving the so-called "mushroom regime" where the PEG chains do not overlap and there are empty spaces between them. As the density increases, the PEG chains cannot maintain the random coil state and must stretch to be accommodated. At higher density when the distance between the PEG chains is smaller than the radius of gyration the chains will be more completely stretched, and the surface is said to be in the "brush regime" (Fig 1.13). Due to the relevance of covalent attachment and chemisorption methods to the work reported in this thesis, a summary of the literature on surface modification with PEG through covalent attachment and chemisorption is now presented.

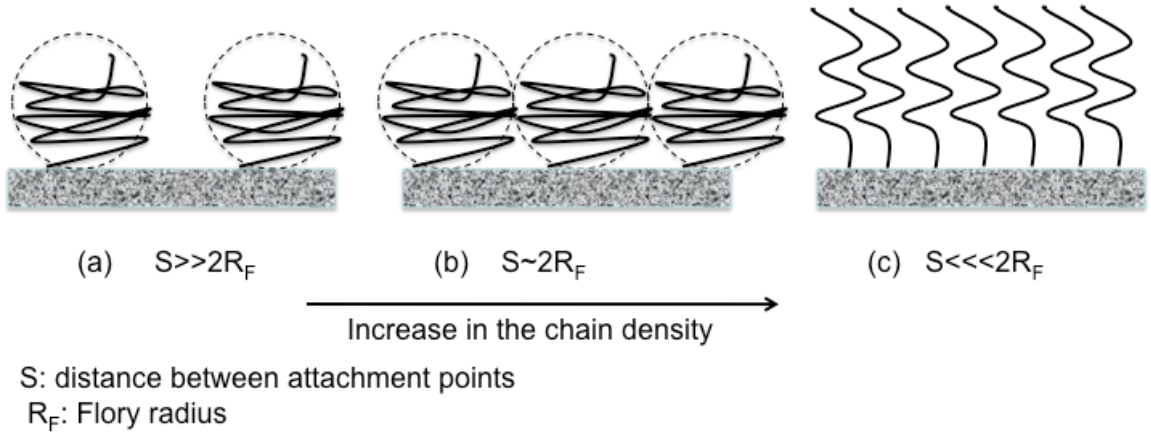

Figure 1. 13 Illustration of PEG regimes upon surface grafting of PEG. Depending on the PEG chain density, the PEG conformation on surface changes from non-overlapping "mushrooms" to fully extended "brushes". (Adapted and redrawn from Ref #[174])

Linear and branched PEGs with various molecular weights were grafted on polystyrene surfaces by Bergstrom et al. The modified surfaces showed significant decreases in Fg adsorption. Branched PEG was less effective than linear PEG [175, 176]. Desai et al modified polyethylene terephthalate with cyanuric chloride-activated PEG and observed a significant reduction in fibrinogen and albumin adsorption as well as platelet adhesion [177]. Another study investigated albumin adsorption and platelet adhesion on PEG grafted to polyaniline films and showed significant reduction in protein adsorption and platelet adhesion on the modified surfaces[178]. Han et al modified polyurethane surfaces with PEG and PEG-SO_3. The PU-PEG surfaces showed lower Fg and albumin adsorption from plasma than the control surfaces [179, 180]. In a study by Kishida et al, cellulose membrane was grafted with PEG-monoacid and PEG-diacid and the grafted membranes showed reduced complement activation [181]. Kim et al modified glass substrate with a monolayer consisting of a lipid and a PEG layer. The modified surfaces were effective in reducing platelet adhesion [182]. Snellings et al investigated protein

adsorption of PEG modified surfaces [183]. Surfaces were prepared by spin coating or chemisorption of PU-PEG or a copolymer of methylmethacrylate and PEG onto gold substrate. These surfaces were shown to be significantly protein resistant.

Several studies investigated the effect of chain density and chain length of PEG on protein adsorption. Grafting of PEG on TiO_2 showed that when ethylene glycol densities were above 15-20 EG/nm^2, very little protein adsorbed to the surfaces (less than 10ng/cm^2) [184]. Sofia et al modified silicon surfaces with PEGs of several molecular weights and densities and showed that with increasing grafting density of PEG, fibronectin and albumin adsorption were reduced and reached zero (below limit of detection) at a PEG density of ~100 ng/cm^2 [185]. They did not observe any dependence on PEG molecular weight in the range of 3400 to 20,000. They found, however, that a higher grafting density of the smaller PEGs was required for low protein adsorption. Unsworth et al studied the effect of chain length, chain density and end group of PEG on protein adsorption using gold as a model substrate. Hydroxy-terminated PEG performed better than methoxy-terminated PEG. Furthermore, the PEG chain density was found to play a more important role than the chain length in reducing Fg adsorption [186]. This study also concluded that there was an optimal chain density of PEG beyond which protein adsorption increased [187]. Archambault et al modified polyurethaneurea with hydroxyl- and amino-terminated PEGs of different chain lengths [188, 189]. The modified surfaces showed significant protein resistance, but no effect of protein size or charge on adsorption to the PEG surfaces was observed. As the chain length of PEG increased, protein adsorption decreased. The amino-terminated PEG surfaces showed

greater protein resistance than the hydroxyl-terminated PEG due to the higher PEG density. Chen et al modified a polyurethane substrate with monobenzyloxy PEG with PEG and monomethoxy PEG as fillers to increase PEG density [190]. They concluded that backfilling with PEG caused the monobenzyloxy PEG chains to stretch, and thus the benzyloxy end groups caused high protein adsorption on these surfaces. Gon et al attached poly L-lysine (PLL)- PEG copolymer on a silica surface that already contained PLL (cationic) patches [191]. They observed a threshold of cationic patch density below which the PEG could keep surfaces protein resistant. In a study by Dong et al, PEGs of different molecular weight ranging from 200 to 4600 were immobilized on polyethylene terephthalate [26]. PEG of MW 2000 gave the best surfaces in terms of antifouling properties. Others have tried to increase PEG surface density by using star (multi arm) PEGs [173, 185, 192]. Grafting of such PEGs has been done on poly(divinylbenzene), poly(vinylidene fluoride) and silicone and the surfaces showed reduced protein adsorption.

Recent studies have shown that despite low protein adsorption on surfaces modified with PEG and other protein resistant polymers, blood coagulation still occurs on these surfaces [167, 193] in some cases as rapidly as on the unmodified controls [167]. Thus it seems that protein resistance such as is conferred by PEG is not sufficient to achieve true blood compatibility. This realization has led to approaches based on bioactive molecules as surface modifiers or on combinations of bioactive and protein resistant molecules.

1.2.3.2 Surface Modification with Bioactive Molecules

Modification with bioactive molecules has the goal of creating surfaces that can promote specific interactions with the biological system. In the case of blood contact, anticoagulants such as heparin have been investigated extensively. As shown in Fig 1.14 and described in details in section 1.1.4 (section on the inhibition of blood coagulation: anticoagulants) of this literature review, heparin catalyzes the inhibition of thrombin and FXa by binding antithrombin.

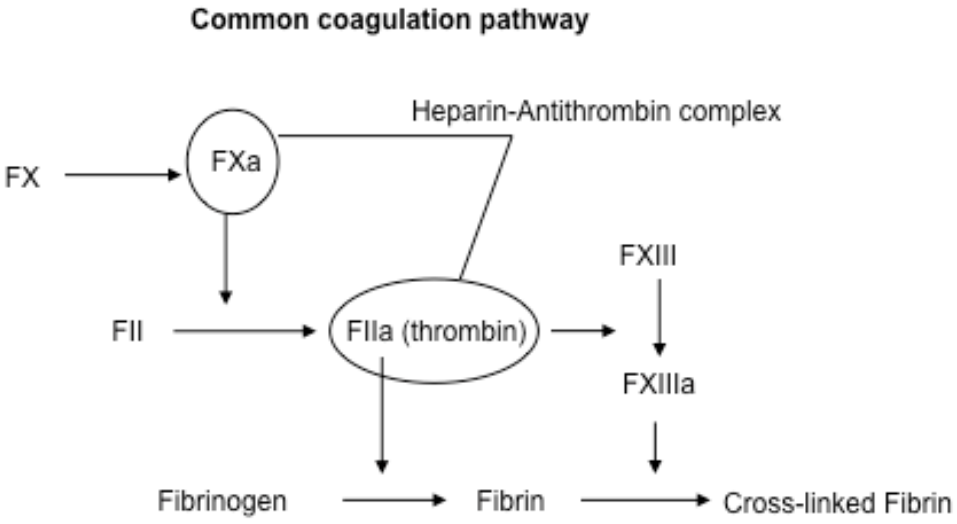

Figure 1. 14 Heparin-antithrombin complex inhibits thrombin and FXa.

Heparin has been used to modify a wide range of biomaterials and several chemistries have been used for surface attachment. Vinyl copolymers modified with heparin showed prolonged blood clotting times especially with poly(hydroxyethyl methacrylate) (HEMA) or polytetraethylene pentamine as spacer/linkers [194]. Polyurethane (PU) substrate was modified with heparin by several groups. Kang and

coworkers [195-197] modified PU surfaces by exposing it to oxygen plasma glow discharge and attached heparin through its amino or carboxyl groups. A higher heparin density was achieved when attachment was via the amino groups. Recently, Lin et al modified polyurethane membrane with heparin using low temperature plasma treatment and poly acrylic acid as a linker. The modified surfaces showed reduced platelet adhesion and prolonged coagulation time [198].

PolyHEMA was also modified with heparin in several studies. Bayramoglu et al grafted heparin on PolyHEMA hydrogels and showed an increase in prothrombin time for the grafted materials [199]. Heparinized polyHEMA microspheres with or without methacrylate polymers as linkers were prepared by Denizli et al. The heparinized microspheres showed longer plasma clotting times than the unmodified ones. The heparinized microspheres with no linker showed the longest clotting time due to a higher heparin density [200]. Duncan et al immobilized heparin on polyHEMA gel using glutaraldehyde as the linker and showed that the modified gels had improved anticoagulant properties [201]. A hydrogel network of polyHEMA and albumin prepared in tube form and coated with heparin, showed reduced platelet adhesion and fibrinogen adsorption compared to the uncoated material [199]. Stents and vascular grafts were modified by heparin in several studies [202-204]. The heparinized stents and vascular grafts generally showed improved anticoagulant properties compared with unmodified ones. Many other natural and synthetic polymers have been modified with heparin, and numerous studies are ongoing [205-211]. Heparin coating is currently used for commercially available medical devices such as stents, oxygenators and vascular grafts

[212-217]. Most of these commercially available devices are coated using the method developed by Larm et al [218]. These surfaces are referred to as Carmeda® BioActive Surfaces (CBAS).

Hirudin has also been used as for surface modification due to its anticoagulant properties and specific interactions with thrombin [219-224]. Berceli et al coated polyester grafts with hirudin and showed reduced local thrombin concentration in an in vitro assay under flow conditions [219]. Seifert et al modified poly(lactide glycolide) with hirudin and observed decreased platelet adhesion and activation on these surfaces. Furthermore, the hirudin-modified surfaces showed prolonged clotting time, similar to that for heparin-modified controls [220]. Phaneuf et al attached hirudin to polycarbonate-urethane and showed high thrombin binding on the modified surfaces [221, 223]. In another study by the same group, hirudin was immobilized on polyethylene terephthalate (Dacron) and high thrombin binding was observed [224]. Lahann et al coated nitinol coronary stents with functionalized poly(paracyclophane) and attached hirudin to the coating. Prolonged clotting times and decreased platelet adhesion were observed for the hirudin- treated stents [222].

Other bioactive molecules used for surface modification include antithrombin-heparin complex (ATH) and peptides with thrombin inhibitory properties. Du et al modified polyurethane catheters with ATH [225]. The modified catheters showed higher AT binding and anti-FXa activity compared with unmodified and heparin modified catheters. The ATH-modified catheters also performed better in an *in vivo* rabbit model [226]. Sun et al chemisorbed three peptides with N-terminal cysteine residues as thrombin

scavengers on gold-coated polyurethanes: Cys-Pro-Arg, Cys-(L)Phe-Pro-Arg, and Cys-(D)Phe-Pro-Arg. The peptide modified surface specifically bound and inhibited thrombin [227]. Martins et al synthesized a heparin binding dipeptide of L-lysine and L-leucine and immobilized it on layers of tetraethylene glycol on a gold substrate [228]. Increased heparin binding was observed on the modified surfaces.

Although all of the above-mentioned heparinized and other "anticoagulant" surfaces have been found to prolong clotting time, they do not prevent clotting ultimately. Indeed no surface has been found or developed which prevents coagulation. Thus "clot-lysing" surfaces capable of dissolving the clot once formed instead of preventing its formation have been proposed [229-236]. These surfaces are designed to capture the proteins of the fibrinolytic system in blood contact. Two key proteins of the fibrinolytic system are plasminogen and tissue plasminogen activator (tPA). Activation of plasminogen by tissue plasminogen activator results in the formation of plasmin. Plasmin degrades fibrin forming fibrin degradation products. A method of attracting plasminogen to blood contacting surfaces is the covalent attachment of lysine which has specific binding sites for plasminogen. In early work by Woodhouse, lysine was attached to polyurethane and the lysine-modified surfaces showed extensive plasminogen adsorption from plasma [229]. Lysine-modified silica glass showed similar behaviour [230]. In the presence of tissue plasminogen activator, the adsorbed plasminogen on the lysinized surfaces enhanced clot lysis [231]. Another approach to "clot lysing" surfaces is the use of lysine-rich coatings. McClung et al attached a coating of lysine-polyacrylamide covalently to a polyurethane substrate. The lysine moieties were attached via either the α-

amino or ε-amino group. With attachment through the α-amino group (ε-amino group free), the surfaces showed specific plasminogen affinity [232, 233]. In follow on work, it was shown that the surfaces with free ε-amino groups had high affinity towards tissue plasminogen activator. Although t-PA affinity was lower than that of plasminogen, surfaces with pre-adsorbed t-PA were able to dissolve blood clots formed around them after plasma contact [234]. In subsequent work, polyethylene tubing was modified with a lysine containing polymer. After exposure to tissue plasminogen activator, the modified surfaces were shown to be effective in dissolving thrombus in a whole blood Chandler Loop experiment [235]. Samoilova et al used the same strategy and modified polyethylene-polystyrene surfaces with polyelectrolyte complexes containing lysine [236]. The L-lysine modified surfaces showed high plasminogen affinity and reduced thrombogenicity in an *in vivo* assay.

1.2.3.3 Surface Modification for Combined Protein Resistance and Bioactivity

Recent research has focused on surfaces that are modified with both a bioactive molecule for specific interactions and an inert/protein resistant component to reduce non-specific interactions (Fig 1.15). The protein resistant molecule is usually an inert, hydrophilic polymer such as polyethylene glycol and the bioactive component, in the context of blood contacting materials, is usually an anticoagulant, a peptide or a protein that can either inhibit clot formation or lyse the clot.

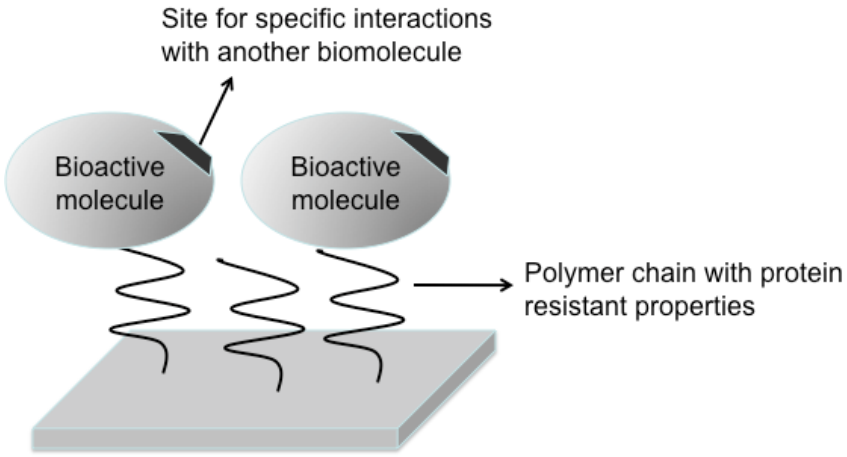

Figure 1. 15 Concept of bioactive, protein resistant surfaces. The protein resistant component is usually a hydrophilic, non-fouling polymer. The bioactive molecule can be an antibody, an enzyme, a protein, a peptide or a polysaccharide. In the context of blood compatibility, the bioactive component usually has anticoagulant or clot lysing properties.

Combinations of heparin and PEG have been used for this purpose. Kim and coworkers modified polyurethaneurea (PUU) surfaces to introduce free NCO groups. They then immobilized PEG and attached heparin. The PUU-PEG-heparin surfaces showed reduced protein adsorption and platelet adhesion *in vitro* compared with the control surfaces. The modified surfaces also showed prolonged occlusion time in an *ex vivo* rabbit shunt experiment [237, 238]. In another study, Kim and coworkers immobilized heparin on a styrene/p-amino styrene copolymer using a PEG spacer. These surfaces showed improved bioactivity in terms of antithrombin binding compared with surfaces prepared by direct immobilization of heparin [239]. Chen et al modified silicone with heparin through a PEG spacer. The modified surfaces showed high antithrombin binding and low fibrinogen adsorption [240]. Xu et al immobilized heparinized poly(oligoethylene glycol monomethacrylate) (poly(OEGMA) brushes on silicon using atom transfer radical polymerization (ATRP) [241]. These surfaces suppressed protein adsorption and platelet adhesion and increased clotting time. In other work heparin was

immobilized on a copolymer of poly(OEGMA) and poly(hydroxysuccinimidyl methacrylate) on silicon [242]. The modified surfaces showed significantly reduced fibrinogen adsorption but high antithrombin binding compared with the unmodified or polymer-only modified surfaces. Antithrombin-heparin complex (ATH) has also been used in combination with PEG. Gold so-modified was shown to be protein resistant and to have high antithrombin adsorption [243, 244].

To create a non-fouling clot lysing surface, a polyurethane was modified by sequential attachment of PEG and ε-amino-free lysine. These surfaces showed reduced non-specific protein adsorption and high plasminogen binding [245]. The effect of PEG chain length on the biological properties of the PEG-lysine surfaces was also investigated. In general PEG of lower chain length was shown to be more effective in terms of a balance of protein resistance, plasminogen adsorption and clot lysis [246]. Poly(dimethyl siloxane) (PDMS) was also modified with both PEG and lysine [247]. The modified surfaces showed reduced fibrinogen adsorption and dissolved clots formed around them after exposure to plasma and tissue plasminogen activator. Poly(hydroxyethyl methacrylate) (polyHEMA) as a protein resistant polymer, was also used in combination with lysine [248]. PolyHEMA was chosen to create surfaces with high hydroxyl functionality for lysine attachment and thus high lysine density. PolyHEMA was graft polymerized on a polyurethane substrate. The lysine-polyHEMA modified polyurethanes showed reduced non-specific protein adsorption and high plasminogen binding capacity.

All of the above-mentioned studies were focused on surface modification for improved blood compatibility relevant to this thesis. The combination of bioactive-

protein resistant molecules has been of interest for other biomedical applications such as biosensors, tissue engineering and protein purification. For example, RGD peptides were immobilized through PEG or poly(OEGMA) or a copolymer of poly(OEGMA) and poly(HEMA) to enhance cell adhesion [249-252]. Another example of this approach is the immobilization of biotin for biosensor applications. This has been done on silicon through poly(ethylene glycol methyl ether methacrylate) (PEGMA), 3-(trimethoxysilyl)propyl methacrylate (TMSMA) and N-acryloxysuccinimide (NAS), or on glass through PEG or on gold through poly(ethylene glycol monomethacrylate) [253-255]. Anticancer drugs were also immobilized on nanoparticles through a PEG spacer with applications in targeted tumor drug delivery [256, 257].

The literature reviewed in this section shows that surfaces with bioactive and protein resistant molecules can be effective in improving blood compatibility. More research in this area, however, is crucial to address outstanding issues such as identification of the optimal ratio of the two components and others. The research reported in this thesis represents attempts to resolve some of these issues.

1.3 References

[1] Williams DF. On the nature of biomaterials. Biomaterials 2009;30:5897-909.
[2] Ratner BD. New Ideas in Biomaterials Science - a Path to Engineered Biomaterials. J Biomed Mater Res 1993;27:837-50.
[3] Williams DF. On the mechanisms of biocompatibility. Biomaterials 2008;29:2941-53.
[4] Muller B. Tailoring biocompatibility: Benefitting patients. Mater Today 2010;13:58-.
[5] Ratner BD, Bryant SJ. Biomaterials: Where we have been and where we are going. Annu Rev Biomed Eng 2004;6:41-75.
[6] Anderson JM, Rodriguez A, Chang DT. Foreign body reaction to biomaterials. Semin Immunol 2008;20:86-100.
[7] Brash JL, Tenhove P. Protein Adsorption Studies on Standard Polymeric Materials. J Biomater Sci Polym Ed 1993;4:591-9.

[8] Courtney JM, Forbes CD. Thrombosis on Foreign Surfaces. Br Med Bull 1994;50:966-81.
[9] Gorbet MB, Sefton MV. Biomaterial-associated thrombosis: roles of coagulation factors, complement, platelets and leukocytes. Biomaterials 2004;25:5681-703.
[10] Courtney JM, Lamba NMK, Sundaram S, Forbes CD. Biomaterials for Blood-Contacting Applications. Biomaterials 1994;15:737-44.
[11] Du H, Chandaroy P, Hui SW. Grafted poly-(ethylene glycol) on lipid surfaces inhibits protein adsorption and cell adhesion. Biochim Biophys Acta-Biomembr 1997;1326:236-48.
[12] Steinberg J, Neumann AW, Absolom DR, Zingg W. Human-Erythrocyte Adhesion and Spreading on Protein-Coated Polymer Surfaces. J Biomed Mater Res 1989;23:591-610.
[13] Barbosa JN, Martins MCL, Freitas SC, Goncalves IC, Aguas AP, Barbosa MA. Adhesion of human leukocytes on mixtures of hydroxyl- and methyl-terminated self-assembled monolayers: Effect of blood protein adsorption. J Biomed Mater Res A 2009;93A:12-9.
[14] Barbosa JN, Barbosa MA, Aguas AP. Inflammatory responses and cell adhesion to self-assembled monolayers of alkanethiolates on gold. Biomaterials 2004;25:2557-63.
[15] Anderson JM. Biological responses to materials. Ann Rev Mater Res 2001;31:81-110.
[16] Hamad OA, Nilsson PH, Wouters D, Lambris JD, Ekdahl KN, Nilsson B. Complement Component C3 Binds to Activated Normal Platelets without Preceding Proteolytic Activation and Promotes Binding to Complement Receptor 1. J Immunol;184:2686-92.
[17] Petsko GAR, D.,. Protein structure and function. 2004.
[18] Petsko GA. Protein structure and function: London : New Science Press ; Sunderland, MA : Sinauer Associates ; Oxford : Blackwell Pub.; 2004.
[19] Norde W. Driving forces for protein adsorption at solid surfaces. In: Biopolymers at interfaces. Malmsten M. (editor). 2nd ed: New York : Marcel Dekker; 2003.
[20] Schmidt DR, Waldeck H, Kao WJ. Protein adsorption on biomaterials in Biological Interactions on Materials Surfaces: Understanding and Controlling protein, Cell, and Tissue Responses. Editors: Puleo, D.A. and Bizios, R.: Springer Science+Business Media, LLC 2009; 2009.
[21] Andrade JD. Principles of protein adsorption. In: Surface and interfacial aspects of biomedical polymers. Andrade JD (Editor). New York : Plenum Press.; 1985.
[22] Gray JJ. The interaction of proteins with solid surfaces. Curr Opin Struct Biol 2004;14:110-5.
[23] Barnthip N, Noh H, Leibner E, Vogler EA. Volumetric interpretation of protein adsorption: Kinetic consequences of a slowly-concentrating interphase. Biomaterials 2008;29:3062-74.
[24] Dee KC, Puleo DA, Bizios R. Protein-surface interactions. In: Dee KC, Puleo DA, Bizios R, editors. An introduction to tissue-biomaterial interactions.: Hoboken, NJ: John Wiley and Sons.; 2002.

[25] Horbett TA. The role of adsorbed proteins in tissue response to biomaterials . In: Ratner BD , Hoffman AS ,
Schoen FJ , Lemons JE , editors. Biomaterials science. An introduction to materials in medicine . : San Diego :Elsevier Academic Press; 2004.
[26] Dong BY, Manolache S, Wong ACL, Denes FS. Antifouling ability of polyethylene glycol of different molecular weights grafted onto polyester surfaces by cold plasma. Polym Bull 2011;66:517-28.
[27] Rechendorff K, Hovgaard MB, Foss M, Zhdanov VP, Besenbacher F. Enhancement of protein adsorption induced by surface roughness. Langmuir 2006;22:10885-8.
[28] Tie Y, Calonder C, Van Tassel PR. Protein adsorption: Kinetics and history dependence. J Colloid Interface Sci 2003;268:1-11.
[29] Young BR, Pitt WG, Cooper SL. Protein Adsorption on Polymeric Biomaterials .2. Adsorption-Kinetics. J Colloid Interface Sci 1988;125:246-60.
[30] Norde W, Haynes CA. Reversibility and the mechanism of protein adsorption. In: Proteins at interfaces II: fudamentals and applications. Horbett T.A. and Brash J.L. (eds): American Chemical Society; 1995.
[31] Andrade JD, Hlady V. Protein Adsorption and Materials Biocompatibility - a Tutorial Review and Suggested Hypotheses. Adv Polym Sci 1986;79:1-63.
[32] Young BR, Pitt WG, Cooper SL. Protein Adsorption on Polymeric Biomaterials .1. Adsorption-Isotherms. J Colloid Interface Sci 1988;124:28-43.
[33] Lundstrom I. Models of Protein Adsorption on Solid-Surfaces. Prog Colloid Polym Sci 1985;70:76-82.
[34] Katira P, Agarwal A, Hess H. A Random Sequential Adsorption Model for Protein Adsorption to Surfaces Functionalized with Poly(ethylene oxide). Adv Mater 2009;21:1599-+.
[35] Mulheran PA, Pellenc D, Bennett RA, Green RJ, Sperrin M. Mechanisms and dynamics of protein clustering on a solid surface. Phys Rev Lett 2008;100.
[36] Aggarwal N, Lawson K, Kershaw M, Horvath R, Ramsden J. Protein adsorption on heterogeneous surfaces. Appl Phys Lett 2009;94.
[37] Ramsden J. Protein adsorption kinetics. In: Biopolymers at interfaces. Malmsten M. (editor). 2nd ed: New York : Marcel Dekker; 2003.
[38] Tilton RD. Protein adsorption kinetics. In: Biopolymers at interfaces. Malmsten M. (editor). 2nd ed: New York : Marcel Dekker; 2003.
[39] Mavropoulos E, Costa AM, Costa LT, Achete CA, Mello A, Granjeiro JM, et al. Adsorption and bioactivity studies of albumin onto hydroxyapatite surface. Colloids Surf B 2011;83:1-9.
[40] Bozgeyik K, Kopac T. Adsorption of Bovine Serum Albumin onto Metal Oxides: Adsorption Equilibrium and Kinetics onto Alumina and Zirconia. Int J Chem Reactor Eng 2010;8.
[41] Johnson RD, Arnold FH. The Temkin Isotherm Describes Heterogeneous Protein Adsorption. Biochim Biophys Acta-Protein Struct Molec Enzym 1995;1247:293-7.
[42] Aeimbhu A, Castle JE, Singjai P. Accounting for the size of molecules in determination of adsorption isotherms by XPS; exemplified by adsorption of chicken egg albumin on titanium. Surf Interface Anal 2005;37:1127-36.

[43] Yang CH. Statistical-Mechanical Aspects of Adsorption Systems Obeying the Temkin Isotherm. J Phys Chem 1993;97:7097-101.
[44] Barnthip N, Parhi P, Golas A, Vogler EA. Volumetric interpretation of protein adsorption: Kinetics of protein-adsorption competition from binary solution. Biomaterials 2009;30:6495-513.
[45] Noh H, Vogler EA. Volumetric interpretation of protein adsorption: Competition from mixtures and the Vroman effect. Biomaterials 2007;28:405-22.
[46] Krishnan A, Siedlecki CA, Vogler EA. Mixology of protein solutions and the Vroman effect. Langmuir 2004;20:5071-8.
[47] Leonard EF, Vroman L. Is the Vroman Effect of Importance in the Interaction of Blood with Artificial Materials. J Biomater Sci Polym Ed 1991;3:95-107.
[48] Brash JL, Scott CF, Tenhove P, Wojciechowski P, Colman RW. Mechanism of Transient Adsorption of Fibrinogen from Plasma to Solid-Surfaces - Role of the Contact and Fibrinolytic Systems. Blood 1988;71:932-9.
[49] Jung IK, Bae JW, Choi WS, Choi JH, Park KD. Surface Graft Polymerization of Poly(ethylene glycol) Methacrylate onto Polyurethane via Thiol-Ene Reaction: Preparation and Characterizations. J Biomater Sci Polym Ed 2009;20:1473-82.
[50] Monroe DM, Hoffman M. What does it take to make the perfect clot? Arterioscler Thromb Vasc Biol 2006;26:41-8.
[51] Vogler EA, Graper JC, Harper GR, Sugg HW, Lander LM, Brittain WJ. Contact Activation of the Plasma Coagulation Cascade .1. Procoagulant Surface-Chemistry and Energy. J Biomed Mater Res 1995;29:1005-16.
[52] Mitropoulos KA. High affinity binding of factor XIIa to an electronegative surface controls the rates of factor XII and prekallikrein activation in vitro. Thromb Res 1999;94:117-29.
[53] Mitropoulos KA. The levels of factor XIIa generated in human plasma on an electronegative surface are insensitive to wide variation in the concentration of FXII, prekallikrein, high molecular weight kininogen or FXI. Thromb Haemost 1999;82:1033-40.
[54] Zhuo R, Siedlecki CA, Vogler EA. Autoactivation of blood factor XII at hydrophilic and hydrophobic surfaces. Biomaterials 2006;27:4325-32.
[55] Vogler EA. Water and the acute biological response to surfaces. J Biomater Sci Polym Ed 1999;10:1015-45.
[56] Vogler EA, Siedlecki CA. Contact activation of blood-plasma coagulation. Biomaterials 2009;30:1857-69.
[57] Cool DE, Edgell CJS, Macgillivray RTA. Characterization of Human Factor-Xii Cdna. Thromb Haemost 1985;54:120-.
[58] Cool DE, Macgillivray RTA. Characterization of the Human Factor-Xii Gene. Thromb Haemost 1987;58:1-.
[59] Colman RW, Schmaier AH. Contact system: A vascular biology modulator with anticoagulant, Profibrinolytic, antiadhesive, and proinflammatory attributes. Blood 1997;90:3819-43.
[60] McMullen BA, Fujikawa K. Amino-Acid Sequence of the Heavy-Chain of Human Alpha-Factor-Xiia (Activated Hageman-Factor). J Biol Chem 1985;260:5328-41.

[61] Becker RC, Spencer FA. Thrombin: Structure, biochemistry, measurement, and status in clinical medicine. J Thromb Thrombolysis 1998;5:215-29.
[62] Bode W. Structure and interaction modes of thrombin. Blood Cells Mol Dis 2006;36:122-30.
[63] Wolberg AS. Thrombin generation and fibrin clot structure. Blood Rev 2007;21:131-42.
[64] Hongbao M, Young J, Shen C. Thrombin. Nat Sci 2008;6:90-3.
[65] Tapparelli C, Metternich R, Cook NS. Structure and Function of Thrombin Receptors. Trends Pharmacol Sci 1993;14:426-8.
[66] Feng L, Andrade JD. Structure and adsorption properties of fibrinogen, in: Proteins at interfaces II: fundamentals and applications, Horbet, T.A. and Brash, J.L. (eds.)1995.
[67] Doolittle RF. X-ray crystallographic studies on fibrinogen and fibrin. J Thromb Haemost 2003;1:1559-65.
[68] Wu YG, Simonovsky FI, Ratner BD, Horbett TA. The role of adsorbed fibrinogen in platelet adhesion to polyurethane surfaces: A comparison of surface hydrophobicity, protein adsorption, monoclonal antibody binding, and platelet adhesion. J Biomed Mater Res A 2005;74A:722-38.
[69] Tsai WB, Grunkemeier JM, Horbett TA. Human plasma fibrinogen adsorption and platelet adhesion to polystyrene. J Biomed Mater Res 1999;44:130-9.
[70] Sivaraman B, Latour RA. The relationship between platelet adhesion on surfaces and the structure versus the amount of adsorbed fibrinogen. Biomaterials;31:832-9.
[71] Shen MC, Horbett TA. The effects of surface chemistry and adsorbed proteins on monocyte/macrophage adhesion to chemically modified polystyrene surfaces. J Biomed Mater Res 2001;57:336-45.
[72] Hu WJ, Eaton JW, Tang LP. Molecular basis of biomaterial-mediated foreign body reactions. Blood 2001;98:1231-8.
[73] Brodbeck WG, Colton E, Anderson JM. Effects of adsorbed heat labile serum proteins and fibrinogen on adhesion and apoptosis of monocytes/macrophages on biomaterials. J Mater Sci-Mater Med 2003;14:671-5.
[74] Rabenstein DL. Heparin and heparan sulfate: structure and function. Nat Prod Rep 2002;19:312-31.
[75] Weitz JI. Low-molecular-weight heparins. N Engl J Med 1997;337:688-98.
[76] Weitz DS, Weitz JI. Update on heparin: what do we need to know? J Thromb Thrombolysis 2010;29:199-207.
[77] CatellaLawson F. Direct thrombin inhibitors in cardiovascular disease. Coronary Artery Dis 1997;8:105-11.
[78] Weitz JI, Hudoba M, Massel D, Maraganore J, Hirsh J. Clot-Bound Thrombin Is Protected from Inhibition by Heparin-Antithrombin-Iii but Is Susceptible to Inactivation by Antithrombin-Iii-Independent Inhibitors. J Clin Invest 1990;86:385-91.
[79] Kettner C, Shaw E. D-Phe-Pro-Argch2c1-a Selective Affinity Label for Thrombin. Thromb Res 1979;14:969-73.
[80] Potzsch B, Muller J, Rox JM. Developmental strategies of novel anticoagulants. Transfusion Med Hemotherapy 2006;33:200-4.

[81] Szyperski T, Guntert P, Stone SR, Wuthrich K. Nuclear-Magnetic-Resonance Solution Structure of Hirudin(1-51) and Comparison with Corresponding 3-Dimensional Structures Determined Using the Complete 65-Residue Hirudin Polypeptide-Chain. J Mol Biol 1992;228:1193-205.
[82] Grutter MG, Priestle JP, Rahuel J, Grossenbacher H, Bode W, Hofsteenge J, et al. Crystal-Structure of the Thrombin Hirudin Complex - a Novel Mode of Serine Protease Inhibition. Embo J 1990;9:2361-5.
[83] Markwardt F. Hirudin - the Promising Antithrombotic. Cardiovasc Drug Rev 1992;10:211-32.
[84] Skrzypczak-Jankun E, Carperos VE, Ravichandran KG, Tulinsky A, Westbrook M, Maraganore JM. Structure of the hirugen and hirulog 1 complexes of [alpha]-thrombin. J Mol Biol 1991;221:1379-93.
[85] Chang JY. The Hirudin-Binding Site of Human Alpha-Thrombin - Identification of Lysyl Residues Which Participate in the Combining Site of Hirudin-Thrombin Complex. J Biol Chem 1989;264:7141-6.
[86] Electricwala A, Hartwell R, Scawen MD, Atkinson T. The Complete Amino-Acid-Sequence of a Hirudin Variant from the Leech Hirudinaria-Manillensis. J Protein Chem 1993;12:365-70.
[87] Chen ZG, Li Y, Mulichak AM, Lewis SD, Shafer JA. Crystal-Structure of Human Alpha-Thrombin Complexed with Hirugen and P-Amidinophenylpyruvate at 1.6 Angstrom Resolution. Arch Biochem Biophys 1995;322:198-203.
[88] Gladwell TD. Bivalirudin: A direct thrombin inhibitor. Clin Ther 2002;24:38-58.
[89] Skrzypczakjankun E, Carperos VE, Ravichandran KG, Tulinsky A, Westbrook M, Maraganore JM. Structure of the Hirugen and Hirulog-1 Complexes of Alpha-Thrombin. Journal of Molecular Biology 1991;221:1379-93.
[90] Mahoney WC, Hermodson MA, Jones B, Powers DD, Corfman RS, Reeck GR. Amino-Acid-Sequence and Secondary Structural-Analysis of the Corn Inhibitor of Trypsin and Activated Hageman-Factor. J Biol Chem 1984;259:8412-6.
[91] Chong GL, Reeck GR. Interaction of Trypsin, Beta-Factor-Xiia, and Plasma Kallikrein with Trypsin-Inhibitor Isolated from Barley-Seeds - a Comparison with the Corn Inhibitor of Activated Hageman-Factor. Thromb Res 1987;48:211-21.
[92] Pedersen LC, Yee VC, Vondassow G, Hazeghazam M, Reeck GR, Stenkamp RE, et al. The Corn Inhibitor of Blood-Coagulation Factor Xiia - Crystallization and Preliminary Crystallographic Analysis. J Mol Biol 1994;236:385-7.
[93] Behnke CA, Yee VC, Le Trong I, Pedersen LC, Stenkamp RE, Kim SS, et al. Structural determinants of the bifunctional corn Hageman factor inhibitor: X-ray crystal structure at 1.95 angstrom resolution. Biochemistry 1998;37:15277-88.
[94] Hazegh-Azam M, Kim SS, Masoud S, Andersson L, White F, Johnson L, et al. The corn inhibitor of activated hageman factor: Purification and properties of two recombinant forms of the protein. Protein Expr Purif 1998;13:143-9.
[95] Swartz MJ, Mitchell HL, Cox DJ, Reeck GR. Isolation and Characterization of Trypsin-Inhibitor from Opaque-2 Corn Seeds. J Biol Chem 1977;252:8105-7.
[96] Rand MD, Lock JB, vantVeer C, Gaffney DP, Mann KG. Blood clotting in minimally altered whole blood. Blood 1996;88:3432-45.

[97] Mann KG, Whelihan MF, Butenas S, Orfeo T. Citrate anticoagulation and the dynamics of thrombin generation. J Thromb Haemost 2007;5:2055-61.
[98] Dargaud Y, Luddington R, Baglin TP. Elimination of contact factor activation improves measurement of platelet-dependent thrombin generation by calibrated automated thrombography at low-concentration tissue factor. J Thromb Haemost 2006;4:1160-1.
[99] Yau JW, Stafford AR, Fredenburgh JC, Brash JL, Weitz JI. Immobilization of corn trypsin inhibitor on a catheter surface reduces its in vitro procoagulant properties. San Antonio, TX: Annual Meeting, Society for Biomaterials; April 2009.
[100] Yau JW. Immobilization of corn trypsin inhibitor attenuates the procoagulant activity of catheter surfaces: McMaster University; 2009.
[101] Colman RW. Hemostasis and thrombosis : basic principles and clinical practice Philadelphia, PA : Lippincott Williams & Wilkins; 2006.
[102] Ruggeri ZM, Mendolicchio GL. Adhesion mechanisms in platelet function. CircRes 2007;100:1673-85.
[103] Savage B, Saldivar E, Ruggeri ZM. Initiation of platelet adhesion by arrest onto fibrinogen or translocation on von Willebrand factor. Cell 1996;84:289-97.
[104] Nieswandt B, Watson SP. Platelet-collagen interaction: is GPVI the central receptor? Blood 2003;102:449-61.
[105] Smith O. Weathering the big chill. Science 2003;299:530-.
[106] Wagner DD, Burger PC. Platelets in inflammation and thrombosis. Arterioscler Thromb Vasc Biol 2003;23:2131-7.
[107] Grunkemeier JM, Tsai WB, Horbett TA. Co-adsorbed fibrinogen and von Willebrand factor augment platelet procoagulant activity and spreading. J Biomater Sci Polym Ed 2001;12:1-20.
[108] Tsai WB, Grunkemeier JM, McFarland CD, Horbett TA. Platelet adhesion to polystyrene-based surfaces preadsorbed with plasmas selectively depleted in fibrinogen, fibronectin, vitronectin, or von Willebrand's factor. J Biomed Mater Res 2002;60:348-59.
[109] Rand ML, Packham MA, Taylor DM, Yeo EL, Gemmell CH, Patil S, et al. The fibrinogen gamma chain dodecapeptide inhibits agonist-induced aggregation of rabbit platelets and fibrinogen binding to rabbit glycoprotein IIb-IIIa. Thromb Haemost 1999;82:1680-6.
[110] Weeterings C, Adelmeijer J, Myles T, de Groot PG, Lisman T. Glycoprotein Ib alpha-mediated platelet adhesion and aggregation to immobilized thrombin under conditions of flow. Arterioscler Thromb Vasc Biol 2006;26:670-5.
[111] Jackson SP. The growing complexity of platelet aggregation. Blood 2007;109:5087-95.
[112] Ferretti S, Paynter S, Russell DA, Sapsford KE, Richardson DJ. Self-assembled monolayers: a versatile tool for the formulation of bio-surfaces. Trac-Trends Anal Chem 2000;19:530-40.
[113] Nuzzo RG, Fusco FA, Allara DL. Spontaneously Organized Molecular Assemblies .3. Preparation and Properties of Solution Adsorbed Monolayers of Organic Disulfides on Gold Surfaces. J Am Chem Soc 1987;109:2358-68.

[114] Biener MM, Biener J, Friend CM. Revisiting the S-Au(111) interaction: Static or dynamic? Langmuir 2005;21:1668-71.
[115] Paik WK, Eu S, Lee K, Chon S, Kim M. Electrochemical reactions in adsorption of organosulfur molecules on gold and silver: Potential dependent adsorption. Langmuir 2000;16:10198-205.
[116] Sellers H, Ulman A, Shnidman Y, Eilers JE. Structure and Binding of Alkanethiolates on Gold and Silver Surfaces - Implications for Self-Assembled Monolayers. J Am Chem Soc 1993;115:9389-401.
[117] Ulman A. Formation and structure of self-assembled monolayers. chem Rev 1996;96:1533-54.
[118] Love JC, Estroff LA, Kriebel JK, Nuzzo RG, Whitesides GM. Self-assembled monolayers of thiolates on metals as a form of nanotechnology. chem Rev 2005;105:1103-69.
[119] Boncheva M, Bruzewicz DA, Whitesides GM. Millimeter-scale self-assembly and its applications. Pure Appl Chem 2003;75:621-30.
[120] Mrksich M, Whitesides GM. Patterning Self-Assembled Monolayers Using Microcontact Printing - a New Technology for Biosensors. Trends Biotechnol 1995;13:228-35.
[121] Troughton EB, Bain CD, Whitesides GM, Nuzzo RG, Allara DL, Porter MD. Monolayer Films Prepared by the Spontaneous Self-Assembly of Symmetrical and Unsymmetrical Dialkyl Sulfides from Solution onto Gold Substrates - Structure, Properties, and Reactivity of Constituent Functional-Groups. Langmuir 1988;4:365-85.
[122] Vericat C, Vela ME, Benitez GA, Gago JAM, Torrelles X, Salvarezza RC. Surface characterization of sulfur and alkanethiol self-assembled monolayers on Au(111). J Phys-Condes Matter 2006;18:R867-R900.
[123] Vericat C, Vela ME, Benitez G, Carro P, Salvarezza RC. Self-assembled monolayers of thiols and dithiols on gold: new challenges for a well-known system. Chem Soc Rev 2010;39:1805-34.
[124] Ron H, Matlis S, Rubinstein I. Self-assembled monolayers on oxidized metals. 2. Gold surface oxidative pretreatment, monolayer properties, and depression formation. Langmuir 1998;14:1116-21.
[125] Benitez G, Vericat C, Tanco S, Lenicov FR, Castez MF, Vela AE, et al. Role of surface heterogeneity and molecular interactions in the charge-transfer process through self-assembled thiolate monolayers on Au(111). Langmuir 2004;20:5030-7.
[126] Gomez-Carrillo SC, Bolcatto PG. Coexistence of root 3 x root 3 and quasi-linear phases of sulfur adsorbed (Theta=1/3) on a gold (111) substrate. Phys Chem Chem Phys 2011;13:461-6.
[127] Smith T. The hydrophilic nature of a clean gold surface. J Colloid Interface Sci 1980;75:51-5.
[128] Dubois LH, Zegarski BR, Nuzzo RG. Molecular Ordering of Organosulfur Compounds on Au(111) and Au(100) - Adsorption from Solution and in Ultrahigh-Vacuum. J Chem Phys 1993;98:678-88.
[129] Yu M, Ascolani H, Zampieri G, Woodruff DP, Satterley CJ, Jones RG, et al. The structure of atomic sulfur phases on Au(111). J Phys Chem C 2007;111:10904-14.

[130] Chidsey CED, Liu GY, Rowntree P, Scoles G. Molecular Order at the Surface of an Organic Monolayer Studied by Low-Energy Helium Diffraction. J Chem Phys 1989;91:4421-3.
[131] Badia A, Lennox RB, Reven L. A dynamic view of self-assembled monolayers. Accounts Chem Res 2000;33:475-81.
[132] Prime KL, Whitesides GM. Self-Assembled Organic Monolayers - Model Systems for Studying Adsorption of Proteins at Surfaces. Science 1991;252:1164-7.
[133] Gooding JJ, Mearns F, Yang WR, Liu JQ. Self-assembled monolayers into the 21(st) century: Recent advances and applications. Electroanalysis 2003;15:81-96.
[134] Tokumitsu S, Liebich A, Herrwerth S, Eck W, Himmelhaus M, Grunze M. Grafting of alkanethiol-terminated poly(ethylene glycol) on gold. Langmuir 2002;18:8862-70.
[135] Singh N, Cui X, Boland T, Husson SM. The role of independently variable grafting density and layer thickness of polymer nanolayers on peptide adsorption and cell adhesion. Biomaterials 2007;28:763-71.
[136] Yeh PYJ, Kainthan RK, Zou YQ, Chiao M, Kizhakkedathu JN. Self-assembled monothiol-terminated hyperbranched polyglycerols on a gold surface: A comparative study on the structure, morphology, and protein adsorption characteristics with linear poly(ethylene glycol)s. Langmuir 2008;24:4907-16.
[137] Estes GM, Seymour RW, Cooper SL. Infrared Studies of Segmented Polyurethane Elastomers. II. Infrared Dichroism. Macromolecules 1971;4:452-8.
[138] Zdrahala RJ, Zdrahala IJ. Biomedical applications of polyurethanes: A review of past promises, present realities, and a vibrant future. J Biomater Applications 1999;14:67-90.
[139] Hentschel T, Munstedt H. Thermoplastic polyurethane - The material used for the Erlanger silver catheter. Infection 1999;27:S43-S5.
[140] Grenier S, Sandig M, Mequanint K. Polyurethane biomaterials for fabricating 3D porous scaffolds and supporting vascular cells. J Biomed Mater Res A 2007;82A:802-9.
[141] Adhikari R, Gunatillake PA, Griffiths I, Tatai L, Wickramaratna M, Houshyar S, et al. Biodegradable injectable polyurethanes: Synthesis and evaluation for orthopaedic applications. Biomaterials 2008;29:3762-70.
[142] Besteiro MC, Guiomar AJ, Goncalves CA, Bairos VA, de Pinho MN, Gil H. Characterization and in vitro hemocompatibility of bi-soft segment, polycaprolactone-based poly(ester urethane urea) membranes. J Biomed Mater Res A 2010;93A:954-64.
[143] Wang DA, Feng LX, Ji J, Sun YH, Zheng XX, Elisseeff JH. Novel human endothelial cell-engineered polyurethane biomaterials for cardiovascular biomedical applications. J Biomed Mater Res A 2003;65A:498-510.
[144] Lamba N.M.K. WKA, Cooper S.L. Polyurethanes in biomedical applications: Boca Raton : CRC Press; 1998.
[145] Huang Y, Lu XY, Qian WP, Tang ZM, Zhong YP. Competitive protein adsorption on biomaterial surface studied with reflectometric interference spectroscopy. Acta Biomater 2010;6:2083-90.
[146] Xu L-C, Runt J, Siedlecki CA. Dynamics of hydrated polyurethane biomaterials: Surface microphase restructuring, protein activity and platelet adhesion. Acta Biomater 2010;6:1938-47.

[147] Xu LC, Siedlecki CA. Microphase separation structure influences protein interactions with poly(urethane urea) surfaces. J Biomed Mater Res A 2009;92A:126-36.
[148] Zheng J, Song W, Huang H, Chen H. Protein adsorption and cell adhesion on polyurethane/Pluronic (R) surface with lotus leaf-like topography. Colloids and Surfaces B-Biointerfaces 2010;77:234-9.
[149] Lee JH, Ju YM, Kim DM. Platelet adhesion onto segmented polyurethane film surfaces modified by addition and crosslinking of PEO-containing block copolymers. Biomaterials 2000;21:683-91.
[150] Tan J, Brash JL. Nonfouling biomaterials based on polyethylene oxide-containing amphiphilic triblock copolymers as surface modifying additives: Solid state structure of PEO-copolymer/polyurethane blends. J Biomed Mater Res A 2008;85A:862-72.
[151] Tan J, Brash JL. Nonfouling biomaterials based on polyethylene oxide-containing amphiphilic triblock copolymers as surface modifying additives: Synthesis and characterization of copolymers and surface properties of copolymer-polyurethane blends. J Appl Polym Sci 2008;108:1617-28.
[152] Alibeik S, Sheardown H, Rizkalla AS, Mequanint K. Protein adsorption and platelet adhesion onto ion-containing polyurethanes. J Biomater Sci Polym Ed 2007;18:1195-210.
[153] Skarja GA, Brash JL. Physicochemical properties and platelet interactions of segmented polyurethanes containing sulfonate groups in the hard segment. J Biomed Mater Res 1997;34:439-55.
[154] Chen KY, Kuo JF, Chen CY. Synthesis, characterization and platelet adhesion studies of novel ion-containing aliphatic polyurethanes. Biomaterials 2000;21:161-71.
[155] Hasirci N, Aksoy EA. Synthesis and modifications of polyprethanes for biomedical purposes. High Perform Polym 2007;19:621-37.
[156] Archambault JG, Brash JL. Protein repellent polyurethane-urea surfaces by chemical grafting of hydroxyl-terminated poly(ethylene oxide): effects of protein size and charge. Colloids Surf B 2004;33:111-20.
[157] Shen MC, Martinson L, Wagner MS, Castner DG, Ratner BD, Horbett TA. PEO-like plasma polymerized tetraglyme surface interactions with leukocytes and proteins: in vitro and in vivo studies. J Biomater Sci Polym Ed 2002;13:367-90.
[158] Brash JL. Exploiting the current paradigm of blood-material interactions for the rational design of blood-compatible materials. J Biomater Sci Polym Ed 2000;11:1135-46.
[159] Shen MC, Pan YV, Wagner MS, Hauch KD, Castner DG, Ratner BD, et al. Inhibition of monocyte adhesion and fibrinogen adsorption on glow discharge plasma deposited tetraethylene glycol dimethyl ether. J Biomater Sci Polym Ed 2001;12:961-78.
[160] Chang Y, Chen SF, Zhang Z, Jiang SY. Highly protein-resistant coatings from well-defined diblock copolymers containing sulfobetaines. Langmuir 2006;22:2222-6.
[161] Zhang Z, Chen SF, Jiang SY. Dual-functional biomimetic materials: Nonfouling poly(carboxybetaine) with active functional groups for protein immobilization. Biomacromolecules 2006;7:3311-5.
[162] Zhang Z, Chen SF, Chang Y, Jiang SY. Surface grafted sulfobetaine polymers via atom transfer radical polymerization as superlow fouling coatings. J Phys Chem B 2006;110:10799-804.

[163] Feng W, Brash JL, Zhu SP. Non-biofouling materials prepared by atom transfer radical polymerization grafting of 2-methacryloloxyethyl phosphorylcholine: Separate effects of graft density and chain length on protein repulsion. Biomaterials 2006;27:847-55.
[164] Jin ZL, Feng W, Zhu SP, Sheardown H, Brash JL. Protein-resistant polyurethane via surface-initiated atom transfer radical polymerization of oligo(ethylene glycol) methacrylate. J Biomed Mater Res A 2009;91A:1189-201.
[165] Osterberg E, Bergstrom K, Holmberg K, Schuman TP, Riggs JA, Burns NL, et al. Protein-Rejecting Ability of Surface-Bound Dextran in End-on and Side-on Configurations - Comparison to Peg. J Biomed Mater Res 1995;29:741-7.
[166] Nojiri C, Okano T, Jacobs HA, Park KD, Mohammad SF, Olsen DB, et al. Blood Compatibility of Peo Grafted Polyurethane and Hema Styrene Block Copolymer Surfaces. J Biomed Mater Res 1990;24:1151-71.
[167] Zhang Z, Zhang M, Chen SF, Horbetta TA, Ratner BD, Jiang SY. Blood compatibility of surfaces with superlow protein adsorption. Biomaterials 2008;29:4285-91.
[168] Lee JH, Lee HB, Andrade JD. Blood Compatibility of Polyethylene Oxide Surfaces. Prog Polym Sci 1995;20:1043-79.
[169] Kingshott P, Thissen H, Griesser HJ. Effects of cloud-point grafting, chain length, and density of PEG layers on competitive adsorption of ocular proteins. Biomaterials 2002;23:2043-56.
[170] Pasut G, Veronese FM. Polymer-drug conjugation, recent achievements and general strategies. Prog Polym Sci 2007;32:933-61.
[171] Thompson MS, Vadala TP, Vadala ML, Lin Y, Riffle JS. Synthesis and applications of heterobifunctional poly(ethylene oxide) oligomers. Polymer 2008;49:345-73.
[172] Pasut G, Veronese FM. PEGylation of proteins as tailored chemistry for optimized bioconjugates. Polymer Therapeutics I: Polymers as Drugs, Conjugates and Gene Delivery Systems2006. p. 95-134.
[173] Gasteier P, Reska A, Schulte P, Salber J, Offenhausser A, Moeller M, et al. Surface grafting of PEO-Based star-shaped molecules for bioanalytical and biomedical applications. Macromol Sci 2007;7:1010-23.
[174] Unsworth LD, Tun Z, Sheardown H, Brash JL. Chemisorption of thiolated poly(ethylene oxide) to gold: surface chain densities measured by ellipsometry and neutron reflectometry. J Colloid Interface Sci 2005;281:112-21.
[175] Bergstrom K, Holmberg K, Safranj A, Hoffman AS, Edgell MJ, Kozlowski A, et al. Reduction of Fibrinogen Adsorption on Peg-Coated Polystyrene Surfaces. J Biomed Mater Res 1992;26:779-90.
[176] Bergstrom K, Osterberg E, Holmberg K, Hoffman AS, Schuman TP, Kozlowski A, et al. Effects of Branching and Molecular-Weight of Surface-Bound Poly(Ethylene Oxide) on Protein Rejection. J Biomater Sci Polym Ed 1994;6:123-32.
[177] Desai NP, Hubbell JA. Biological Responses to Polyethylene Oxide Modified Polyethylene Terephthalate Surfaces. J Biomed Mater Res 1991;25:829-43.

[178] Chen YJ, Kang ET, Neoh KG, Wang P, Tan KL. Surface modification of polyaniline film by grafting of poly(ethylene glycol) for reduction in protein adsorption and platelet adhesion. Synth Met 2000;110:47-55.
[179] Han DK, Park KD, Ryu GH, Kim UY, Min BG, Kim YH. Plasma protein adsorption to sulfonated poly(ethylene oxide)-grafted polyurethane surface. J Biomed Mater Res 1996;30:23-30.
[180] Han DK, Ryu GH, Park KD, Jeong SY, Kim YH, Min BG. Adsorption Behavior of Fibrinogen to Sulfonated Polyethyleneoxide-Grafted Polyurethane Surfaces. J Biomater Sci Polym Ed 1993;4:401-13.
[181] Kishida A, Mishima K, Corretge E, Konishi H, Ikada Y. Interactions of Poly(Ethylene Glycol)-Grafted Cellulose Membranes with Proteins and Platelets. Biomaterials 1992;13:113-8.
[182] Kim K, Kim C, Byun Y. Preparation of a PEG-grafted phospholipid Langmuir-Blodgett monolayer for blood-compatible material. J Biomed Mater Res 2000;52:836-40.
[183] Snellings G, Vansteenkiste SO, Corneillie SI, Davies MC, Schacht EH. Protein adhesion at poly(ethylene glycol) modified surface. Adv Mater 2000;12:1959-+.
[184] Dalsin JL, Lin LJ, Tosatti S, Voros J, Textor M, Messersmith PB. Protein resistance of titanium oxide surfaces modified by biologically inspired mPEG-DOPA. Langmuir 2005;21:640-6.
[185] Sofia SJ, Premnath V, Merrill EW. Poly(ethylene oxide) grafted to silicon surfaces: Grafting density and protein adsorption. Macromolecules 1998;31:5059-70.
[186] Unsworth LD, Sheardown H, Brash JL. Polyethylene oxide surfaces of variable chain density by chemisorption of PEO-thiol on gold: Adsorption of proteins from plasma studied by radiolabelling and immunoblotting. Biomaterials 2005;26:5927-33.
[187] Unsworth LD, Sheardown H, Brash JL. Protein resistance of surfaces prepared by sorption of end-thiolated poly(ethylene glycol) to gold: Effect of surface chain density. Langmuir 2005;21:1036-41.
[188] Archambault JG, Brash JL. Protein repellent polyurethane-urea surfaces by chemical grafting of hydroxyl-terminated poly(ethylene oxide): effects of protein size and charge. Colloids and Surfaces B-Biointerfaces 2004;33:111-20.
[189] Archambault JG, Brash JL. Protein resistant polyurethane surfaces by chemical grafting of PEO: amino-terminated PEO as grafting reagent. Colloids and Surfaces B-Biointerfaces 2004;39:9-16.
[190] Chen H, Hu XY, Zhang YX, Li D, Wu ZK, Zhang T. Effect of chain density and conformation on protein adsorption at PEG-grafted polyurethane surfaces. Colloids and Surfaces B-Biointerfaces 2008;61:237-43.
[191] Gon S, Santore MM. Single Component and Selective Competitive Protein Adsorption in a Patchy Polymer Brush: Opposition between Steric Repulsions and Electrostatic Attractions. Langmuir 2011;27:1487-93.
[192] Heuts J, Salber J, Goldyn AM, Janser R, Moller M, Klee D. Bio-functionalized star PEG-coated PVDF surfaces for cytocompatibility-improved implant Components. J Biomed Mater Res A;92A:1538-51.

[193] Hansson KM, Tosatti S, Isaksson J, Wettero J, Textor M, Lindahl TL, et al. Whole blood coagulation on protein adsorption-resistant PEG and peptide functionalised PEG-coated titanium surfaces. Biomaterials 2005;26:861-72.
[194] Marconi W, Benvenuti F, Piozzi A. Covalent bonding of heparin to a vinyl copolymer for biomedical applications. Biomaterials 1997;18:885-90.
[195] Kang IK, Baek DK, Lee YM, Sung YK. Synthesis and surface characterization of heparin-immobilized polyetherurethanes. Journal of Polymer Science Part a-Polymer Chemistry 1998;36:2331-8.
[196] Kang IK, Kwon OH, Lee YM, Sung YK. Preparation and surface characterization of functional group-grafted and heparin-immobilized polyurethanes by plasma glow discharge. Biomaterials 1996;17:841-7.
[197] Bae JS, Seo EJ, Kang IK. Synthesis and characterization of heparinized polyurethanes using plasma glow discharge. Biomaterials 1999;20:529-37.
[198] Lin WC, Tseng CH, Yang MC. In-vitro hemocompatibility evaluation of a thermoplastic polyurethane membrane with surface-immobilized water-soluble chitosan and heparin. Macromol Sci 2005;5:1013-21.
[199] Bayramoglu G, Yilmaz M, Batislam E, Arica MY. Heparin-coated poly(hydroxyethyl methacrylate/albumin) hydrogel networks: In vitro hemocompatibility evaluation for vascular biomaterials. J Appl Polym Sci 2008;109:749-57.
[200] Denizli A. Heparin-immobilized poly(2-hydroxyethylmethacrylate)-based microspheres. J Appl Polym Sci 1999;74:655-62.
[201] Duncan AC, Boughner D, Campbell G, Wan WK. Preparation and characterization of a poly(2-hydroxyethyl methacrylate) biomedical hydrogel. Eur Polym J 2001;37:1821-6.
[202] Christensen K, Larsson R, Emanuelsson H, Elgue G, Larsson A. Effects on blood compatibility in vitro by combining a direct P2Y(12) receptor inhibitor and heparin coating of stents. Platelets 2006;17:318-27.
[203] Chandy T, Rao GHR. Evaluation of heparin immobilized chitosan-PEG microbeads for charcoal encapsulation and endotoxin removal. Artif Cells Blood Substit Immobil Biotechnol 2000;28:65-77.
[204] Almlöf M, Kristensen EME, Siegbahn H, Åqvist J. Molecular dynamics study of heparin based coatings. Biomaterials 2008;29:4463-9.
[205] Jao WC, Lin CH, Hsieh JY, Yeh YH, Liu CY, Yang MC. Effect of immobilization of polysaccharides on the biocompatibility of poly(butyleneadipate-co-terephthalate) films. Polym Adv Technol 2010;21:543-53.
[206] Wang S, Zhang Y, Wang H, Dong Z. Preparation, characterization and biocompatibility of electrospinning heparin-modified silk fibroin nanofibers. Int J Biol Macromol 2011;48:345-53.
[207] Baldwin AD, Kiick KL. Polysaccharide-Modified Synthetic Polymeric Biomaterials. Biopolymers 2010;94:128-40.
[208] Yang Z, Wang J, Luo R, Maitz MF, Jing F, Sun H, et al. The covalent immobilization of heparin to pulsed-plasma polymeric allylamine films on 316L stainless steel and the resulting effects on hemocompatibility. Biomaterials 2010;31:2072-83.

[209] Steffen HJ, Schmidt J, Gonzalez-Elipe A. Biocompatible surfaces by immobilization of heparin on diamond-like carbon films deposited on various substrates. Surf Interface Anal 2000;29:386-91.
[210] Murugesan S, Mousa S, Vijayaraghavan A, Ajayan PM, Linhardt RJ. Ionic liquid-derived blood-compatible composite membranes for kidney dialysis. J Biomed Mater Res Part B 2006;79B:298-304.
[211] Tsai CC, Chang Y, Sung HW, Hsu JC, Chen CN. Effects of heparin immobilization on the surface characteristics of a biological tissue fixed with a naturally occurring crosslinking agent (genipin): an in vitro study. Biomaterials 2001;22:523-33.
[212] Svenmarker S, Sandstrom E, Karlsson T, Haggmark S, Jansson E, Appelblad M, et al. Neurological and general outcome in low-risk coronary artery bypass patients using heparin coated circuits. Eur J Cardio-Thorac Surg 2001;19:47-53.
[213] Ovrum E, Brosstad F, Holen EA, Tangen G, Abdelnoor M, Oystese R. Complete heparin-coated (CBAS) cardio-pulmonary bypass and reduced systemic heparin dose; Effects on coagulation and fibrinolysis. Eur J Cardio-Thorac Surg 1996;10:449-55.
[214] Kocsis JF, Llanos G, Holmer E. Heparin-coated stents. J Long-Term Eff Med Implants 2000;10:19-45.
[215] Cornelius RM, Sanchez J, Olsson P, Brash JL. Interactions of antithrombin and proteins in the plasma contact activation system with immobilized functional heparin. J Biomed Mater Res A 2003;67A:475-83.
[216] Davidson I, Hackerman C, Kapadia A, Minhajuddin A. Heparin bonded hemodialysis e-PTFE grafts result in 20% clot free survival benefit. J Vasc Access 2009;10:153-6.
[217] Bindslev L, Bohm C, Jolin A, Jonzon KH, Olsson P, Ryniak S. Extracorporeal Carbon-Dioxide Removal Performed with Surface-Heparinized Equipment in Patients with Ards. Acta Anaesthesiol Scand 1991;35:125-31.
[218] Larm O, Larsson R, Olsson P. A New Non-Thrombogenic Surface Prepared by Selective Covalent Binding of Heparin Via a Modified Reducing Terminal Residue. Biomaterials Medical Devices and Artificial Organs 1983;11:161-73.
[219] Berceli SA, Phaneuf MD, LoGerfo PW. Evaluation of a novel hirudin-coated polyester graft to physiologic flow conditions: Hirudin bioavailability and thrombin uptake. J Vasc Surgery 1998;27:1117-27.
[220] Seifert B, Romaniuk P, Groth T. Covalent immobilization of hirudin improves the haemocompatibility of polylactide-polyglycolide in vitro. Biomaterials 1997;18:1495-502.
[221] Phaneuf MD, Szycher M, Berceli SA, Dempsey DJ, Quist WC, LoGerfo FW. Covalent linkage of recombinant hirudin to a novel ionic poly(carbonate) urethane polymer with protein binding sites: Determination of surface antithrombin activity. Artif Organs 1998;22:657-65.
[222] Lahann J, Klee D, Pluester W, Hoecker H. Bioactive immobilization of r-hirudin on CVD-coated metallic implant devices. Biomaterials 2001;22:817-26.
[223] Phaneuf MD, Dempsey DJ, Bide MJ, Szycher M, Quist WC, LoGerfo FW. Bioengineering of a novel small diameter polyurethane vascular graft with covalently bound recombinant hirudin. Asaio J 1998;44:M653-M8.

[224] Phaneuf MD, Berceli SA, Bide MJ, Quist WC, LoGerfo FW. Covalent linkage of recombinant hirudin to poly(ethylene terephthalate) (Dacron): Creation of a novel antithrombin surface. Biomaterials 1997;18:755-65.
[225] Du YJ, Brash JL, McClung G, Berry LR, Klement P, Chan AKC. Protein adsorption on polyurethane catheters modified with a novel antithrombin-heparin covalent complex. J Biomed Mater Res A 2007;80A:216-25.
[226] Du YJ, Klement P, Berry LR, Tressel P, Chan AKC. In vivo rabbit acute model tests of polyurethane catheters coated with a novel antithrombin-heparin covalent complex. Thromb Haemost 2005;94:366-72.
[227] Sun XL, Sheardown H, Tengvall P, Brash JL. Peptide modified gold-coated polyurethanes as thrombin scavenging surfaces. J Biomed Mater Res 2000;49:66-78.
[228] Martins MCL, Curtin SA, Freitas SC, Salgueiro P, Ratner BD, Barbosa MA. Molecularly designed surfaces for blood deheparinization using an immobilized heparin-binding peptide. J Biomed Mater Res A 2008;88A:162-73.
[229] Woodhouse KA, Brash JL. Adsorption of Plasminogen from Plasma to Lysine-Derivatized Polyurethane Surfaces. Biomaterials 1992;13:1103-8.
[230] Woodhouse KA, Brash JL. Plasminogen Adsorption to Sulfonated and Lysine Derivatized Model Silica Glass Materials. J Colloid Interface Sci 1994;164:40-7.
[231] Woodhouse KA, Weitz JI, Brash JL. Lysis of surface-localized fibrin clots by adsorbed plasminogen in the presence of tissue plasminogen activator. Biomaterials 1996;17:75-7.
[232] McClung WG, Clapper DL, Hu SP, Brash JL. Adsorption of plasminogen from human plasma to lysine-containing surfaces. J Biomed Mater Res 2000;49:409-14.
[233] McClung WG, Clapper DL, Hu SP, Brash JL. Lysine-derivatized polyurethane as a clot lysing surface: conversion of adsorbed plasminogen to plasmin and clot lysis in vitro. Biomaterials 2001;22:1919-24.
[234] McClung WG, Clapper DL, Anderson AB, Babcock DE, Brash JL. Interactions of fibrinolytic system proteins with lysine-containing surf aces. J Biomed Mater Res A 2003;66A:795-801.
[235] McClung W, Babcock DE, Brash JL. Fibrinolytic properties of lysine-derivatized polyethylene in contact with flowing whole blood (Chandler Loop model). J Biomed Mater Res A 2007;81A:644-51.
[236] Samoilova NA, Krayukhina MA, Novikova SP, Babushkina TA, Volkov IO, Komarova LI, et al. Polyelectrolyte thromboresistant affinity coatings for modification of devices contacting blood. J Biomed Mater Res A 2007;82A:589-98.
[237] Park KD, Kim WG, Jacobs H, Okano T, Kim SW. Blood Compatibility of Spuu-Peo-Heparin Graft-Copolymers. J Biomed Mater Res 1992;26:739-56.
[238] Park KD, Piao AZ, Jacobs H, Okano T, Kim SW. Synthesis and Characterization of Spuu-Peo-Heparin Graft-Copolymers. Journal of Polymer Science Part a-Polymer Chemistry 1991;29:1725-37.
[239] Byun Y, Jacobs HA, Kim SW. Heparin Surface Immobilization through Hydrophilic Spacers - Thrombin and Antithrombin-Iii Binding-Kinetics. J Biomater Sci Polym Ed 1994;6:1-13.

[240] Chen H, Chen Y, Sheardown H, Brook MA. Immobilization of heparin on a silicone surface through a heterobifunctional PEG spacer. Biomaterials 2005;26:7418-24.
[241] Xu FJ, Li YL, Kang ET, Neoh KG. Heparin-coupled poly(poly(ethylene glycol) monomethacrylate)-Si(111) hybrids and their blood compatible surfaces. Biomacromolecules 2005;6:1759-68.
[242] Zhang YX, Yu QA, Huang H, Zhou F, Wu ZQ, Yuan L, et al. A surface decorated with diblock copolymer for biomolecular conjugation. Soft Matter 2010;6:2616-8.
[243] Sask KN, Zhitomirsky I, Berry LR, Chan AKC, Brash JL. Surface modification with an antithrombin-heparin complex for anticoagulation: Studies on a model surface with gold as substrate. Acta Biomater 2010;6:2911-9.
[244] Sask KN, McClung WG, Berry LR, Chan AKC, Brash JL. Immobilization of an antithrombin-heparin complex on gold: Anticoagulant properties and platelet interactions. Acta Biomater 2011;7:2029-34.
[245] Chen H, Zhang YX, Li D, Hu XY, Wang L, McClung WG, et al. Surfaces having dual fibrinolytic and protein resistant properties by immobilization of lysine on polyurethane through a PEG spacer. J Biomed Mater Res A 2009;90A:940-6.
[246] Li D, Chen H, McClung WG, Brash JL. Lysine-PEG-modified polyurethane as a fibrinolytic surface: Effect of PEG chain length on protein interactions, platelet interactions and clot lysis. Acta Biomater 2009;5:1864-71.
[247] Chen H, Wang L, Zhang YX, Li D, McClung WG, Brook MA, et al. Fibrinolytic poly(dimethyl siloxane) surfaces. Macromol Sci 2008;8:863-70.
[248] Li D, Chen H, Wang SS, Wu ZQ, Brash JL. Lysine-poly(2-hydroxyethyl methacrylate) modified polyurethane surface with high lysine density and fibrinolytic activity. Acta Biomater;7:954-8.
[249] Choi WS, Bae JW, Lim HR, Joung YK, Park JC, Kwon IK, et al. RGD peptide-immobilized electrospun matrix of polyurethane for enhanced endothelial cell affinity. Biomed Mater 2008;3.
[250] Tugulu S, Silacci P, Stergiopulos N, Klok HA. RGD - Functionalized polymer brushes as substrates for the integrin specific adhesion of human umbilical vein endothelial cells. Biomaterials 2007;28:2536-46.
[251] Raynor JE, Petrie TA, Garcia AJ, Collard DM. Controlling cell adhesion to titanium: Functionalization of poly[oligo(ethylene glycol)methacrylate] brushes with cell-adhesive peptides. Adv Mater 2007;19:1724-+.
[252] Lavanant L, Pullin B, Hubbell JA, Klok HA. A Facile Strategy for the Modification of Polyethylene Substrates with Non-Fouling, Bioactive Poly(poly(ethylene glycol) methacrylate) Brushes. Macromol Sci 2010;10:101-8.
[253] Park SJ, Lee KB, Choi IS, Langer R, Jon SY. Dual functional, polymeric self-assembled monolayers as a facile platform for construction of patterns of biomolecules. Langmuir 2007;23:10902-5.
[254] Sun XL, Yang LC, Chaikof EL. Chemoselective immobilization of biomolecules through aqueous Diels-Alder and PEG chemistry. Tetrahedron Lett 2008;49:2510-3.
[255] Lee BS, Chi YS, Lee KB, Kim YG, Choi IS. Functionalization of poly(oligo(ethylene glycol)methacrylate) films on gold and Si/SiO2 for immobilization of proteins and cells: SPR and QCM studies. Biomacromolecules 2007;8:3922-9.

[256] Bhattacharya R, Patra CR, Earl A, Wang SF, Katarya A, Lu L, et al. Attaching folic acid on gold nanoparticles using noncovalent interaction via different polyethylene glycol backbones and targeting of cancer cells. Nanomed-Nanotechnol Biol Med 2007;3:224-38.
[257] Ye L, Letchford K, Heller M, Liggins R, Guan D, Kizhakkedathu JN, et al. Synthesis and Characterization of Carboxylic Acid Conjugated, Hydrophobically Derivatized, Hyperbranched Polyglycerols as Nanoparticulate Drug Carriers for Cisplatin. Biomacromolecules 2011;12:145-55.

CHAPTER 2. OBJECTIVES AND CONTRIBUTIONS TO ARTICLES

2.1 Objectives

From the discussion in chapter 1, it is clear that despite numerous research studies on the modification of biomaterials for improved blood compatibility, thrombosis and clot formation remain problematic. Since these phenomena are initiated by blood protein adsorption, it is of interest to control protein-surface interactions in order to minimize or, ideally, eliminate thrombotic complications.

Research has shown that non-specific protein adsorption can be minimized using hydrophilic polymers such as polyethylene glycol (PEG). Modification with appropriate bioactive molecules has also proved beneficial, often by promotion of adsorption of a specific protein such that clot formation is inhibited. A combination of these two strategies can be employed to create surfaces that reduce non-specific adsorption while inhibiting thrombus formation.

With the above in mind the objectives of this thesis were:

1. To explore the combined effects of polyethylene glycol and bioactive molecules in controlling protein-surface interactions for improved blood compatibility.
2. To determine the optimal ratio of PEG:bioactive molecule on the surface.
3. To explore two methods of dual surface modification designated “direct” and “sequential”. In the sequential method surfaces were modified first with PEG. The immobilized PEG was then reacted with the bioactive molecule. In the direct

method, a conjugate of PEG and the bioactive molecule was first prepared and then immobilized on the surface.

Gold was used first as a model substrate and the following surfaces were prepared, characterized and studied in terms of their interactions with blood proteins:

- Gold modified with PEG and hirudin. Hirudin was chosen on the basis of its anticoagulant properties through its specific interactions with thrombin.
- Gold modified with PEG and corn trypsin inhibitor (CTI). CTI was chosen based on its anticoagulant properties through its specific interactions with clotting factor XIIa.

Polyurethane was used as a substrate having applicability to real blood-contacting devices (catheters, intra-aortic balloon pumps etc) and was modified with PEG and CTI using a sequential method.

2.2 Contributions to the Articles

This thesis contains four articles (Chapters 3-6). The following describes my contributions. I was responsible for the design and performance of the projects, including literature searches, experiments and data analysis. I prepared the first draft of all four papers and the initial responses to the comments of the journal reviewers. I then worked with my supervisors on the subsequent drafts of the papers. In the case of papers 2, 3 and 4, Dr. Jeffrey Weitz and Jonathan Yau provided general assistance with corn trypsin inhibitor, its modification with Traut's reagent, and background on its use as a factor XIIa inhibitor.

CHAPTER 3. SURFACE MODIFICATION WITH PEG AND HIRUDIN FOR PROTEIN RESISTANCE AND THROMBIN NEUTRALIZATION IN BLOOD CONTACT

Authors: **Sara Alibeik**, Shiping Zhu, John L. Brash

Publication Information: Colloids and Surfaces B: Biointerfaces

Acceptance Date: July 7, 2010

Working Hypothesis:

Improved blood compatibility may be obtained by surface modification using a combination of PEG for protein resistant properties and hirudin for thrombin inhibition. The method of modification may play a role on plasma proteins-surface interactions.

Surface Modification with PEG and Hirudin for Protein Resistance and Thrombin Neutralization in Blood Contact

Sara Alibeik, Shiping Zhu, John L. Brash

School of Biomedical Engineering and Dept of Chemical engineering, McMaster University, Hamilton, Ontario, Canada

Corresponding author: JL Brash
School of Biomedical Engineering
McMaster University
Hamilton, ON Canada L8S 4L8
Ph: 905 525 9140 x 24946
Fax: 905 528 1054
email: brashjl@mcmaster.ca

Abstract

In this work, we hypothesize that a surface modified with both polyethylene glycol (PEG) and hirudin may provide a non-fouling, thrombin-neutralizing surface suitable for blood contacting applications. With gold as a model substrate we used two different approaches to the preparation of such a surface: (1) a "direct" method in which PEG was conjugated to hirudin and the conjugate was then immobilized on the gold; (2) a "sequential" method in which PEG was immobilized on the gold and hirudin then attached to the immobilized PEG. The surfaces were characterized by water contact angle, ellipsometry and XPS. The biological properties were investigated by measuring protein adsorption (fibrinogen and thrombin) from buffer and plasma: thrombin inhibition was measured using a chromogenic substrate assay. Hirudin immobilization was found to be more efficient on surfaces prepared by the "direct" method. "Sequential" surfaces, however, despite having a lower density of hirudin, showed greater biological activity (thrombin binding and inhibition).

Key words: Blood compatibility, hirudin, PEG, gold, protein resistant surface, antithrombin.

1. Introduction

Biomaterials used in blood contacting devices trigger protein adsorption and cell adhesion [1] resulting in failure of the device, most commonly due to thrombosis and embolization. Among several strategies used for the modification of biomaterials to overcome these problems, incorporation of hydrophilic polymers (eg polyethylene glycol) to reduce nonspecific protein adsorption has been widely investigated [2-5]. Also attachment of a biologically active biomolecule to the biomaterial surface can promote beneficial interactions between the surface and blood proteins [6-8]. Researchers have also investigated the attachment of biomolecules such as heparin to the surface through a PEG spacer [7, 9] with the objective of improving the ability of the biomolecule to interact with its target.

Another approach is to combine the protein resistance of PEG with the specific activity of the biomolecule [10]. In the present study, we investigated such a bifunctional surface modified with PEG and hirudin to provide both protein resistance and thrombin inhibition. The peptide hirudin is a very strong inhibitor of both soluble and clot-bound thrombin. It has a molecular weight of 6.9 kDa and contains 65 amino acid residues [11]. The N-terminal of hirudin can bind to the apolar binding site of thrombin. The C-terminal can interact with the anion-binding exosite of thrombin. The Pro46-Lys47-Pro48 sequence of hirudin may occupy the basic specificity pocket near the active site of thrombin. Hirudin is thus able to inhibit both free and fibrin-bound thrombin [12].

Surfaces with immobilized hirudin have been investigated previously [13-16]; however none of these combined hirudin with PEG, and thus they could potentially

adsorb other proteins besides the target thrombin, some of which (eg fibrinogen) are undesirable. In this work we used gold surface as the substrate for a number of reasons. First, gold is inert and nontoxic. Second, the reactivity of the gold with thiol and disulfide functions provides a means of grafting a variety of biomolecules with high grafting density [17].

Gold surfaces were modified with PEG and hirudin using two different approaches. In the first approach, referred to as the direct method, a conjugate of PEG and hirudin was synthesized and then chemisorbed to gold. In the second approach, referred to as the sequential method, PEG was first chemisorbed to gold and hirudin was then attached via reaction with the PEG.

2. Materials and methods

(2, 2'-Dithiobisethylhepa(ethylene glycolic) acid)-N-hydroxy succinimidyl ester (PEG-NHS ester disulfide) (MW=1109.3) was purchased from Polypure AS (Oslo, Norway). α-hydroxy-ω-thiol terminated polyethylene glycol (MW=1100) was purchased from Polymer Source (Montreal). Hydrogen peroxide, ammonium hydroxide, ethanol and Atroxin snake venom were purchased from Sigma-Aldrich (Oakville, ON). Hirudin (Refludan® (lepirudin)) was purchased from Bayer HealthCare Pharmaceuticals (Wayne, NJ). Lepirudin is a recombinant hirudin derived from yeast cells. It is identical to hirudin from leeches except for substitution of leucine for isoleucine at the N-terminal and the absence of a sulfate group on the tyrosine at position 63. Silicon wafers sputter-coated with titanium and then gold (1000Å) were purchased from Silicon Valley

Microelectronics (Santa Clara, CA) and were cut into 0.5 x 0.5 cm pieces. Antithrombin-depleted plasma (AT<0.01 U/mL) was purchased from Affinity Biologicals (Ancaster, ON). Chromogenic substrate for thrombin, S-2238, was purchased from DiPharma Group (West Chester, Ohio).

2.1 Surface preparation

Gold-coated silicon wafers were cleaned in a solution containing one part 30% hydrogen peroxide, one part 30% ammonium hydroxide and five parts water at 85ºC for 5 min. They were then rinsed three times, 5 min each time, with deionized water before transferring to chemisorption solutions. The surfaces were modified using two methods.

Method 1. Direct.

A conjugate of PEG and hirudin was prepared by reaction of PEG-NHS ester disulfide (1 mM) with hirudin (0.5 mg/mL) in phosphate-buffered saline (PBS, pH=7.4) (NHS reacts with $-NH_2$ of hirudin). The reaction product was characterized by MALDI-mass spectrometry. The conjugate was attached to gold coated silicon by chemisorption through the disulfide group in the PEG moiety. This reaction was carried out at room temperature for 3 h, then at 4ºC under nitrogen purge for 16 h.

Method 2. Two-step, sequential.

PEG-NHS ester disulfide (1 mM) was first attached to gold surface by chemisorption for 2 h under nitrogen purge at room temperature. Hirudin (0.5 mg/mL)

was then attached to the chemisorbed PEG (NHS reacts with -NH_2 of hirudin) by incubation at room temperature for 3 h, then at 4ºC under nitrogen purge for 16 h.

A surface prepared by chemisorption of SH-PEG-OH of MW 1100 (1 mM) to gold was used as a "control". The reaction was carried out for 2 h at room temperature under nitrogen purge.

At the end of each modification step, surfaces were rinsed three times, five minutes each time, with deionized water. They were dried and stored under nitrogen or were used immediately for characterization and biological activity experiments.

2.2 Mass Spectrometry

The molecular weights of the hirudin sample and the PEG-hirudin conjugate were determined by matrix-assisted laser desorption-ionization time of flight (MALDI-TOF) mass spectrometry to confirm the conjugation reaction (Waters/Micromass MALDI MicroMX).

2.3 Surface characterization

Water contact angles were measured using the sessile drop method with a Ramé-Hart NRL C.A. goniometer (Mountain Lakes, NJ). Advancing and receding angles were determined. The thickness of chemisorbed layers on the modified surfaces was measured by ellipsometry using a self-nulling, single wavelength (6328Å) ellipsometer (Exacta 2000). The incident angle was 70º and the refractive index and extinction coefficient for the gold substrate were taken as 0.2 and 3.5 respectively. The refractive indices for PEG

modified surfaces and PEG-protein modified surfaces were taken as 1.475 and 1.465 respectively [18-20]. X-ray photoelectron spectroscopy (XPS) was conducted using a Thermo Scientific K-Alpha instrument. Surface chemical compositions were determined based on low resolution spectra at 90º and 20º takeoff angles.

2.4 Determination of hirudin surface density

Hirudin was labeled with ^{125}I using the ICl method [21, 22]. Direct and sequential attachments to gold were carried out using the labeled hirudin. Densities were calculated by counting radioactivity and comparing to a solution of the labeled hirudin of known concentration [21].

2.5 Protein and blood interactions

Thrombin adsorption from buffer, from serum and from plasma depleted of antithrombin and fibrinogen (AT-Fg) were studied using ^{125}I-labeled thrombin. Thrombin was labeled with ^{125}I by the Iodogen method and was used as a tracer (10% of total thrombin concentration) [23]. Total thrombin concentration was 0.06 mg/mL in all adsorption experiments from serum and AT-Fg depleted plasma. Serum was prepared by adding 25 mM $CaCl_2$ to pooled normal citrated human plasma (PNP) at 37ºC (1:1 v/v) and centrifuging to remove the clot. To prepare AT-Fg depleted plasma, Atroxin (snake venom) was added to AT-depleted plasma. After 15 min incubation at 37ºC the plasma was centrifuged to remove the clot. Solutions for adsorption consisted of 50% serum or AT-Fg depleted plasma, and 50% phosphate buffered saline (PBS) containing “cold” NaI

to suppress free ^{125}I-iodide uptake by gold [24]. In experiments to measure thrombin adsorption as a function of serum concentration, the initial serum was serially diluted using PBS-NaI buffer. Fibrinogen adsorption from 50% pooled normal citrated human plasma was also carried out using ^{125}I-labeled Fg as a tracer. Fg was labeled using the ICl method.

Immunoblotting of proteins eluted from the surfaces by SDS after a 2 h exposure to serum was carried out as described elsewhere [25]. The proteins were eluted by incubating the surfaces with 2% SDS for 16 h [26]. The eluates were run on reduced SDS-PAGE (12%) gels and transferred to polyvinylidene fluoride (PVDF) membranes. The membranes were cut into 3 mm strips and incubated in sequence with primary and enzyme-conjugated secondary antibodies followed by NBT/BCIP substrate (Pierce, Rockford, IL) to visualize the protein bands. In these experiments, the surface areas, the volumes of buffer used to elute, and the eluate volumes loaded on the gels were the same for all surfaces. Comparisons among the surfaces are thus valid. It should be mentioned that this approach depends on the elutability of adsorbed proteins by SDS. One cannot be certain that all proteins are SDS-elutable, but previous experiments using radiolabelled proteins have shown that elutability of several proteins from gold is greater than 90% [24].

The ability of the modified surfaces to inhibit thrombin in a contacting fluid was investigated using a chromogenic substrate assay. Surfaces were incubated with 100 μL of 0.01 mg/mL thrombin solution in PBS for 1 h in a 96-well plate format. 100 μL of 500 nM chromogenic substrate (S-2238) solution was then added to the wells. The optical

density was recorded as a function of time at 405 nm. A decrease in thrombin activity is expected if interaction with the surface inhibits thrombin. Residual thrombin activity in the solution was calculated from a standard curve constructed by measuring the rate of the thrombin-substrate reaction using a series of thrombin solutions of known concentration.

3. Results and discussion

3.1 PEG-Hirudin conjugation

MALDI-Mass spectrometry showed that after reaction with PEG, the molecular weight of hirudin increased, thus confirming conjugation (Fig 1). Hirudin has a molecular weight of 6.9 kDa. It contains 3 lysine residues and one N-terminal amino group leading to the possibility of conjugates containing 1, 2, 3, and 4 PEGs. The peaks seen at around 7.9, 8.9, 9.9 and 10.9 kDa suggest that conjugates were formed in the range of molecular weights expected for species containing 1 to 4 PEGs per hirudin. It appears that the product containing 3 PEGs, possibly indicating substitution of the three internal lysine residues, is the most abundant.

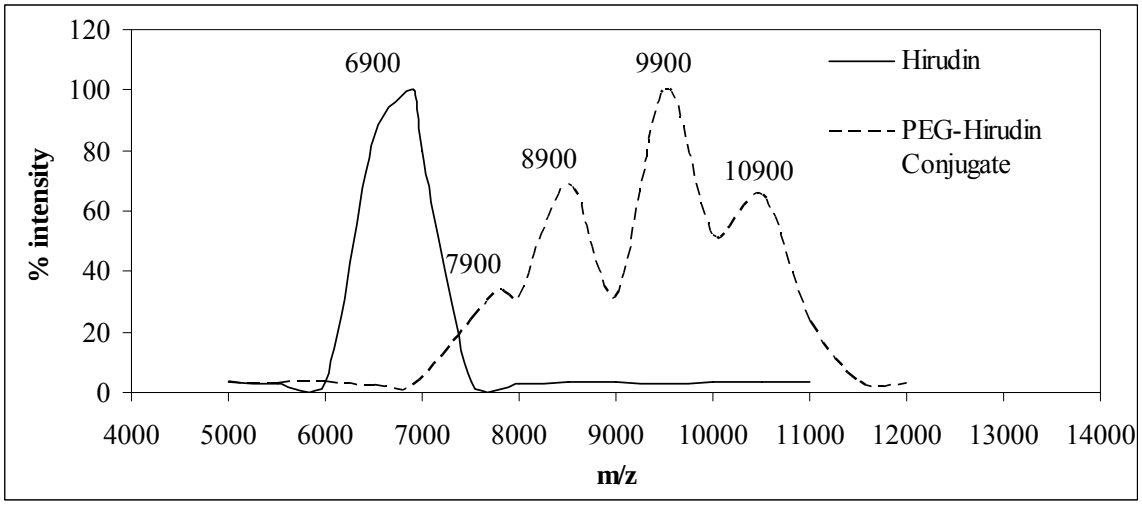

Fig 1. MALDI-MS of hirudin before and after conjugation to PEG.

3.2 Contact angles

Water contact angles (Fig 2) decreased after treatment of the gold substrate with HS-PEG-OH. The angles were not significantly different on the PEG-hirudin surfaces compared to the PEG-alone surfaces. All of the modified surfaces, with advancing angles between 30º and 40º and receding angles less than 30º, are more hydrophilic than the unmodified gold. Surfaces with angles in the 30 to 40º range may be viewed as less hydrophilic than might be expected for a layer of PEG. It has been reported by Cohen Stuart et al [27] that the contact angles of PEG-modified surfaces are affected by adsorption of the surface-tethered PEG at the air-water interface which prevents decrease of the contact angles to very low values even for a good solvent.

The contact angles were similar for the PEG-hirudin surfaces whether formed by the direct or sequential method, suggesting that similar surface compositions were achieved in both cases.

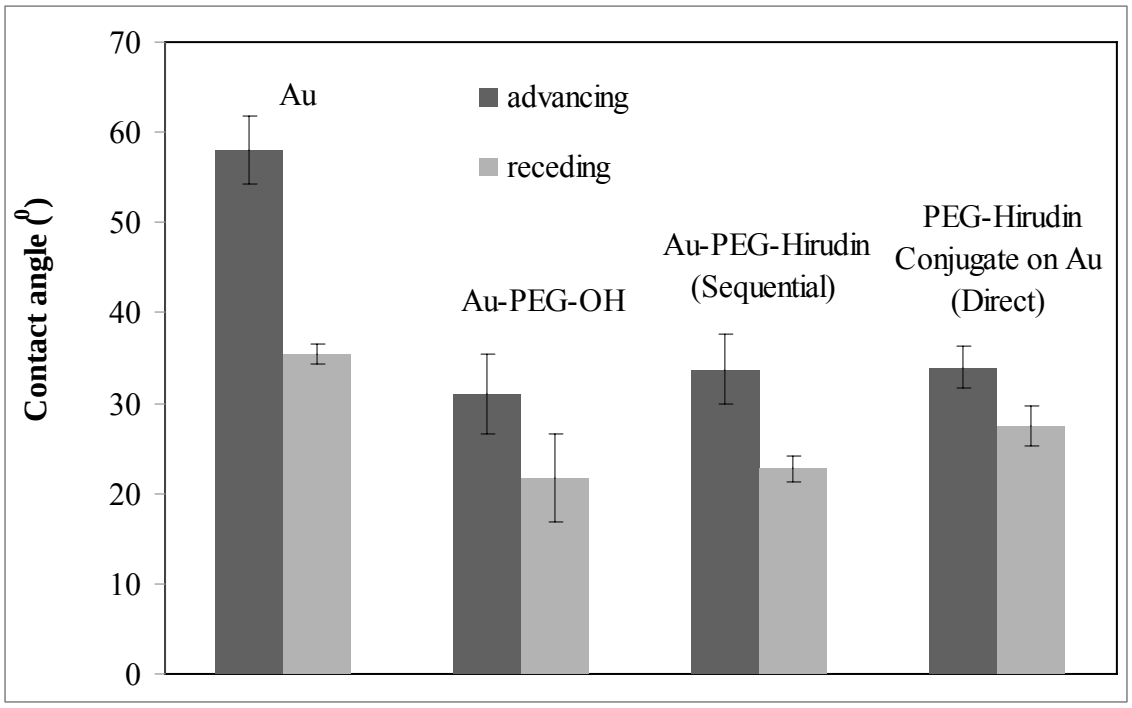

Fig 2. Water contact angles for gold and modified gold surfaces. Data are mean ±SD, n>9.

3.3 Ellipsometry

From ellipsometry data (Table 1) the film thicknesses ranged from 14 to 31 Å and were in the order: Au-PEG-OH < Au-PEG-Hirudin (sequential) < Au-PEG-Hirudin (direct). Among the three immobilized species, PEG-OH with a molecular weight of 1100 Da gave the film with the smallest thickness. The species on hirudin surfaces prepared by the sequential method consist of PEG of effective MW 550 (half the 1100 Da disulfide) and hirudin of MW 6900 Da attached to the PEG. The species on surfaces prepared by the direct method are conjugates with an average MW of ~9900 Da. The thickness data obtained by ellipsometry thus correlate well with the relative MWs (and presumably the relative sizes) of the three modifier species.

Table 1. Ellipsometry data for control and modified surfaces (mean±SD, n=6)

Surface	Film Thickness (Å)
Au-PEG-OH	14±4
Au-PEG-Hirudin (sequential)	27±8
Au-PEG-Hirudin (direct)	31±9

3.4 Surface chemical composition from XPS

Low resolution XPS data are shown in Table 2. The unmodified gold surface consisted mainly of gold with some contamination, mainly carbonaceous material with trace levels of N, O and S [28]. Contamination was kept to a minimum by storage of the cleaned gold surfaces under nitrogen. The gold content was lower on the PEG-alone and PEG-hirudin surfaces, while the carbon, oxygen and nitrogen contents were higher, confirming the presence of PEG and hirudin on these surfaces. As expected the carbon, oxygen, and nitrogen contents were greater on the PEG-hirudin surfaces than on the PEG-alone surfaces. At 20º take-off angle, the gold content decreased for PEG-alone and PEG-hirudin surfaces compared with the 90º take-off angle, and the carbon, oxygen and nitrogen contents increased confirming the attachment of PEG and PEG-hirudin.

To compare surface composition from XPS with data on hirudin uptake by radiolabeling, the XPS data for PEG-alone and PEG-hirudin surfaces were re-analyzed after subtracting the gold content. The compositions were then calculated based on carbon, oxygen, nitrogen and sulfur. The values of each element were also calculated based on the quantity of hirudin as determined by radiolabeling (see section 3.5). XPS gave higher carbon and oxygen contents than radiolabeling, probably due to contamination of the gold "seen" by XPS but not by radiolabeling. For nitrogen the

radiolabeling and XPS values were very close. For example, for the PEG-hirudin surfaces prepared by both the sequential and direct methods, the normalized XPS values at 20º take-off angle were 3.1% and 3.6% respectively compared to values of 4% and 6% respectively based on radiolabeled hirudin uptake. The lower nitrogen content from XPS may also be due to contamination causing an increase in carbon and oxygen and, therefore, a decrease in nitrogen on a percentage basis.

Table 2. Composition of control and PEG-Hirudin modified surfaces determined by XPS

90º angle	Au%	C%	N%	O%	S%	%N (from normalized XPS data)	%N (from labeled hirudin uptake)
Au	82.3	14.8	0.7	0.7	0.9		
Au-PEG-OH	58.5	27.5	1.1	7.1	5.9		
Au-PEG-Hirudin (sequential)	39.1	42.1	1.3	15.3	2.3	2.2	4
Au-PEG-Hirudin (direct)	56.4	28.4	2.1	7.8	5.3	4.8	6
20º angle							
Au	51.0	41.6	1.6	4.2	1.6		
Au-PEG-OH	34.4	44.0	2.4	11.9	7.2		
Au-PEG-Hirudin (sequential)	23.4	54.6	2.4	17.6	2.1	3.1	4
Au-PEG-Hirudin (direct)	29.7	48.8	2.6	13.2	5.7	3.6	6

Data are means of two determinations. Precision ~5%.

3.5 Determination of hirudin density on PEG-hirudin surfaces

^{125}I-labeled hirudin was used to determine the densities of hirudin on the PEG-hirudin surfaces. The densities on surfaces prepared by the direct and sequential methods were 11±0.1 and 7.8±0.1 ng/cm^2 respectively, i.e., uptake on the "direct" surfaces was significantly higher than on the "sequential". When preparing surfaces by the sequential method, PEG is immobilized first, and it is expected that hirudin reaction at these PEG surfaces will be impeded by the inherent protein resistance of the PEG; this may account for the lower density of hirudin on these surfaces. The higher density of hirudin on the

direct surfaces does not necessarily mean that they will be more effective in binding and inhibiting thrombin since the conformation and availability of thrombin binding sites on hirudin should also play a role. Data bearing on these considerations are discussed in the next sections.

To estimate the coverage of hirudin on the PEG-hirudin surfaces, a monolayer of hirudin was calculated by assuming hirudin shape as a 25 Å diameter sphere [16]. Based on these dimensions a monolayer of hirudin should contain 0.06 $\mu g/cm^2$ implying coverage of hirudin on the sequential and direct surfaces of 11% and 16% respectively. These apparently low values are probably due to the effect of the PEG: on the sequential surface it may impede the access of hirudin for reaction at the surface; on the direct surface the reactivity of the conjugate may be reduced due to the masking effects of the PEG.

3.6 Protein interactions

Fibrinogen adsorption from plasma

Fibrinogen adsorption from plasma after 3 h (Fig 3) was low on all the surfaces (20-35 ng/cm^2). Although higher on the PEG-hirudin surfaces than on the PEG-alone, the adsorbed quantities were very close. Based on statistical analysis (student t-test) the Au-PEG-OH and sequential surfaces were in fact not significantly different, whereas the Au-PEG-OH and direct surfaces were different ($p < 0.05$). These data demonstrate the protein resistance of the PEG-hirudin surfaces, and show that the protein resistance of the PEG component is not greatly compromised by the presence of the hirudin.

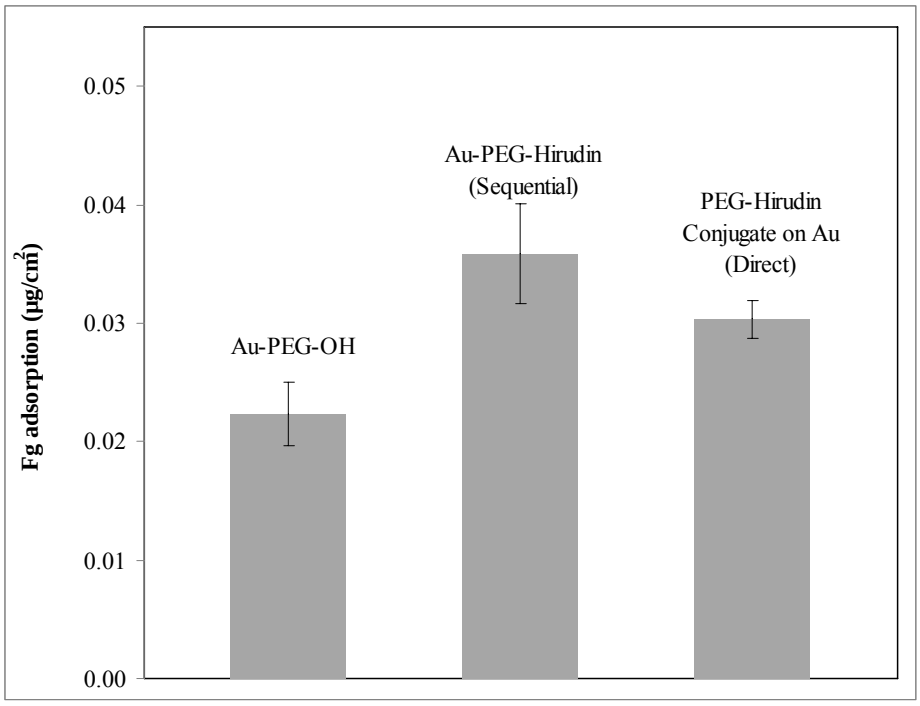

Fig 3. Fg adsorption from 50% plasma on PEG-alone and PEG-hirudin surfaces. Adsorption time, 3 h. Data are mean ±SD, n=3.

Thrombin adsorption from buffer, serum and AT-Fg depleted plasma

For an exposure time of 2 h, thrombin uptake from PBS on the PEG-hirudin surfaces was significantly greater than on the PEG-alone surface (Fig 4), suggesting specific interactions of the immobilized hirudin with thrombin. Similarly thrombin uptake from serum was significantly greater on the PEG-hirudin surfaces compared to the PEG-alone (Fig 5), and slightly, but not significantly, greater on the sequential compared to the direct surface. The latter difference, seen also in the buffer data (Fig 4), may be due to the limited availability of hirudin molecules to interact with thrombin when the hirudin is conjugated to (and to some extent buried in) multiple PEGs so that its thrombin binding sites may be "hidden". Thrombin adsorption levels from buffer were significantly higher

than from serum. This is to be expected due to the competitive multi-protein environment in serum.

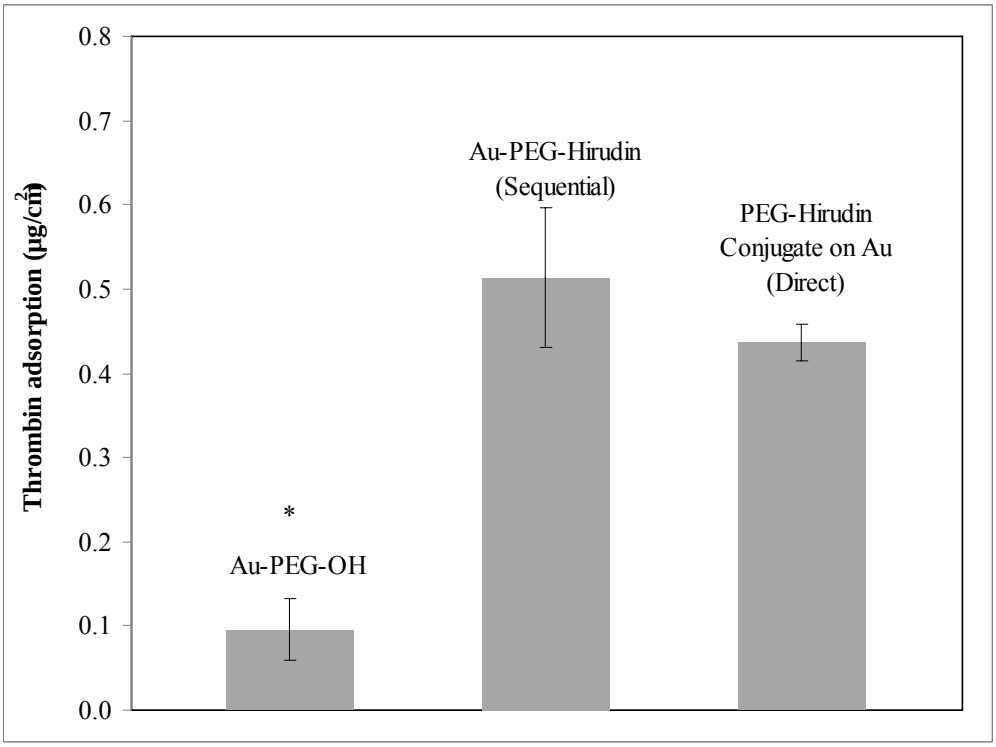

Fig 4. Thrombin adsorption from PBS buffer on PEG-alone and PEG-hirudin modified surfaces. Thrombin concentration was 0.1 mg/mL. Adsorption time, 2 h. Data are mean ±SD, n=3.

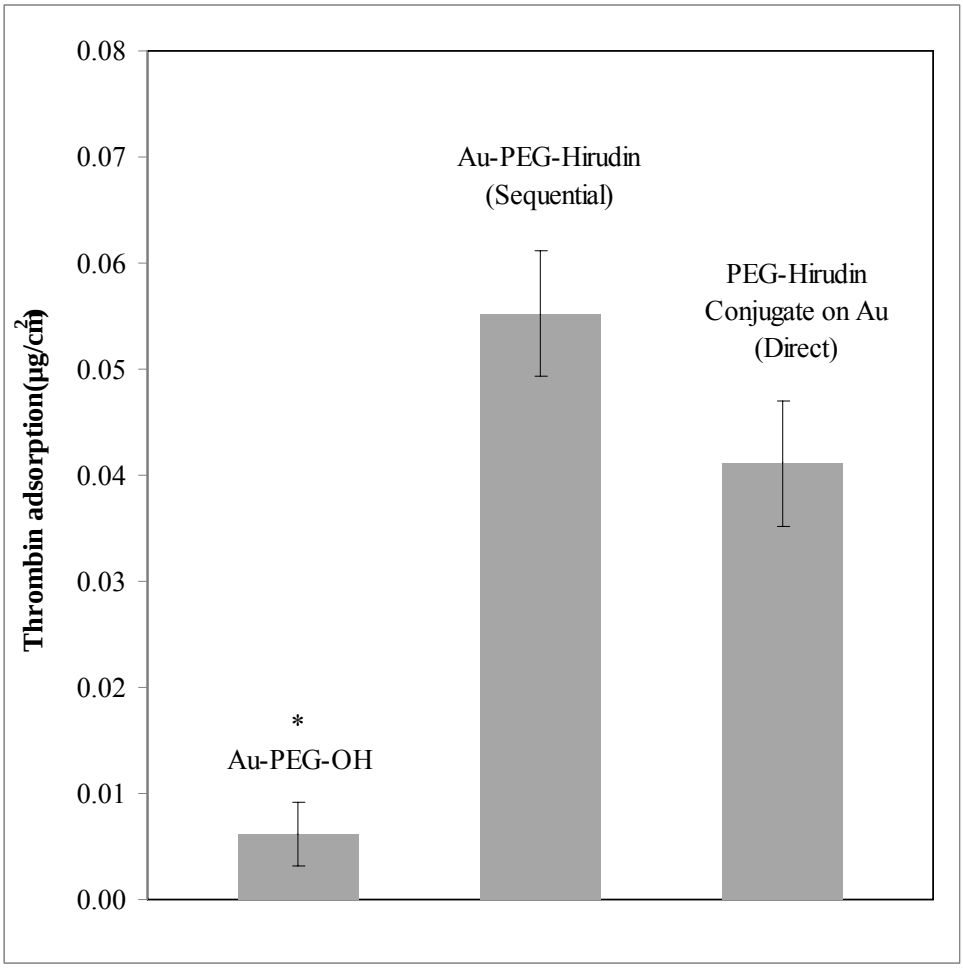

Fig 5. Thrombin uptake from 50% serum on PEG-alone and PEG-Hirudin modified surfaces. Thrombin in serum at a final concentration of 0.06 mg/mL. Adsorption time, 2h. Data are mean ±SD, n=3.

Adsorption of thrombin from serum as a function of time from 2 to 100 min (Fig 6) again showed consistently and significantly greater uptake on the PEG-hirudin surfaces than on the PEG-alone, and the sequential surfaces showed greater thrombin uptake than the direct surfaces, presumably due to the greater availability of hirudin to interact with thrombin. In 50% serum, and to a lesser extent in 1% serum, adsorption on the hirudin surfaces increased with time up to about 30 min and then appeared to decrease. To

investigate whether this maximum was indicative of a Vroman effect, whereby initially adsorbed thrombin would be replaced by other proteins at longer time [29], thrombin uptake at a fixed time of 2 h as a function of serum dilution was investigated [29]. As shown in Fig 7, thrombin uptake increased monotonically with increasing serum concentration, suggesting that the apparent maximum in adsorption observed in the kinetics (Fig 6) was probably not due to a Vroman effect. In fact, a Vroman effect is unlikely if the thrombin is bound to hirudin via its active site since that interaction is reported to be essentially irreversible [30].

Plasma depleted of Fg and AT was also used for thrombin adsorption studies. It seemed important to investigate thrombin uptake from a blood-like fluid that, unlike serum, contains most of the clotting factors. Since adding thrombin to plasma with Fg present would cause clot formation, fibrinogen had to be removed. AT also had to be removed since it binds to thrombin and thus would interfere with thrombin-hirudin interactions. The kinetics of thrombin uptake from AT-Fg depleted plasma (Fig 8) was similar to thrombin uptake from serum. The adsorbed quantities, however, were smaller. For the PEG-hirudin surfaces, adsorption from AT-Fg depleted plasma (Fig 8) was about half as much as from serum (Fig 6). We have no definitive explanation for this difference. Clearly the two fluids are of different composition as indicated, and this may account for the variation in thrombin uptake. Thrombin adsorption to the PEG-hirudin surfaces is significantly higher than to the PEG-alone surfaces thus supporting the conclusion that the interaction is specific.

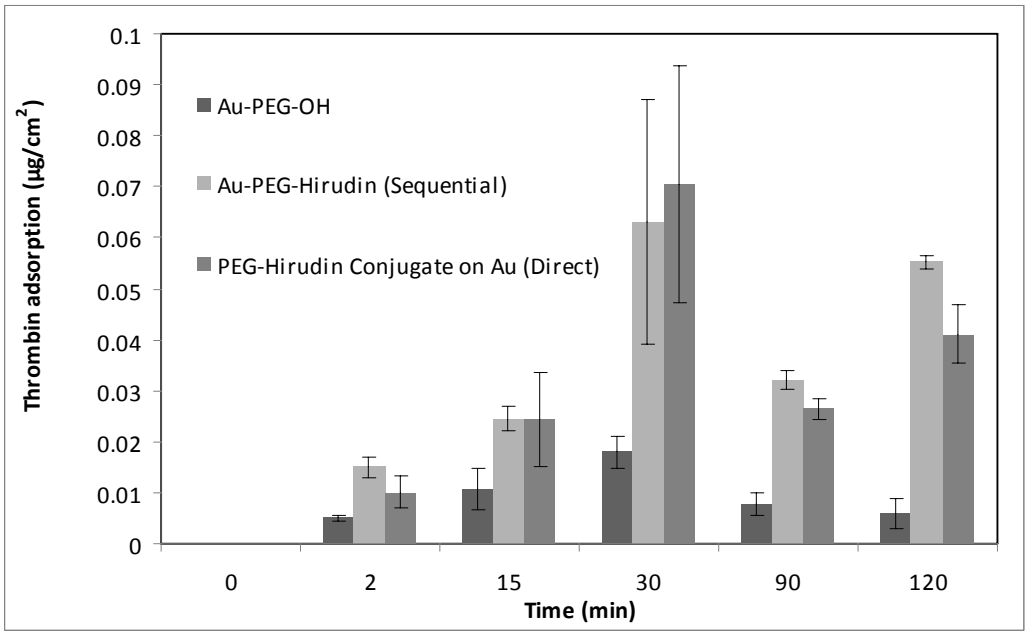

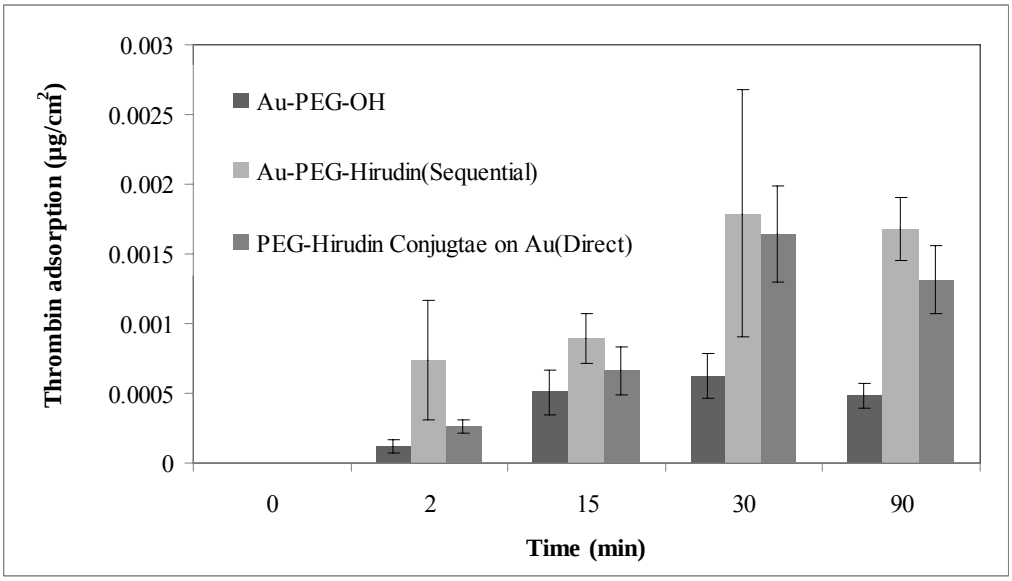

Fig 6. Kinetics of thrombin uptake to PEG-alone and PEG-hirudin surfaces from a) 50% serum, b) 1% serum. Thrombin concentration in serum was 0.06 mg/mL. Data are mean ±SD, n=3.

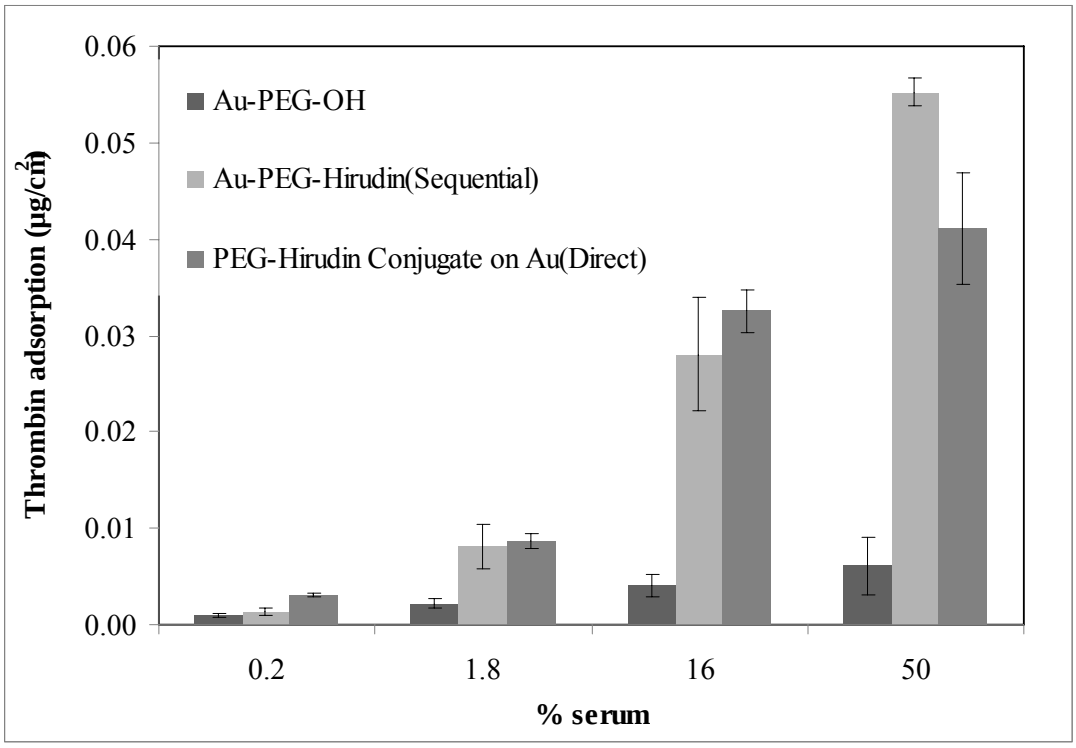

Fig 7. Effect of serum concentration on thrombin uptake on PEG-alone and PEG-hirudin surfaces. Thrombin added to 50% serum was 0.06 mg/mL. Adsorption time, 2h. Data are mean ±SD, n=3.

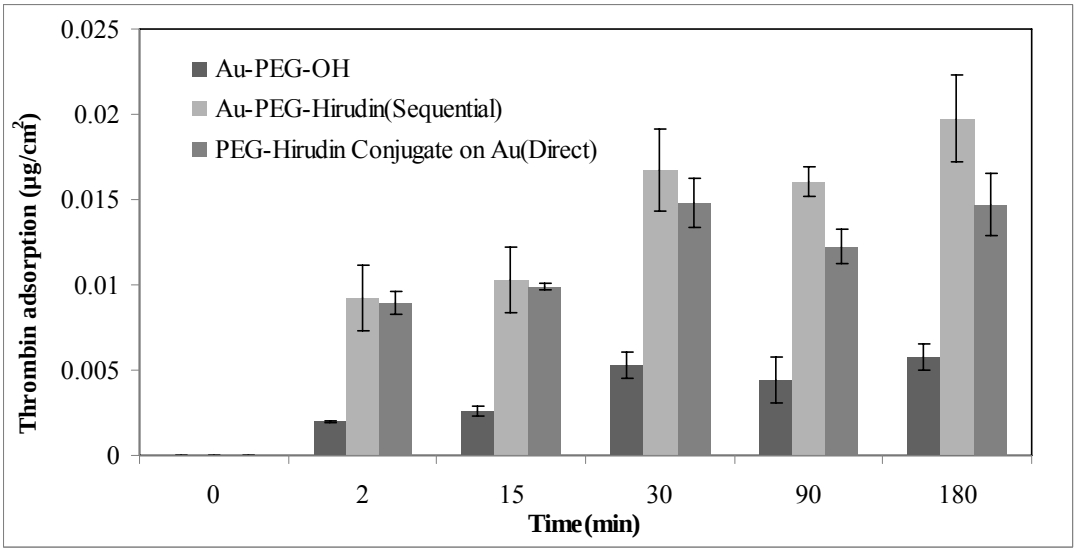

Fig 8. Kinetics of thrombin uptake from 50% AT-Fg depleted plasma. Thrombin added to 50% AT-Fg depleted plasma to give 0.06 mg/mL. Data are mean ±SD, n=3.

Immunoblots of serum proteins eluted from surfaces

To investigate the interactions of serum proteins more generally with these surfaces, we performed SDS PAGE and Western blotting on proteins eluted from the surfaces after exposure to serum.

For serum exposure, the PEG-alone and PEG-hirudin surfaces showed similar blot patterns (Fig 9). Antibodies against nine different blood proteins were used, and most of the proteins probed for were found in the eluates from all of the modified surfaces. The responses were generally weak, however, suggesting that these PEG-hirudin surfaces have a low affinity for serum protein adsorption due to the presence of PEG; also it appears that on the PEG-hirudin surfaces PEG resists proteins to about the same extent as on the PEG-alone surfaces.

For the thrombin blot it should be noted that the antibody against thrombin also reacts with thrombin-antithrombin (TAT) complex. TAT complex (MW ~90 kDa) was observed on all of the surfaces. The response for thrombin (37 kDa) was greater for the PEG-hirudin surfaces than for the PEG-alone surface, providing additional support for the specific interaction of PEG-hirudin surfaces with thrombin. The PEG-hirudin sequential surface again showed the highest thrombin adsorption from serum probably due to the greater availability of hirudin when sequentially attached.

It is seen that the response to apo AI was among the strongest for the proteins investigated, again indicating the high surface activity of this protein as has been found previously [31].

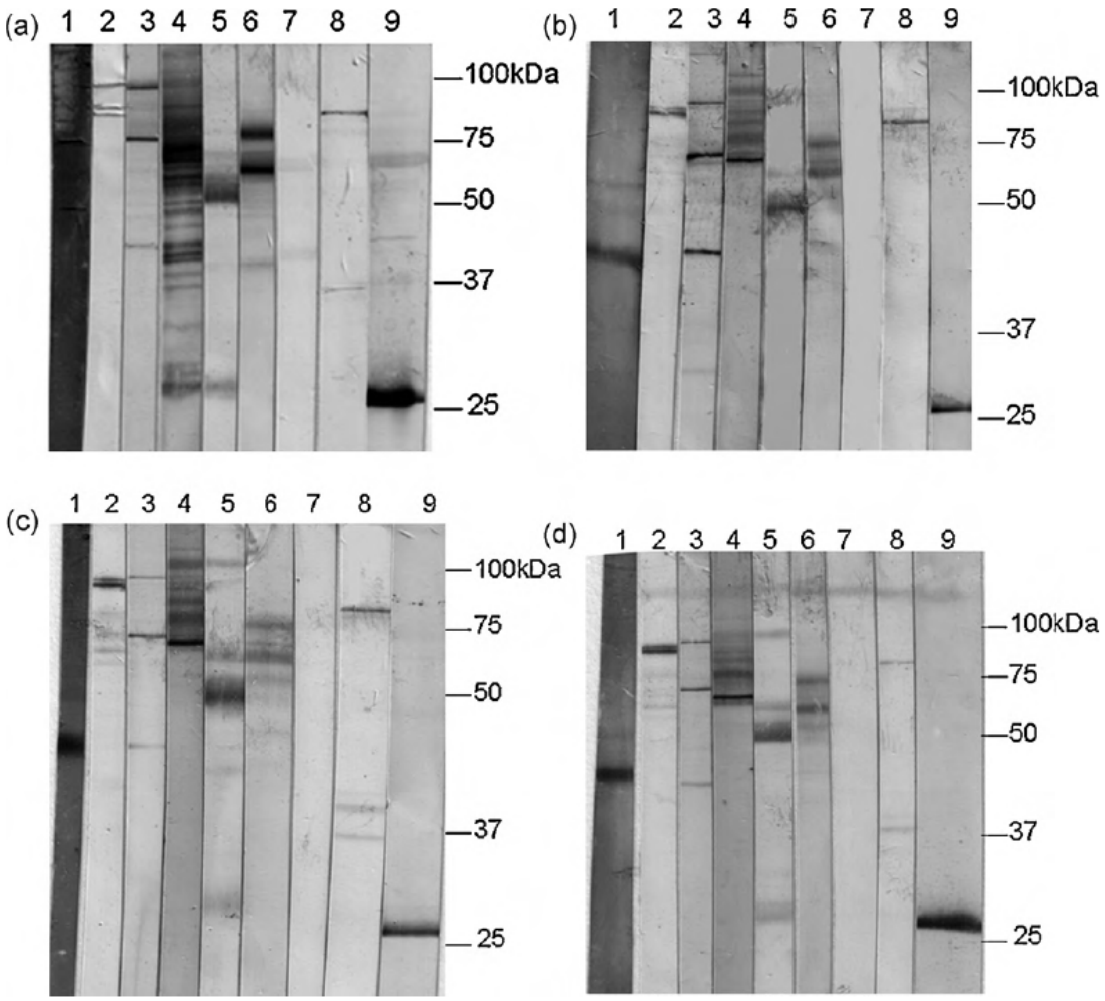

Fig 9. Immunoblots of serum proteins eluted from surfaces exposed to serum for 3h: (a) Serum (b)PEG-OH surface (c)sequential surface and (d)direct surface
1. HMWK, 2. Plasminogen, 3. C3, 4. Albumin, 5. IgG, 6. Vitronectin, 7. Protein C, 8. Thrombin, 9. Apolipoprotein-AI.

3.7 Activity of adsorbed thrombin

The thrombin-inhibitory activity of PEG-hirudin surfaces was measured using a chromogenic substrate assay. Cleavage of the chromogenic substrate by active thrombin results in a color change due to the formation of paranitroaniline (pNA), and the rate of pNA formation increases with increasing concentration of active thrombin.

To measure thrombin inhibition by PEG-hirudin surfaces, the surfaces were incubated with 100 μL of 0.01 mg/mL thrombin solution and the decrease in active thrombin concentration was determined. A standard curve for thrombin concentration was constructed using a series of thrombin solutions of known concentration. Using the standard curve, it was found that 50% and 25% of the initial thrombin quantities in the incubation solutions were inhibited by the sequential and direct surfaces, respectively, whereas no thrombin was inhibited by the PEG-alone surfaces (Fig 10). Thus it is concluded that hirudin retained its antithrombin activity when attached or conjugated to PEG on these surfaces.

The bound hirudin appeared to be more active when attached by the "sequential" than by the "direct" method. This observation correlates with the thrombin adsorption data showing higher adsorption on the sequential surfaces. Thrombin adsorption on the "sequential" surfaces was about 10% greater on the "direct" surfaces (radiolabeling data), but thrombin activity (chromogenic assay) was about 25% greater. The "masking" of hirudin molecules when directly conjugated to PEG (average of three PEGs per hirudin) may be responsible for this difference since on the direct surfaces, the N-terminal amino group of hirudin might not be as available as on the sequential surfaces. Furthermore, in

the case of the direct surfaces most of the thrombin uptake is probably due to interaction with the C-terminal of hirudin since the N-terminal is used in conjugation. The N-terminal of hirudin inhibits the catalytic site of thrombin which is the main site for the interaction of thrombin with the chromogenic substrate [32, 33]. Therefore, if immobilized hirudin does not inhibit the active site of thrombin then the site would be available to react with the chromogenic substrate and less thrombin inhibition would be observed in the activity assay.

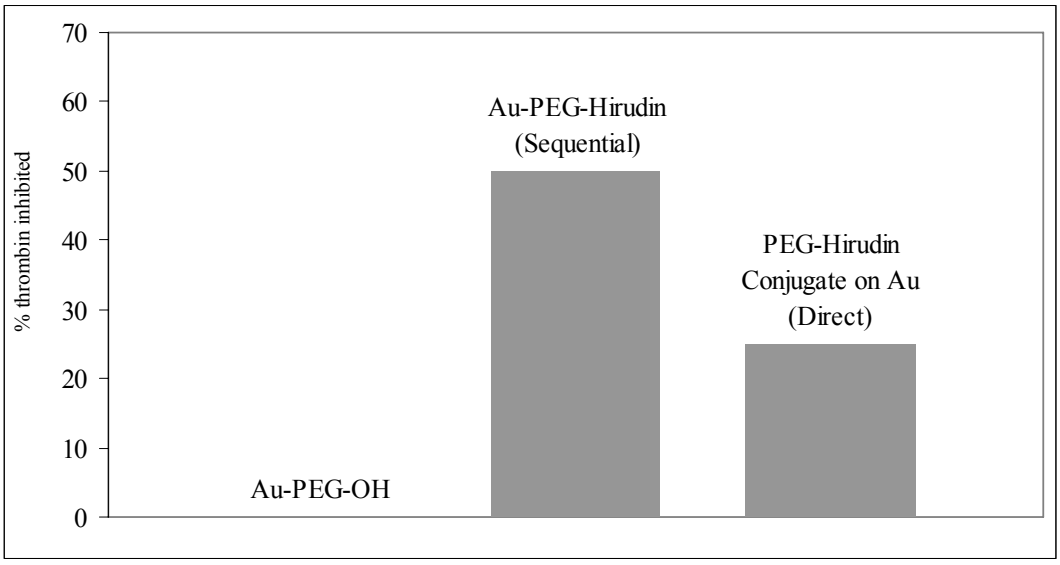

Fig 10. Inhibitory activity of PEG-hirudin surfaces measured by chromogenic substrate assay. Surfaces were incubated with thrombin (0.01mg/mL) for 1 h. Chromogenic substrate was then added and OD at 405 nm was measured. Rate of OD change was measured and compared with a standard curve (n=2).

4. Conclusions

Surfaces modified with PEG and hirudin were prepared using two methods described as “direct” and “sequential”. Contact angle, ellipsometry, XPS and experiments with labeled hirudin confirmed the modification of the surfaces. Protein interactions were

studied by radiolabeling and immunoblotting methods. Thrombin showed more extensive adsorption to the PEG-hirudin surfaces than to the PEG-alone surfaces. Adsorption was similar on both types of hirudin surface. These results indicate that the PEG-hirudin surfaces are generally protein resistant and that they interact specifically with thrombin. When PEG-hirudin surfaces were incubated with thrombin solutions, the enzymatic activity decreased suggesting retention of thrombin inhibitory activity of the immobilized hirudin. Hirudin attached via previously immobilized PEG (sequential surface) showed greater thrombin inhibitory activity than when attached as a preformed PEG conjugate (direct surface), probably due to masking of binding sites by PEG in the conjugate.

Acknowledgements

Work supported by NSERC (Canada) and the Canadian Institutes of Health Research (CIHR). An NSERC (PGS/D) scholarship to S. Alibeik is gratefully acknowledged.

References

[1] B.D. Ratner and S.J. Bryant, Annu. Rev. Biomed. Eng., 6 (2004) 41.
[2] N.A. Alcantar, E.S. Aydil and J.N. Israelachvili, J. Biomed. Mater. Res., 51 (2000) 343.
[3] M.C. Shen, L. Martinson, M.S. Wagner, D.G. Castner, B.D. Ratner and T.A. Horbett, J. Biomater. Sci. Polym. Ed., 13 (2002) 367.
[4] M.C. Tanzi, Expert Review of Medical Devices, 2 (2005) 473.
[5] H. Chen, Z. Zhang, Y. Chen, M.A. Brook and H. Sheardown, Biomaterials, 26 (2005) 2391.
[6] J.L. Brash, J. Biomater. Sci. Polym. Ed., 11 (2000) 1135.
[7] Y.J. Du and J.L. Brash, J. Appl. Polym. Sci., 90 (2003) 594.
[8] W.G. McClung, D.L. Clapper, A.B. Anderson, D.E. Babcock and J.L. Brash, J. Biomed. Mater. Res. A, 66A (2003) 795.
[9] J.S. Bae, E.J. Seo and I.K. Kang, Biomaterials, 20 (1999) 529.
[10] H. Chen, Y.X. Zhang, D. Li, X.Y. Hu, L. Wang, W.G. McClung and J.L. Brash, J. Biomed. Mater. Res. A, 90A (2009) 940.
[11] F. Markwardt, Cardiovasc. Drug Rev., 10 (1992) 211.

[12] M.G. Grutter, J.P. Priestle, J. Rahuel, H. Grossenbacher, W. Bode, J. Hofsteenge and S.R. Stone, Embo J., 9 (1990) 2361.
[13] M.D. Phaneuf, M. Szycher, S.A. Berceli, D.J. Dempsey, W.C. Quist and F.W. LoGerfo, Artif. Organs, 22 (1998) 657.
[14] B. Seifert, P. Romaniuk and T. Groth, Biomaterials, 18 (1997) 1495.
[15] J. Lahann, D. Klee, W. Pluester and H. Hoecker, Biomaterials, 22 (2001) 817.
[16] M.K. Horne and K.J. Brokaw, Thromb. Res., 112 (2003) 111.
[17] S. Ferretti, S. Paynter, D.A. Russell, K.E. Sapsford and D.J. Richardson, Trac-Trends Anal. Chem., 19 (2000) 530.
[18] L.D. Unsworth, Z. Tun, H. Sheardown and J.L. Brash, J. Colloid Interface Sci., 281 (2005) 112.
[19] S. Tokumitsu, A. Liebich, S. Herrwerth, W. Eck, M. Himmelhaus and M. Grunze, Langmuir, 18 (2002) 8862.
[20] S. Tosatti, S.M. De Paul, A. Askendal, S. VandeVondele, J.A. Hubbell, P. Tengvall and M. Textor, Biomaterials, 24 (2003) 4949.
[21] W.G. McClung, D.L. Clapper, S.P. Hu and J.L. Brash, J. Biomed. Mater. Res., 49 (2000) 409.
[22] M.E. Price, R.M. Cornelius and J.L. Brash, Biochim. Biophys. Acta-Biomembr., 1512 (2001) 191.
[23] L.C. Knight, A.Z. Budzynski and S.A. Olexa, Thromb. Haemost., 46 (1981) 593.
[24] Y.J. Du, R.M. Cornelius and J.L. Brash, Colloids and Surfaces B-Biointerfaces, 17 (2000) 59.
[25] A. Yamazaki, F.M. Winnik, R.M. Cornelius and J.L. Brash, Biochim. Biophys. Acta-Biomembr., 1421 (1999) 103.
[26] H. Sheardown, R.M. Cornelius and J.L. Brash, Colloids and Surfaces B-Biointerfaces, 10 (1997) 29.
[27] M.A.C. Stuart, W.M. de Vos and F.A.M. Leermakers, Langmuir, 22 (2006) 1722.
[28] X.L. Sun, H. Sheardown, P. Tengvall and J.L. Brash, J. Biomed. Mater. Res., 49 (2000) 66.
[29] J.L. Brash, C.F. Scott, P. Tenhove, P. Wojciechowski and R.W. Colman, Blood, 71 (1988) 932.
[30] V. De Filippis, G. Colombo, I. Russo, B. Spadari and A. Fontana, Biochemistry, 41 (2002) 13556.
[31] R.M. Cornelius, J. Archambault and J.L. Brash, Biomaterials, 23 (2002) 3583.
[32] J. Lahann, W. Pluster, T. Rodon, M. Fabry, D. Klee, H.G. Gattner and H. Hocker, Macromol. Sci., 2 (2002) 82.
[33] Q.D. Dang and E. Dicera, J. Protein Chem., 13 (1994) 367.

CHAPTER 4. SURFACE MODIFICATION WITH POLYETHYLENE GLYCOL-CORN TRYPSIN INHIBITOR CONJUGATE FOR INHIBITION OF CONTACT FACTOR PATHWAY ON BLOOD-CONTACTING SURFACES

Authors: **Sara Alibeik**, Shiping Zhu, Jonathan W. Yau, Jeffrey I. Weitz, John L. Brash

Publication Information: In Press, Acta Bioamterialia, 2011

Acceptance Date: July 25, 2011

Working Hypothesis:

Improved blood compatibility may be obtained by surface modification using a combination of PEG for protein resistant properties and corn trypsin inhibitor for inhibition of contact factor pathway of coagulation cascade. The method of modification may play a role on the interactions of surface with plasma proteins.

Surface modification with polyethylene glycol-corn trypsin inhibitor conjugate for inhibition of contact factor pathway on blood-contacting surfaces

Sara Alibeik[a], Shiping Zhu[a,b], Jonathan W. Yau[a], Jeffrey I. Weitz[a,c] and John L. Brash[a,b*]

[a] School of Biomedical Engineering, McMaster University, 1280 Main St. West, Hamilton, ON, Canada, L8S 4K1

[b] Department of Chemical Engineering, McMaster University, 1280 Main St. West, Hamilton, ON, Canada, L8S 4L7

[c] Departments of Medicine and Biochemisrty and Biomedical Sciences, McMaster University, 1280 Main St. West, Hamilton, ON, Canada, L8S 4L8

*Corresponding author: JL Brash,
School of Biomedical Engineering
McMaster University
Hamilton, ON
Canada L8S 4L8
Ph: 905 525 9140 x 24946
Fax: 905 528 1054
email: brashjl@mcmaster.ca

Abstract

Blood contacting surfaces bind plasma proteins and trigger coagulation by activating factor XII (FXII). The objective of this work is to develop blood contacting surfaces having the dual properties of protein resistance and inhibition of coagulation. Gold was used as a model substrate because it is amenable to facile modification using gold-thiol chemistry and to detailed surface characterization. The gold was modified with both polyethylene glycol (PEG) and corn trypsin inhibitor (CTI), a potent and specific inhibitor of activated FXII (FXIIa). Two methods of surface modification were developed; sequential and direct. In the sequential method, PEG was first chemisorbed on gold; CTI was then attached to the PEG. In the direct method, a conjugate of PEG and CTI was first prepared; the conjugate was then immobilized on gold. The surfaces were characterized by water contact angle and XPS. Biointeractions with the modified surfaces were assessed by measuring fibrinogen adsorption from buffer and plasma and by immunoblot analysis of eluted proteins after plasma exposure. Inhibition of FXIIa, autoactivation of FXII, and clotting times of plasma in contact with the surfaces were also measured. Both the sequential and direct surfaces showed reduced protein adsorption, increased FXIIa inhibition and longer clotting times compared with controls. Although the CTI density was lower on surfaces prepared using the sequential method, surfaces so prepared exhibited greater CTI activity than those generated by the direct method. It is concluded that the activity of immobilized PEG-CTI depends on the method of attachment and that immobilized CTI may be useful to render biomaterials more blood compatible.

Key words: Corn trypsin inhibitor, PEG, protein resistance, anticoagulant, blood compatibility.

1. Introduction

Current blood contacting devices have limitations because they trigger thrombus formation [1] resulting in device failure. Protein adsorption is the first event when blood contacts the material in such devices; this leads to platelet adhesion and thrombin generation [1-3]. Approaches to this problem have focused on reducing protein adsorption by modifying surfaces with hydrophilic polymers such as polyethylene glycol [4-7]. Attachment of bioactive molecules has also been investigated as a means of promoting the specific adsorption of proteins that may endow the surface with anticoagulant or antithrombotic properties [8, 9]. Heparin, for example, can attenuate clot formation by binding antithrombin and enhancing its capacity to inhibit thrombin, factor Xa and other clotting enzymes [10]. In more recent studies, combinations of PEG and bioactive molecules have been used to modify surfaces [11, 12].

Most of the bioactive molecules used for surface modification to prevent clot formation target the later stages of the coagulation cascade [9, 12-14]. In this work we focus on the first step of the coagulation cascade, i.e. the activation of FXII to FXIIa. Corn trypsin inhibitor (CTI) was used as the surface modifier to bind and inhibit FXIIa. CTI, a ~12,500 Da protein derived from corn kernels, is a known specific and potent inhibitor of FXIIa [15, 16]. In other work in our labs, commercial catheter surfaces were modified with CTI [17] and showed improved blood compatibility compared with unmodified catheters. In the work reported here, two different methods of surface modification using both PEG to inhibit nonspecific protein adsorption and CTI to inhibit

coagulation were developed. Gold was used as a model substrate because it is amenable to facile modification via gold-thiol chemistry and to detailed surface characterization.

It should be recognized that CTI inhibits FXIIa by formation of a 1:1 molar complex and thus on a surface inhibition will be limited by the amount of CTI present. Heparin, which inhibits activation of later steps in the coagulation pathway, does so by a catalytic mechanism and is thus in principle "renewable". It is important to point out, however, that by blocking upstream at the root cause of surface-induced activation of clotting, as anticipated for CTI, a stoichiometric inhibitor may be effective.

2. Materials and methods

(2,2'-Dithiobisethylhepa(ethylene glycolic) acid)-N-succinimidyl ester (PEG-NHS ester disulfide), MW=1109 (A, Fig 1a), was from Polypure AS (Oslo, Norway). Maleimide PEG amine (MW=2000, B, Fig 1a) was from JenKem Technology USA Inc. (Allen, TX). α-hydroxy-ω-thio polyethylene glycol (MW=1100, D in Fig 1a) was from Polymer Source Inc. (Montreal). Hydrogen peroxide, ammonium hydroxide, ethanol, 2-iminothiolane-HCl (Traut's reagent) and ethylene diamine tetraacetic acid (EDTA) were from Sigma-Aldrich (Oakville, ON). CTI was from Haematologic Technologies Inc. (Essex Junction, VT). FXII and FXIIa were from Enzyme Research Laboratories (South Bend, IN). Pefachrome XIIa, a FXIIa-directed chromogenic substrate, was from Pentapharm Ltd. (Basel, Switzerland). PD-10 desalting columns were from GE Healthcare (Baie d'Urfe, Quebec). Silicon wafers sputter-coated with titanium and then gold (1000Å), from Silicon Valley Microelectronics Inc. (Santa Clara, CA), were cut into

0.5 x 0.5 cm squares. The plasma used in the experiments was from blood collected from a minimum of 10 healthy volunteers. The volunteers were aspirin-free and antihistamine-free for a minimum of 10 days prior to donating. Blood was collected into polypropylene centrifuge tubes containing acid citrate dextrose (ACD, 1 part ACD, 6 parts whole blood) and mixed gently. It was centrifuged for 5 min at 2500 x g to give platelet rich plasma (PRP). The supernatant was centrifuged again for 5 min at 2500 x g to give platelet poor plasma (PPP). The plasma was stored at -70ºC. This procedure has ethics approval from McMaster University (McMaster University ethics protocol #04-046).

2.1 Surface preparation

A solution containing one part 30% hydrogen peroxide, one part 30% ammonium hydroxide and five parts water was used to clean the gold-coated silicon wafers (5 min, 85ºC). Cleaned surfaces were rinsed with deionized water three times, five minutes each time, prior to the modification procedure.

To convert the primary amino groups of CTI to thiol groups, CTI was incubated with a 5-fold molar excess of 2-iminothiolane-HCl (Traut's reagent) for 1 h at room temperature in phosphate buffered saline (PBS)-2mM EDTA (pH 8) and dialyzed against PBS-2 mM EDTA (pH 6) for 16 h to remove residual reagent (Fig 1b, reaction (I)). The thiol-modified CTI (Thiol-CTI) was then used for conjugation to PEG and surface modification. Gold surfaces were modified using either a sequential or a direct method.

For the sequential method, PEG-NHS ester disulfide (1 mM in ethanol) was first immobilized on gold by chemisorption for 2 h at room temperature under nitrogen purge.

This was followed by incubation with maleimide PEG amine (1 mM in buffer) for 2 h at room temperature and then with thiol-CTI (15 μM in buffer) for 2 h at room temperature and for 16 h at 4ºC (Fig 1b, reaction (II)).

For the direct method, maleimide PEG amine was reacted with thiol-CTI (1:5 molar ratio) for 2 h at 37°C and 16 h at 4ºC (Fig 1b, reaction (III)). Excess PEG was removed using a PD-10 column equilibrated with PBS (pH 7.4). Amine-PEG-CTI conjugate was then reacted with PEG-NHS ester disulfide (1 mM in buffer) for 16 h at 4°C. Excess PEG was removed using a PD-10 column with PBS (pH 7.4) as eluent. The final conjugate (concentration, 15 μM in buffer) was immobilized on gold by chemisorption under nitrogen purge for 2 h at room temperature and 16 h at 4ºC.

Gold coated silicon wafers and surfaces prepared by chemisorption of SH-PEG-OH (1 mM) (Fig 1b, reaction (IV)) and chemisorption of thiol-CTI (15 μM in buffer) on gold (Fig 1b, reaction (V)) were used as controls.

At the end of each step of surface modification, surfaces were rinsed three times with deionized water, 5 min each time. They were either used immediately for characterization and biointeraction experiments or were dried and stored under nitrogen.

2.2 Mass Spectrometry

Matrix-assisted laser desorption/ionization, time of flight (MALDI-TOF) mass spectra of CTI, thiol-CTI and PEG-CTI conjugates were obtained with a view to confirming the conjugation reactions (Waters/Micromass MALDI Micro MX).

a) Chemicals

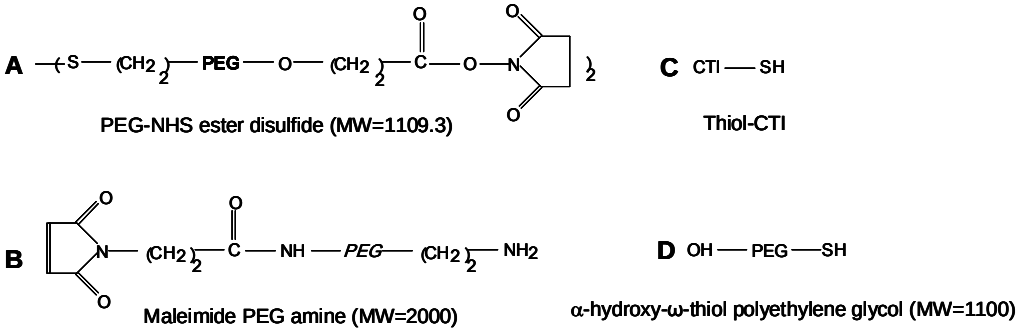

b) Surface modification procedure

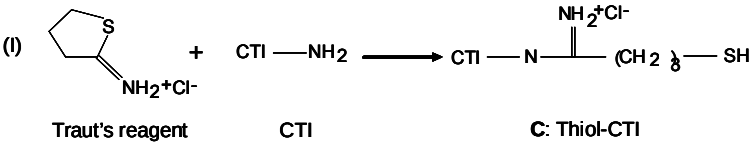

Sequential method

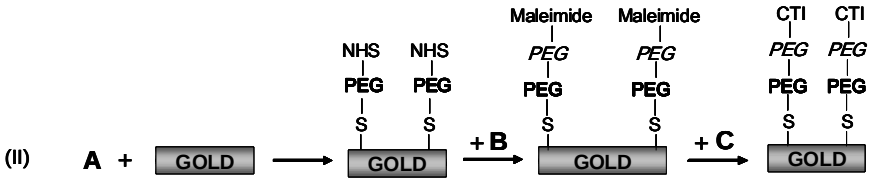

Direct method

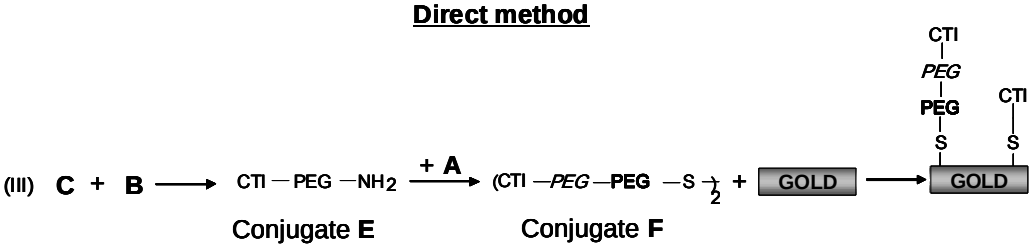

Control surfaces

Fig 1

Fig 1. a) Reagents used in the surface modification reactions, and b) Surface modification reactions. (I) Introducing thiol groups to CTI. (II) Sequential method. (III) Direct method. (IV) Au-PEG-OH control surface. (V) Au-CTI control surface.

2.3 Surface characterization

Advancing and receding water contact angles were measured using the sessile drop method (Ramé-Hart NRL C.A. goniometer, Mountain Lakes, NJ)). A self-nulling, single wavelength (6328Å) ellipsometer (Exacta 2000) was used to measure the thickness of chemisorbed layers on the modified surfaces. The incident angle was 70º. For the gold substrate, the refractive index and extinction coefficient were taken as 0.2 and 3.5 respectively [12]. For PEG-modified surfaces and PEG-CTI modified surfaces, the refractive indices were taken as 1.475 and 1.465 respectively [18, 19]. X-ray photoelectron spectroscopy (XPS) was conducted using a Thermo Scientific Theta Probe instrument. Low resolution spectra were obtained to determine surface chemical compositions. Take off angles of 70º, 50º and 30º were used (angles defined with respect to the normal; smaller angle, greater sampling depth).

2.4 Determination of CTI surface density

Thiol-CTI and PEG-CTI conjugates were labeled with ^{125}I using the Iodo-gen method [20]. Sequential and direct surfaces were prepared as described in section 2.1 using the radiolabeled protein and radiolabeled conjugate, respectively. CTI density on the surfaces was determined by counting radioactivity and comparing with solutions of known concentration [21].

2.5 Protein and blood interactions

Fibrinogen (Fg) adsorption from buffer and plasma was studied using ^{125}I-labeled Fg (ICl method) as a tracer added to the buffer solution or plasma [22]. Total Fg concentration for the buffer experiments was 1 mg/mL. For the plasma experiments, solutions consisted of 50% pooled normal citrated human plasma and 50% phosphate buffered saline (PBS). Cold NaI (0.218 g/L) was added to suppress free radioactive iodide adsorption to the gold [23].

SDS-PAGE and immunoblot analyses of proteins eluted from the surfaces after 3 h exposure to pooled normal citrated human plasma were carried out. Details are given elsewhere [24]. The proteins were eluted by incubation with 2% SDS for 16 h. The eluates were run on reduced SDS-PAGE (12%) gels and transferred to polyvinylidene fluoride (PVDF) membranes for blotting. 3 mm wide strips of membrane were incubated with primary and enzyme-conjugated secondary antibodies and then with NBT/BCIP substrate (Pierce, Rockford, IL) to visualize the protein bands.

A chromogenic substrate assay was used to determine the activity of the synthesized thiol-CTI and PEG-CTI conjugates in solution. 6 μL of a 1 mg/mL solution of thiol-CTI or PEG-CTI conjugate was added to 150 μL of 50 nM FXIIa solution in TBS (pH 7.4) containing 2 mM $CaCl_2$, 12.5 μM $ZnCl_2$ and 15.4 μM bovine serum albumin (BSA). After 1 h incubation at room temperature, 50 μL of 1.6 mM chromogenic substrate (Pefachrome) solution was added and samples were immediately placed in a UV-vis plate reader. The optical density was recorded at 405 nm as a function of time.

The ability of the modified surfaces to bind and inhibit FXIIa was also investigated using a chromogenic substrate assay. Surfaces were incubated with 100 μL of 25 nM FXIIa solution in TBS (pH 7.4) containing 2 mM $CaCl_2$, 12.5 μM $ZnCl_2$ and 15.4 μM BSA in a 96-well plate format for 1 h at room temperature. 50 μL of a 1.6 mM solution of chromogenic substrate (Pefachrome) solution was then added to the wells. The plate was immediately placed in a UV-vis plate reader and the optical density was recorded at 405 nm as a function of time.

FXII autoactivation was measured using the chromogenic substrate assay in multiwell plate format. Surfaces were incubated with 100 μL of 50 nM FXII in TBS (pH 7.4) containing 2 mM $CaCl_2$, 12.5 μM $ZnCl_2$ and 15.4 μM BSA for 15 min at room temperature. 33 μL of a 1.6 mM solution of chromogenic substrate was then added and the optical density at 405 nm recorded as a function of time.

Clotting time was measured for thiol-CTI and CTI conjugates in solution. 5 μg of each was added to 96-well plates and incubated with 100 μL of pooled normal citrated human plasma for 15 min at 37˚C. 100 μL of 0.025 M $CaCl_2$ was then added to each well and optical density at 405 nm was recorded. On surfaces, clotting times were measured by incubating surfaces with 100 μL of pooled normal citrated human plasma for 15 min at 37˚C and then adding 100 μL of 0.025 M $CaCl_2$. Optical density at 405 nm was recorded. The time to reach half maximum was estimated using the instrument software.

2.6. Statistical analysis

Analysis of variance (ANOVA) was carried out to determine whether significant differences existed in groups of data. The Student t-test was conducted as a post-hoc test to compare surface pairs. Differences were considered significant for $p < 0.05$. Data are reported as mean ± SD.

3. Results and discussion

3.5 PEG-CTI conjugation

MALDI mass spectra of CTI were obtained before and after thiolation. The expected molecular weight increase of about 137 Da, corresponding to the addition of a molecule of Traut's reagent, was observed (Fig 2a and 2b). This result confirms that one primary amino group of CTI, most probably the N-terminal, was converted to thiol. Fig 2a shows the mass spectrum of the CTI before any modification. CTI molecular weight reported in the literature ranges from 12,000 to 14,000 Da [15, 16]. The spectrum showed two main peaks at 12,930 m/z and 13,230 m/z (Fig 2a). It has been observed by mass spectrometry that CTI exists in three forms which differ in the number amino acid residues [25]. From Fig 2a it appears that our sample contained two forms. When CTI was modified with Traut's reagent (Fig 2b) the peaks shifted by ~100 amu, indicating that both forms were modified.

MALDI-MS of the product of reaction of HS-CTI with maleimide-PEG-amine (Fig 2c) showed two major peaks centered at 13,350 and 15,500 m/z. These are attributed to unchanged HS-CTI and HS-CTI conjugated to maleimide-PEG-amine (MW 2000 Da),

respectively. The area ratio of these peaks indicates that the reaction product consisted of about 1/3 conjugated and 2/3 unchanged HS-CTI. On reaction of PEG-NHS ester disulfide (A in Fig 1, MW 1109 Da) with this mixture an increase of ~1000 m/z was observed in the higher mass peak indicating that the CTI-PEG-NH_2 conjugate (E) was converted to disulfide-PEG-CTI conjugate F (Fig 2d) essentially quantitatively. The product of these reactions, containing disulfide-PEG-CTI conjugate and unchanged HS-CTI, was used for surface modification by the direct method (reaction (III), Fig 1b).

From the MALDI-MS data, it is clear that for surfaces prepared by the direct method (reaction III, Fig 1b) the modifier solution contained unconjugated thiol-CTI as well as PEG-conjugated CTI in the ratio of ~2:1. Chemisorption of unconjugated thiol-CTI as well as PEG-CTI conjugate to the gold substrate would therefore be expected to occur as indicated.

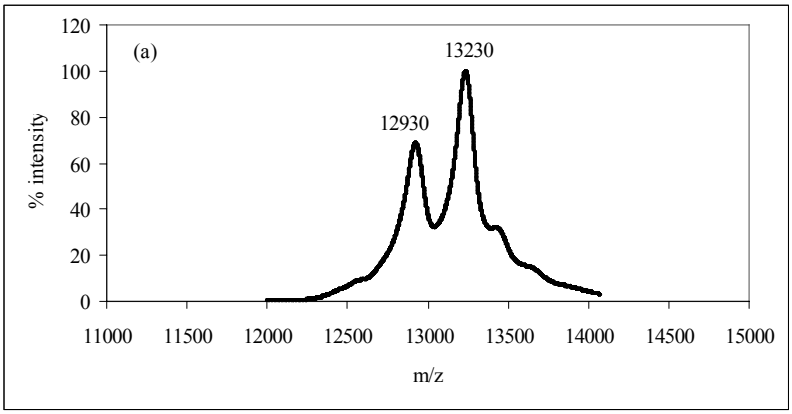
(a)
13230
12930
% intensity
m/z
120
100
80
60
40
20
0
11000
11500
12000
12500
13000
13500
14000
14500
15000

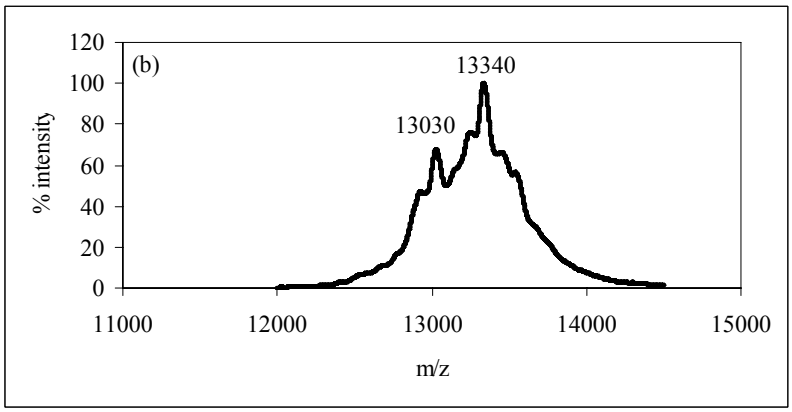
(b)
13340
13030
% intensity
m/z
120
100
80
60
40
20
0
11000
12000
13000
14000
15000

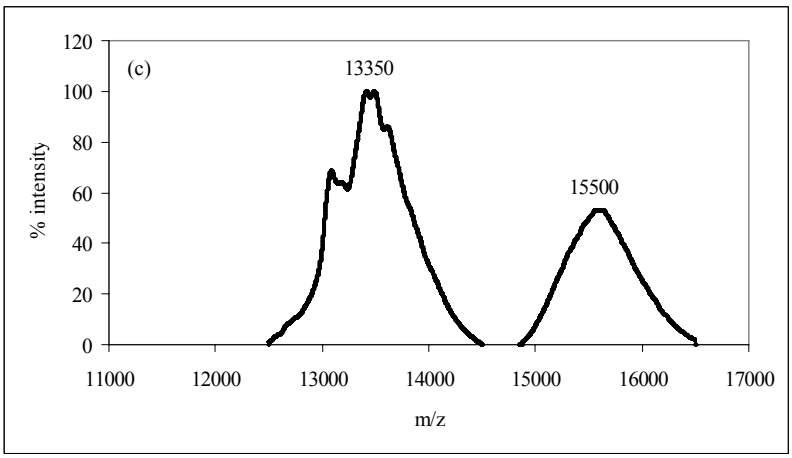
(c)
13350
15500
% intensity
m/z
120
100
80
60
40
20
0
11000
12000
13000
14000
15000
16000
17000

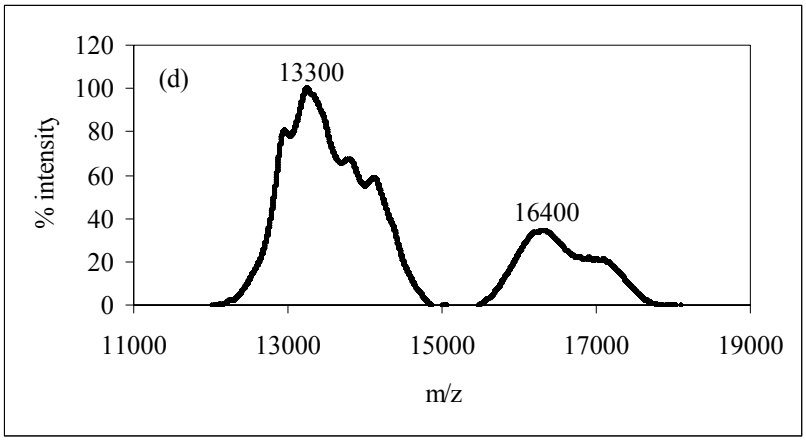

Fig 2. MALDI-MS of CTI: (a) Before modification. (b) After thiol modification. (c) After conjugation to amino-PEG-maleimide. (d) After conjugation to PEG-NHS ester disulfide.

3.6 Surface characterization and composition

The water contact angles decreased significantly upon PEG attachment to gold (Fig 3). The angles were higher on the PEG-CTI surfaces than on the PEG-alone surface, suggesting that introduction of CTI caused an increase in hydrophobicity.

The direct method gave surfaces of higher contact angle than the sequential method. Two factors may be responsible: first, initial immobilization of PEG by the sequential method may create a relatively dense layer of PEG of low contact angle; second, the higher density of CTI obtained by the direct method. The angles were similar on the Au-CTI and direct surfaces indicating that the latter contained a significant quantity of CTI chemisorbed directly to gold.

The thickness of the modifying layers ranged from 10 to 23 Å as determined by ellipsometry (Table 1). The lowest value was seen on the PEG-alone surface. The thickness was higher and similar for the other three surfaces.

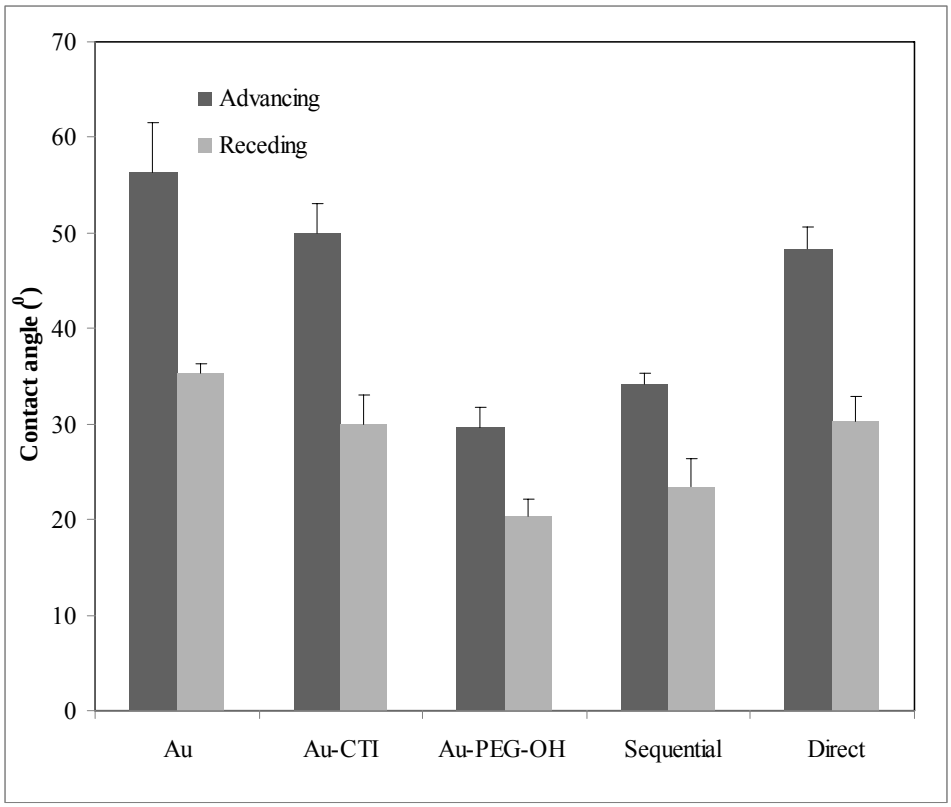

Fig 3. Water contact angles for gold and modified gold surfaces. Data are mean ± SD, n>9.

Table 1. Ellipsometry data for control and modified surfaces (mean±SD, n=6)

Surface	Film Thickness (Å)
Au-PEG-OH	10 ±3
Au-CTI	18±8
Sequential	23 ±5
Direct	21 ±9

To determine the density of CTI on the modified surfaces, ^{125}I-labeled thiol-CTI or ^{125}I-labeled PEG-CTI conjugate were used to prepare sequential and direct surfaces. ^{125}I-labeled thiol-CTI was chemisorbed to bare gold to prepare Au-CTI surfaces. The bare gold surface showed the highest CTI density (Fig 4). With 10 cysteine residues (albeit

involved in disulfide bonds) and one free cysteine introduced by Traut's reagent, CTI is expected to chemisorb extensively to gold. The sequential surface showed lower CTI density than the direct, possibly due to the resistance of the pre-immobilized PEG layer to the "approach" of CTI. A similar result was obtained in work on PEG-hirudin modified surfaces [12]. The higher CTI density on the direct surface correlates with the higher water contact angle.

Surface area coverage of CTI on the modified surfaces was estimated by assuming the dimensions of CTI to be similar to those of lysozyme (MW, 14,000 Da; 45Å x 30Å x 30Å) [26]. A close packed monolayer of CTI having these dimensions should contain 0.16-0.25 μg/cm^2 depending on orientation; CTI coverage was thus estimated as 28 to 44% of monolayer for the sequential surface, and 64-100% for the direct. On the bare gold surface, coverage was very close to 100%.

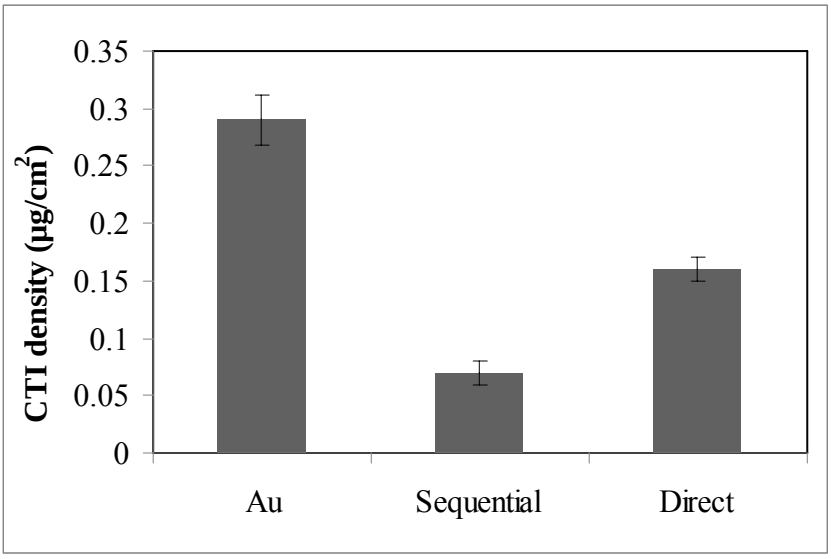

Fig 4. CTI density on PEG-CTI surfaces. Data are mean ± SD, n=9.

Low resolution XPS data (Fig 5) showed that the unmodified gold surface was contaminated with carbon- and oxygen-containing materials. Such contamination is difficult to prevent in a typical laboratory environment [27]. It is believed to be largely displaced when thiols are chemisorbed [27, 28]. To minimize contamination, surfaces were freshly cleaned and stored under nitrogen prior to XPS. As seen in Fig 5, the gold content was lower on the modified surfaces than on the unmodified gold at all take-off angles, while the carbon, oxygen and sulfur contents were higher, confirming the presence of PEG and CTI on these surfaces. Increases in sulfur content on Au-PEG-OH and Au-PEG-CTI surfaces compared with unmodified gold were due to sulfur from the thiolated PEG-OH and PEG-CTI. On the PEG-CTI surfaces, sulfur also originates from the 10 cysteine residues of CTI [16].

On the PEG-alone surface, the C:O ratio was close to 2:1 at all angles corresponding to PEG itself.

As expected, nitrogen was present on the CTI surfaces due to the amino and amide groups of CTI. Since the CTI density was higher on the direct surface, a higher content of nitrogen was expected for this surface, but this was not observed. We have no explanation at present for this observation.

At 70º take-off angle (smallest sampling depth, closest to surface), the gold content was lower than at 30º for all surfaces. For the CTI surfaces carbon, oxygen and nitrogen were greater, thus further confirming the presence of PEG and PEG-CTI.

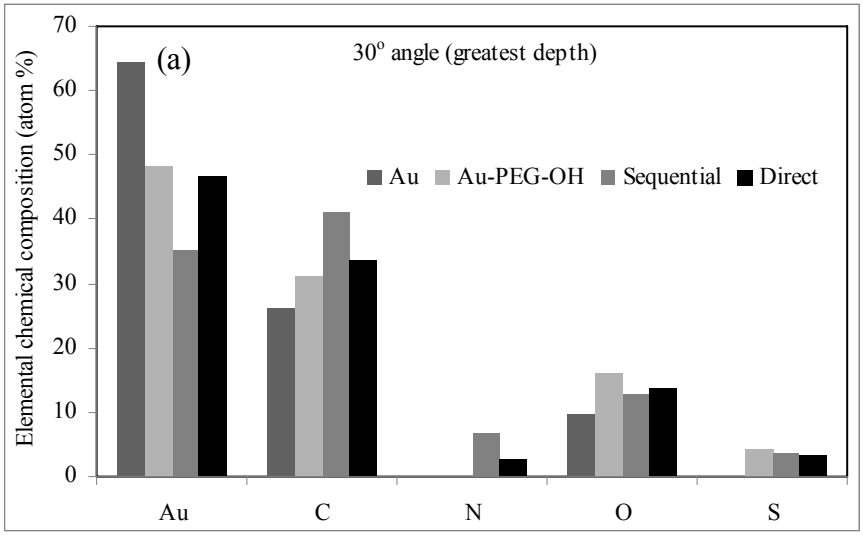
(a)
30° angle (greatest depth)
Au
Au-PEG-OH
Sequential
Direct
Elemental chemical composition (atom %)
70
60
50
40
30
20
10
0
Au
C
N
O
S

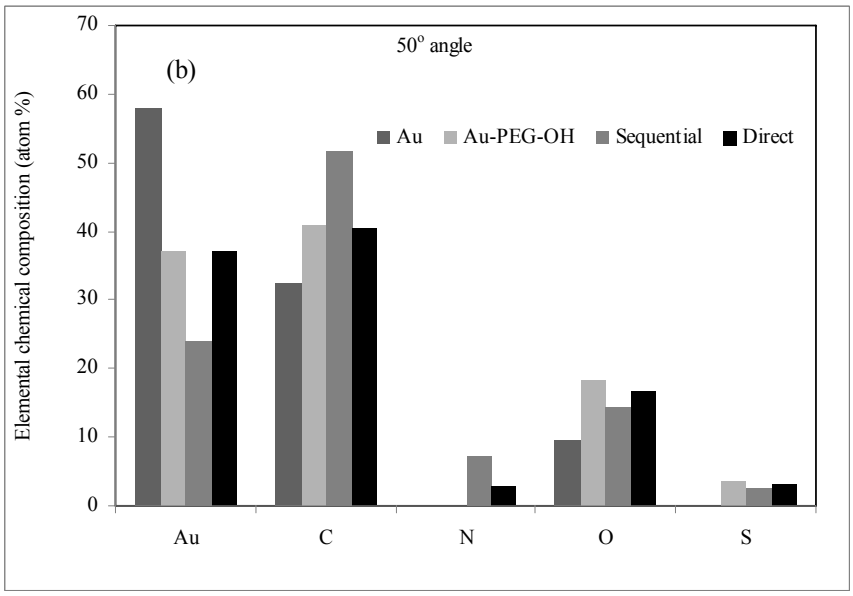
(b)
50° angle
Au
Au-PEG-OH
Sequential
Direct
Elemental chemical composition (atom %)
70
60
50
40
30
20
10
0
Au
C
N
O
S

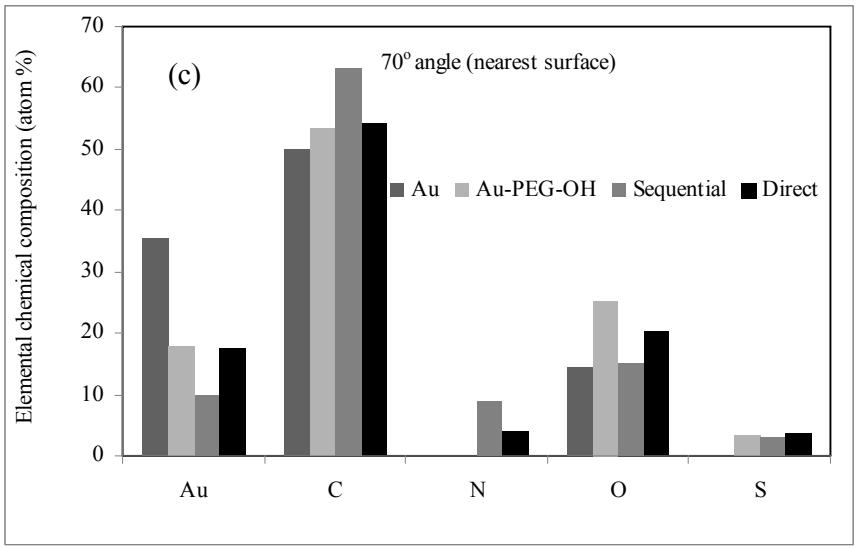

Fig 5. Composition of surfaces from XPS. (a) 30° take off angle, (b) 50° angle, (c) 70° angle. Data are mean of two determinations. Data precision ~5%. Take off angles are relative to the vertical: smaller value, greater sampling depth.

3.3 Biointeractions

Fibrinogen adsorption from buffer and plasma

An important consideration was whether PEG on the surface retains its protein resistance when conjugated to CTI. Fibrinogen was chosen for these experiments as an abundant blood protein and one which is relevant in the context of blood contacting materials. Adsorption from both buffer and plasma (Fig 6) was found to decrease significantly on the PEG-alone, Au-CTI and PEG-CTI surfaces compared with the gold. It should be noted that an additional PEG alone control is included. For this surface the PEG MW was 2500, the same as for the PEG-CTI surfaces, and the end group was maleimide (see Fig 1, reaction sequence II). The sequential surface showed adsorption from buffer similar to the PEG-alone surfaces, whereas the Au-CTI and direct surfaces showed significantly higher adsorption. The initially immobilized PEG layer on the

sequential surface may be responsible for this difference. Based on the CTI density measurements, relatively low CTI coverage was achieved on the sequential surface so that it is unlikely that all of the PEG chains were "covered" by CTI. These "free" PEG chains could contribute to the low fibrinogen adsorption on this surface. On the direct surface, the presence of significant CTI not conjugated to PEG may also contribute to the higher adsorption seen on this surface.

In the multi-protein environment of plasma, both the direct and sequential surfaces adsorbed amounts of fibrinogen similar to the PEG-alone surfaces while the Au-CTI showed the highest adsorption among the modified surfaces. The data thus show that both the sequential and direct surfaces are protein resistant and that the PEG retained its resistance when conjugated to CTI. As expected, adsorption from plasma was generally much lower than from buffer for all surfaces. This is undoubtedly due to the competition for surface sites by other plasma components.

Immunoblot analysis of plasma proteins eluted from surfaces

Immunoblot data are shown in Fig 7. Antibodies directed against nine plasma proteins were used in these experiments. All of the proteins probed for were in general detected. The band intensities, however, varied from surface to surface and were lower on the PEG-alone (Fig 7b) and PEG-CTI surfaces (Fig 7c-7d) than on the unmodified gold, again indicating the protein resistant characteristics of the modified surfaces. For Fg, the band intensities were lower on the PEG-alone and PEG-CTI blots than on the unmodified gold. This trend is consistent with the labeled Fg adsorption data (Fig 6). The C3,

HMWK and vitronectin band intensities were also lower for the PEG-alone and PEG-CTI surfaces. These data support the conclusion that immobilized PEG retains its protein resistant properties when attached to CTI.

A band at 110 kDa was observed for high molecular weight kininogen (HMWK) on the plasma blot (not shown). On the surfaces two bands were observed at ~56 kDa and 46 kDa indicative of contact phase activation [29]. On the plasma blot, a band at 80 kDa was seen for FXII. The antibody directed against FXII also binds to FXIIa so the blots reflect both forms. The gold surface showed the strongest FXII band at 80 kDa most likely due to the chemisorption of FXIIa to gold. The CTI surfaces showed faint bands at 80 kDa while the PEG-only surface showed no band. Although these data are not quantitative and are not indicative of the inhibition of adsorbed FXIIa on the CTI surfaces, they may suggest that a more specific interaction with FXIIa took place on the CTI surfaces compared with the PEG-only surface.

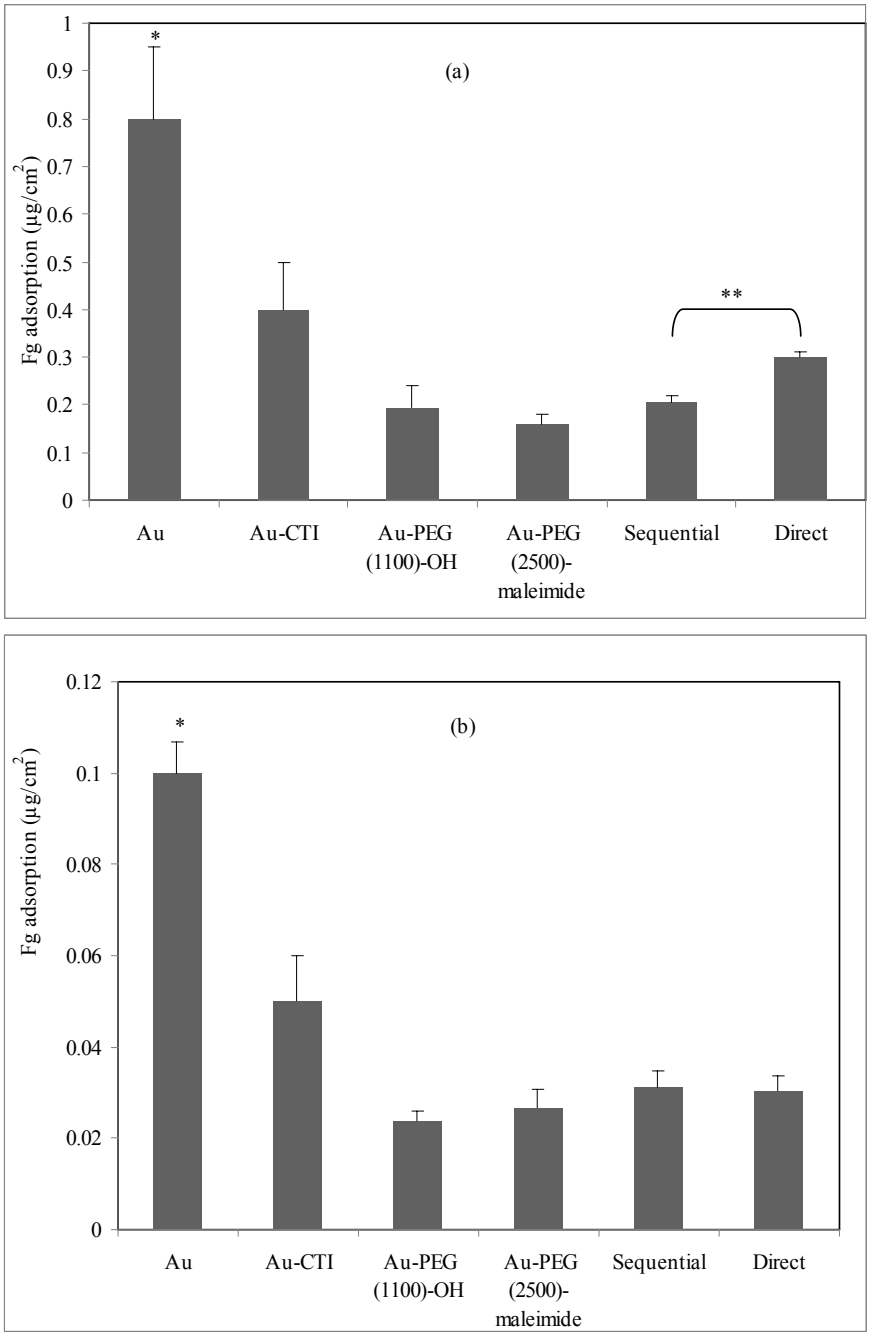

Fig 6. Fibrinogen adsorption from: (a) buffer, (b) 50% plasma. Adsorption time, 3 h. Data are mean ± SD, n=3. * indicates significant difference Au vs. other surfaces. ** indicates significant difference direct vs. sequential ($p<0.05$, Student's t-test).

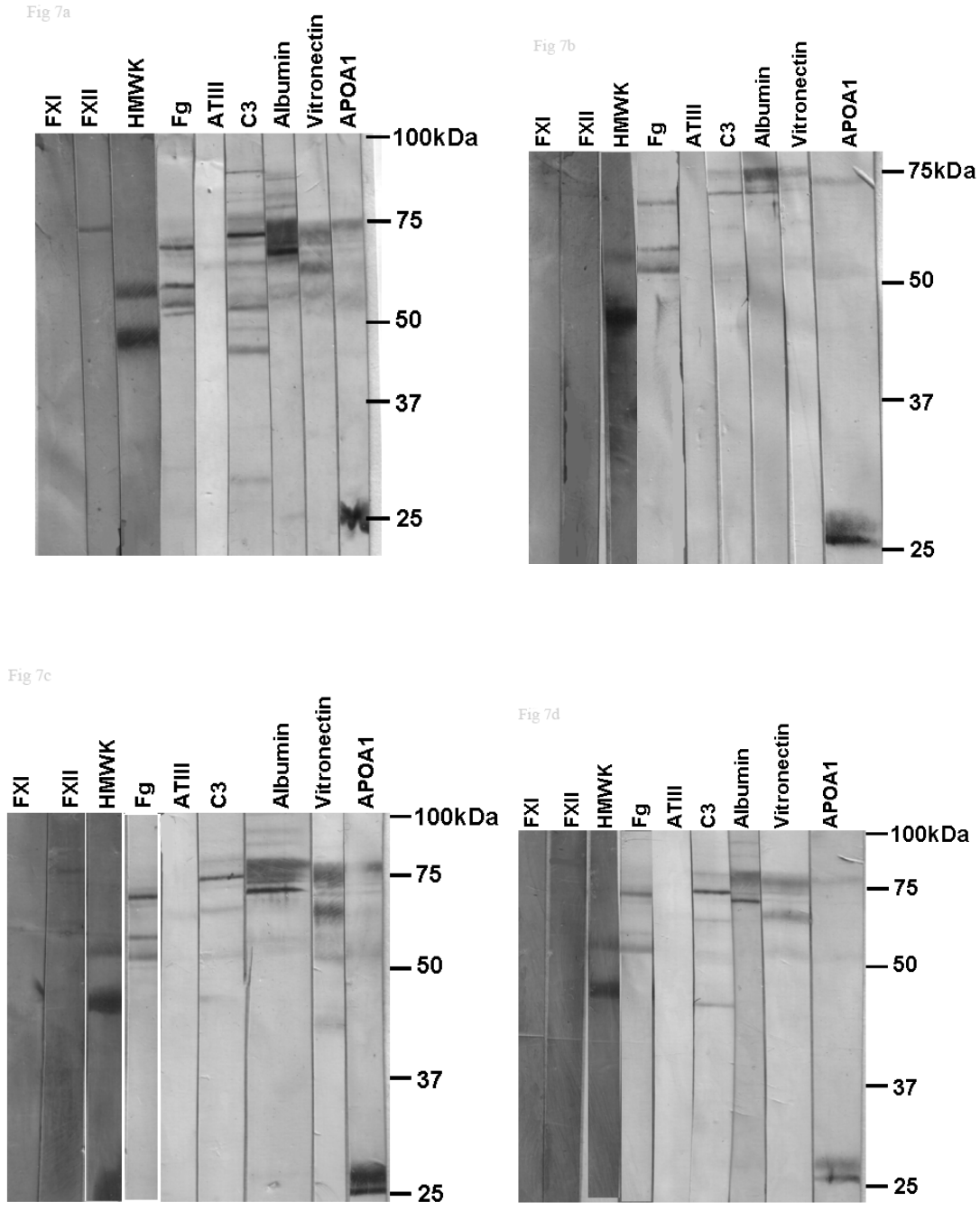

Fig 7. Immunoblots of plasma proteins eluted from surfaces exposed to plasma for 3 h. (a) Au surface, (b) Au-PEG-OH surface, (c) Sequential surface, (d) Direct surface.

FXIIa inhibition by thiol-CTI and PEG-CTI conjugates in solution

A chromogenic substrate assay was used to determine the activity of the synthesized thiol-CTI and PEG-CTI conjugates prior to surface immobilization. A solution of unmodified CTI was used as control. CTI and thiol-CTI showed 100% inhibition of FXIIa in these experiments, indicating that thiol modification did not affect the activity of the CTI. This result was not unexpected since the active site of CTI is at arginine 36-leucine 37, remote from the thiol modification sites. The PEG-CTI conjugate showed a small (not statistically significant) decrease in activity (Fig 8), possibly due to masking of the active site of FXIIa by PEG. Clearly the synthesized thiol-CTI and PEG-CTI retained significant anti-FXIIa activity.

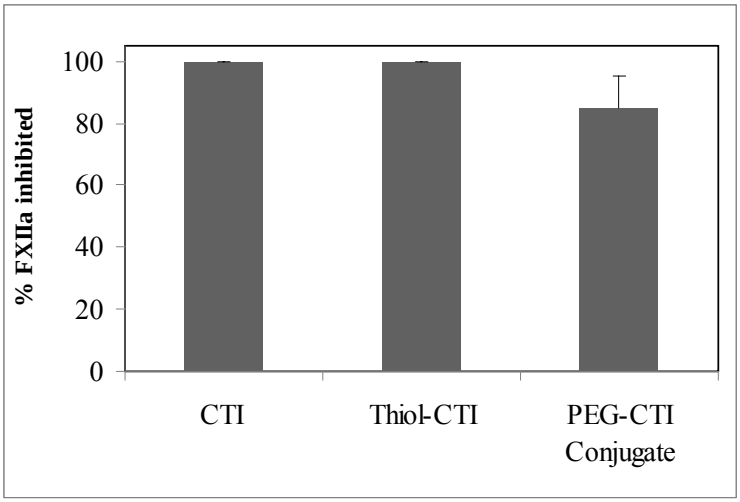

Fig 8. CTI activity after thiol modification and conjugation. Data are mean ± SD, n=3.

FXIIa inhibition by surfaces

Surfaces were incubated for 1 h with FXIIa solution prior to adding the substrate. Chromogenic substrate was then added to determine residual FXIIa activity (Fig 9). For

this experiment a new control surface was included to check on the specificity of surface CTI interactions with FXIIa. This surface was prepared by the sequential attachment of PEG and α-lactalbumin in the same manner as for the PEG-CTI sequential surface. α-Lactalbumin was chosen since it has a molecular weight of 14.2 kDa close to that of CTI. As seen in Figure 9, the PEG-CTI surface prepared by the sequential method inhibited a significantly higher fraction of CTI than the gold, PEG-alone and PEG-lactalbumin surfaces. The PEG-CTI surface prepared by the direct method, also inhibited a higher fraction of FXIIa than the Au, PEG-alone and PEG-lactalbumin surfaces. It thus appears that the PEG-CTI surfaces interact with FXIIa in a manner involving the active site to a greater extent than do the unmodified gold, PEG-alone and PEG-lactalbumin surfaces. The sequential surface inhibited more FXIIa than the direct, possibly due to the more favourable orientation of CTI on this surface. Although having significantly higher CTI density, FXIIa inhibition on the Au-CTI surface was not significantly different than the PEG-CTI.

It should be emphasized that the chromogenic assay as used in this work measures residual FXIIa in the solution following incubation with the surface. The surface can have a number of effects in this situation: nonspecific adsorption such that the active site of the adsorbed FXIIa is inaccessible to a substrate; nonspecific adsorption such that the active site is accessible; or specific adsorption involving the CTI-FXIIa interaction. It is difficult to distinguish among these effects. However, the greater inhibition on the CTI surfaces compared with the controls (especially the PEG-lactalbumin surface) suggests

that specific FXIIa-CTI interactions are occurring on these surfaces. It is likely that at higher CTI density, a much greater degree of specificity could be achieved.

To compare the different surfaces with respect to FXIIa interactions more specifically, plasma eluates were run on a single gel and blotted with an anti-FXII antibody which binds to FXIIa at 80 kDa. The data (not shown) were inconclusive, but a somewhat stronger band at 80 kDa was observed on the PEG-CTI surfaces compared with the PEG-alone and gold surfaces, again suggesting specific interactions of CTI with FXIIa.

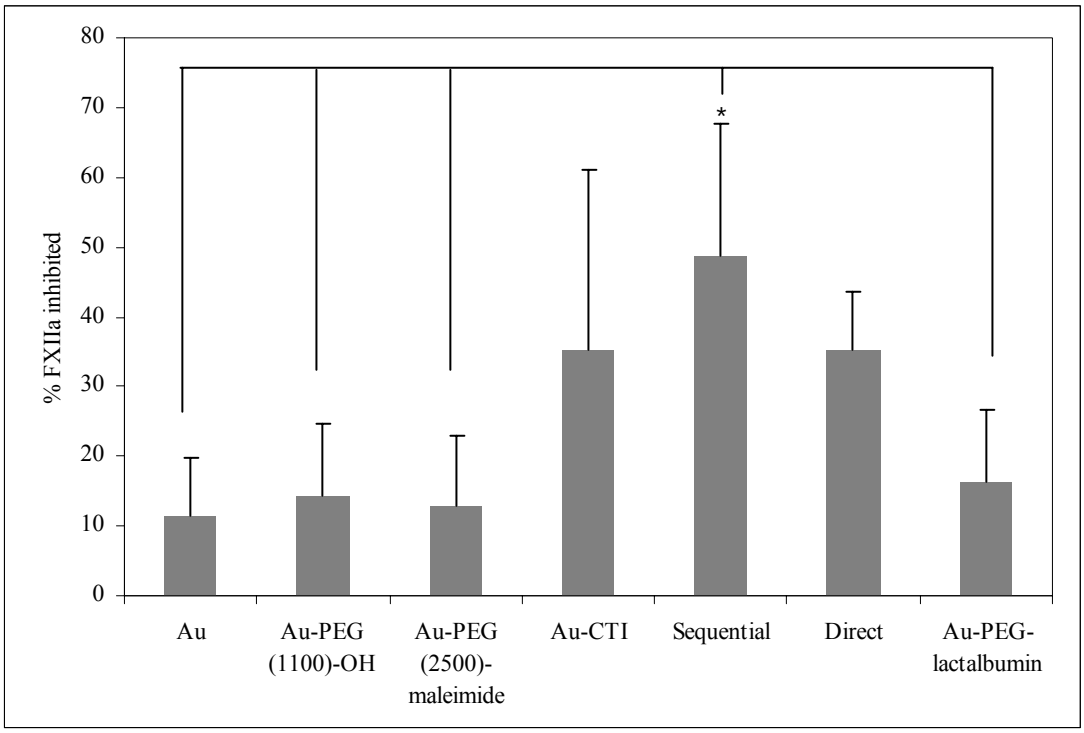

Fig 9. Activity of FXIIa solutions after incubation with control and PEG-CTI surfaces. Data are mean ± SD, n > 3. * Indicates significant difference ($p<0.05$, Student's t-test).

FXII autoactivation

FXII autoactivation on the various surfaces was also investigated. Autoactivation refers to putative conformational changes in FXII that occur upon adsorption, which

initiate activation to FXIIa [30, 31]. Surfaces were incubated with FXII solution and FXIIa generation was measured using the chromogenic substrate assay. The Au-CTI, sequential and direct surfaces showed significantly reduced FXIIa generation compared with the control gold and PEG-alone surfaces (Fig 10). These data suggest that the CTI on these modified surfaces inhibits FXII autoactivation, most likely by "neutralizing" FXIIa as it forms. In this sense the autoactivation data might be seen as the net effect of autoactivation and inhibition. Similar to the findings in the FXIIa inhibition experiments, the sequential surfaces were slightly, but not significantly, more effective than the direct and Au-CTI surfaces.

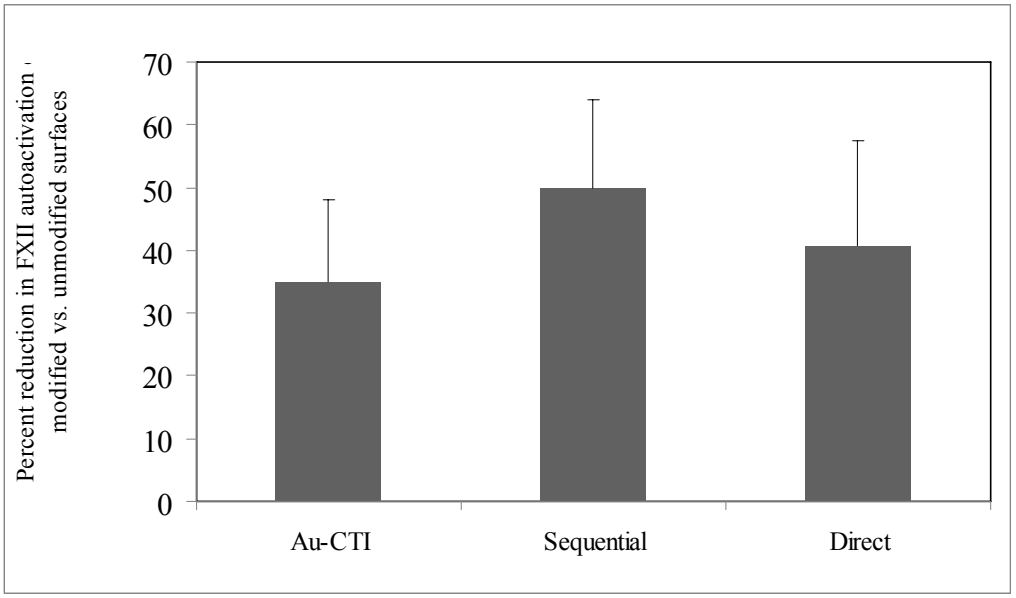

Fig 10. FXII autoactivation on PEG-CTI surfaces. Data are percent reduction in FXII autoactivation compared to control Au and Au-PEG-OH surfaces. Data are mean ± SD, n=3.

Plasma clotting times

The clotting time of plasma in the presence of 5 μg of thiol-CTI or PEG-CTI increased from 700 ± 200 s to 1,200 ± 100 s and 1,000 ± 150 s. respectively. The clotting time of plasma containing a comparable amount of unmodified CTI (5 μg) was 1,200 ± 189 s. Thus the clotting time did not change after thiol or PEG modification of CTI and its anticoagulant activity was retained.

Plasma clotting times were measured to compare the PEG-CTI surfaces with the control surfaces in terms of their procoagulant activity. The surfaces were placed in contact with citrated plasma and after incubation, the plasma was recalcified and turbidity versus time measurements were taken. The time to reach half maximum optical density was recorded (Fig 11). When no surface was present, the plasma clotted at 570 ± 80 s. For Au, Au-CTI and Au-PEG-OH the clotting times decreased to 490±105, 480±150 and 420±30 s, respectively. The PEG-CTI surfaces showed significantly longer clotting times than the Au and Au-PEG-OH. This result is in line with the FXIIa inhibition data (Fig 8). Also consistent with the inhibition data, the clotting time was longer on the sequential surface than on the direct. It is noteworthy that the Au-CTI surface (with a higher CTI density than either of the PEG-CTI surfaces) did not prolong the clotting time, suggesting that the CTI is more effectively deployed when conjugated to PEG.

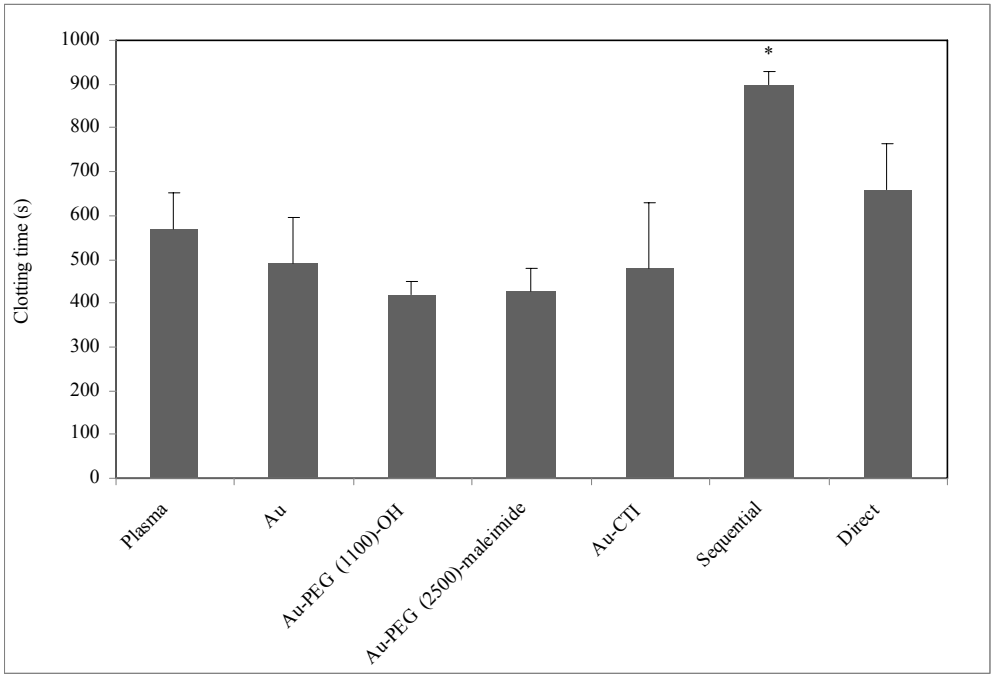

Fig 11. Plasma clotting times. Data are mean ± SD, n=3. * Indicates significant difference sequential vs. Au, Au-PEG-OH, Au-PEG-maleimide and Au-CTI surfaces ($p<0.05$, Student's t-test).

4. Conclusions

Two methods designated "sequential" and "direct" were used to modify gold with PEG and CTI. Several differences were observed between these surfaces. In particular although the CTI density was greater, the anti-FXIIa activity was lower on the direct surface. The reasons for this seeming paradox are unclear. On the sequential surface it is expected that the CTI molecules would be attached by reaction with the pre-immobilized PEG layer via the thiol end group of CTI, possibly presenting the CTI in an orientation that is favorable for interaction with FXIIa. On the other hand, it may be that the PEG moieties of the preformed conjugates (direct surface) have a masking effect on the CTI component that inhibits CTI-FXIIa interactions. Also the direct surface likely has a

significant proportion of its CTI linked directly to gold due to residual HS-CTI in the PEG-CTI conjugate reagent (reaction sequence III, Fig 1b). CTI attached in this way is of relatively low bioactivity. Thus on the Au-CTI surface (no PEG), the density of CTI was significantly higher than on the PEG-containing sequential and direct surfaces. The Au-CTI surfaces, however, were less effective in terms of anti-FXIIa activity and were less protein resistant. PEG thus appears to provide the twin benefits of protein resistance and enhancement of bioactivity due to a more favorable presentation of the CTI molecules.

Both types of PEG-CTI modified surface showed protein resistance similar to the Au-PEG surface without CTI, suggesting that the PEG retained its protein resistance when conjugated to CTI. These observations may also indicate that some "free" PEG was present on the PEG-CTI surfaces. It may also be that even with CTI present, the surfaces remain in a highly and appropriately hydrated state similar to that of a PEG-alone surface.

Overall it is concluded that modification of surfaces to inhibit the contact coagulation pathways, specifically using CTI to inhibit FXIIa, may be a useful approach for improving blood compatibility.

Acknowledgements

Work supported by the Natural Sciences and Engineering Research Council of Canada (NSERC) and the Canadian Institutes of Health Research (CIHR).

References

[1] Brash JL. Exploiting the current paradigm of blood-material interactions for the rational design of blood-compatible materials. J Biomater Sci Polym Ed 2000;11:1135-46.

[2] Ratner BD, Bryant SJ. Biomaterials: Where we have been and where we are going. Annu Rev Biomed Eng 2004;6:41-75.
[3] Chen H, Yuan L, Song W, Wu ZK, Li D. Biocompatible polymer materials: Role of protein-surface interactions. Prog Polym Sci 2008;33:1059-87.
[4] Shen MC, Martinson L, Wagner MS, Castner DG, Ratner BD, Horbett TA. PEO-like plasma polymerized tetraglyme surface interactions with leukocytes and proteins: in vitro and in vivo studies. J Biomater Sci Polym Ed 2002;13:367-90.
[5] Unsworth LD, Sheardown H, Brash JL. Polyethylene oxide surfaces of variable chain density by chemisorption of PEO-thiol on gold: Adsorption of proteins from plasma studied by radiolabelling and immunoblotting. Biomaterials 2005;26:5927-33.
[6] Jin ZL, Feng W, Zhu SP, Sheardown H, Brash JL. Protein-resistant polyurethane via surface-initiated atom transfer radical polymerization of oligo(ethylene glycol) methacrylate. J Biomed Mater Res A 2009;91A:1189-201.
[7] Heath DE, Cooper SL. Design and characterization of PEGylated terpolymer biomaterials. J Biomed Mater Res A 2010;94A:1294-302.
[8] McClung WG, Clapper DL, Anderson AB, Babcock DE, Brash JL. Interactions of fibrinolytic system proteins with lysine-containing surf aces. J Biomed Mater Res A 2003;66A:795-801.
[9] Du YJ, Brash JL, McClung G, Berry LR, Klement P, Chan AKC. Protein adsorption on polyurethane catheters modified with a novel antithrombin-heparin covalent complex. J Biomed Mater Res A 2007;80A:216-25.
[10] Bae JS, Seo EJ, Kang IK. Synthesis and characterization of heparinized polyurethanes using plasma glow discharge. Biomaterials 1999;20:529-37.
[11] Chen H, Zhang YX, Li D, Hu XY, Wang L, McClung WG, et al. Surfaces having dual fibrinolytic and protein resistant properties by immobilization of lysine on polyurethane through a PEG spacer. J Biomed Mater Res A 2009;90A:940-6.
[12] Alibeik S, Zhu S, Brash JL. Surface modification with PEG and hirudin for protein resistance and thrombin neutralization in blood contact. Colloids Surf B 2010;81:389-96.
[13] Chen H, Chen Y, Sheardown H, Brook MA. Immobilization of heparin on a silicone surface through a heterobifunctional PEG spacer. Biomaterials 2005;26:7418-24.
[14] Sun XL, Sheardown H, Tengvall P, Brash JL. Peptide modified gold-coated polyurethanes as thrombin scavenging surfaces. J Biomed Mater Res 2000;49:66-78.
[15] Hojima Y, Pierce JV, Pisano JJ. Hageman-Factor Fragment Inhibitor in Corn Seeds - Purification and Characterization. Thromb Res 1980;20:149-62.
[16] Mahoney WC, Hermodson MA, Jones B, Powers DD, Corfman RS, Reeck GR. Amino-Acid-Sequence and Secondary Structural-Analysis of the Corn Inhibitor of Trypsin and Activated Hageman-Factor. J Biol Chem 1984;259:8412-6.
[17] Yau JW, Stafford AR, Fredenburgh JC, Brash JL, Weitz JI. Immobilization of corn trypsin inhibitor on a catheter surface reduces its in vitro procoagulant properties. Annual Meeting of Society for Biomaterials. San Antonio, TX2009.
[18] Tosatti S, De Paul SM, Askendal A, VandeVondele S, Hubbell JA, Tengvall P, et al. Peptide functionalized poly(L-lysine)-g-poly(ethylene glycol) on titanium: resistance to protein adsorption in full heparinized human blood plasma. Biomaterials 2003;24:4949-58.

[19] Unsworth LD, Tun Z, Sheardown H, Brash JL. Chemisorption of thiolated poly(ethylene oxide) to gold: surface chain densities measured by ellipsometry and neutron reflectometry. J Colloid Interface Sci 2005;281:112-21.
[20] Knight LC, Budzynski AZ, Olexa SA. Radiolabeling of Fibrinogen Using the Lodogen Technique. Thromb Haemost 1981;46:593-6.
[21] McClung WG, Clapper DL, Hu SP, Brash JL. Adsorption of plasminogen from human plasma to lysine-containing surfaces. J Biomed Mater Res 2000;49:409-14.
[22] Price ME, Cornelius RM, Brash JL. Protein adsorption to polyethylene glycol modified liposomes from fibrinogen solution and from plasma. Biochim Biophys Acta-Biomembr 2001;1512:191-205.
[23] Du YJ, Cornelius RM, Brash JL. Measurement of protein adsorption to gold surface by radioiodination methods: suppression of free iodide sorption. Colloids and Surfaces B-Biointerfaces 2000;17:59-67.
[24] Yamazaki A, Winnik FM, Cornelius RM, Brash JL. Modification of liposomes with N-substituted polyacrylamides: identification of proteins adsorbed from plasma. Biochim Biophys Acta-Biomembr 1999;1421:103-15.
[25] Behnke CA, Yee VC, Le Trong I, Pedersen LC, Stenkamp RE, Kim SS, et al. Structural determinants of the bifunctional corn Hageman factor inhibitor: X-ray crystal structure at 1.95 angstrom resolution. Biochemistry 1998;37:15277-88.
[26] Jin ZL, Feng W, Beisser K, Zhu SP, Sheardown H, Brash JL. Protein-resistant polyurethane prepared by surface-initiated atom transfer radical graft polymerization (ATRgP) of water-soluble polymers: Effects of main chain and side chain lengths of grafts. Colloids and Surfaces B-Biointerfaces 2009;70:53-9.
[27] Troughton EB, Bain CD, Whitesides GM, Nuzzo RG, Allara DL, Porter MD. Monolayer Films Prepared by the Spontaneous Self-Assembly of Symmetrical and Unsymmetrical Dialkyl Sulfides from Solution onto Gold Substrates - Structure, Properties, and Reactivity of Constituent Functional-Groups. Langmuir 1988;4:365-85.
[28] Ferretti S, Paynter S, Russell DA, Sapsford KE, Richardson DJ. Self-assembled monolayers: a versatile tool for the formulation of bio-surfaces. Trac-Trends Anal Chem 2000;19:530-40.
[29] Cornelius RM, Brash JL. Adsorption from plasma and buffer of single- and two-chain high molecular weight kininogen to glass and sulfonated polyurethane surfaces. Biomaterials 1999;20:341-50.
[30] Citarella F, Wuillemin WA, Lubbers YTP, Hack CE. Initiation of contact system activation in plasma is dependent on factor XII autoactivation and not on enhanced susceptibility of factor XII for kallikrein cleavage. Br J Haematol 1997;99:197-205.
[31] Zhuo R, Siedlecki CA, Vogler EA. Autoactivation of blood factor XII at hydrophilic and hydrophobic surfaces. Biomaterials 2006;27:4325-32.

CHAPTER 5. DUAL SURFACE MODIFICATION WITH PEG AND CORN TRYPSIN INHIBITOR (CTI): EFFECT OF PEG:CTI RATIO ON PROTEIN RESISTANCE AND ANTICOAGULANT PROPERTIES

Authors: **Sara Alibeik**, Shiping Zhu, Jonathan W. Yau, Jeffrey I. Weitz, John L. Brash

Publication Information: Submitted for Publication, 2011

Working Hypothesis:

On dual functional PEG-CTI surfaces, varying the ratio of PEG: bioactive molecule may affect protein resistance and bioactivity. In particular, it is important to address whether there is an optimum ratio of PEG: bioactive molecule on such surfaces and whether protein resistant properties of PEG are affected by conjugation to bioactive molecule.

Dual surface modification with PEG and corn trypsin inhibitor (CTI): effect of PEG:CTI ratio on protein resistance and anticoagulant properties

Sara Alibeik[a], Shiping Zhu[a,b], Jonathan W. Yau[a], Jeffrey I. Weitz[a,c] and John L. Brash[a,b*]

[a] School of Biomedical Engineering, McMaster University, 1280 Main St. West, Hamilton, ON, Canada, L8S 4K1

[b] Department of Chemical Engineering, McMaster University, 1280 Main St. West, Hamilton, ON, Canada, L8S 4L7

[c] Departments of Medicine and Biochemisrty and Biomedical Sciences, McMaster University, 1280 Main St. West, Hamilton, ON, Canada, L8S 4L8

Corresponding author: JL Brash,
School of Biomedical Engineering
McMaster University
Hamilton, ON
Canada L8S 4L8
Ph: 905 525 9140 x 24946
Fax: 905 528 1054
email: brashjl@mcmaster.ca

Abstract

The objective of this study was to investigate the bioactivity and protein resistant properties of dual functioning surfaces modified with PEG for protein resistance and corn trypsin inhibitor (CTI) for anticoagulant effect. Surfaces on gold substrate were prepared with varying ratios of free PEG to CTI-conjugated PEG. Two methods designated, respectively, "sequential" and "direct" were used. For sequential surfaces, PEG was first immobilized on gold and the surfaces were incubated with CTI at varying concentration. For direct surfaces, a PEG-CTI conjugate was synthesized and gold surfaces were modified using solutions of the conjugate of varying concentration. The CTI density on these surfaces was measured using radiolabeled CTI. Water contact angles were measured and the thickness of PEG-CTI layers was determined by ellipsometry. Fibrinogen adsorption from buffer and human plasma, and adsorption from binary solutions of fibrinogen and α-lactalbumin were investigated using radiolabeling methods. Bioactivity of the surfaces was evaluated via their effects on FXIIa inhibition and plasma clotting time. It was found that as the ratio of CTI-conjugated PEG to free PEG increased, bioactivity increased but protein resistance was relatively constant. It is concluded that on these surfaces conjugation of PEG to CTI does not greatly compromise the protein resistance of the PEG but results in improved interactions between the CTI and the "target" protein FXIIa. At the same CTI density, sequential surfaces were more effective in terms of inhibiting FXIIa and prolonging clotting time.

Key words: polyethylene glycol-protein conjugate, surface modification, protein resistant surface, bioactive surface, blood compatibility, anticoagulant.

INTRODUCTION

Thrombus and clot formation on blood contacting devices is initiated by protein adsorption[1-3] and leads to device failure[4,5]. Inhibition of protein adsorption by hydrophilic polymers such as polyethylene glycol (PEG) has been investigated extensively[6-9]. Polymer chain flexibility and water interactions are believed to contribute to the protein resistance of PEG-modified surfaces.

Surface modification with bioactive molecules has also been investigated[10-13]. In general the bioactive molecule has specific binding affinity for a "target" in the blood, e.g. heparin with affinity for antithrombin, giving an anticoagulant effect. Combinations of PEG with bioactive molecules have also been investigated[14-16]. Such surfaces may be considered to be "dual-functioning", i.e. inhibitory of non-specific protein adsorption and having bioactivity involving the adsorption of a specific protein. Questions arising with respect to such surfaces include: Does PEG retain its protein resistance in the presence of the bioactive molecule? What are the effects of the ratio of PEG to bioactive molecule on biointeractions? Is there an optimal ratio that maximizes both protein resistance and bioactivity?

In this communication, we address the question of a possible optimal composition in a system in which gold is modified with PEG and corn trypsin inhibitor (CTI), a potent and specific inhibitor of factor XIIa [17]. CTI is expected to inhibit contact activation and thus provide an anticoagulant effect. Surfaces were modified using two methods[16]; these are referred to as "sequential" and "direct". For sequential surfaces, PEG was first immobilized on gold and the surfaces then treated with CTI. For direct surfaces, a PEG-

CTI conjugate was synthesized and gold was incubated with the conjugate. Surfaces with varying ratios of PEG-to-CTI were prepared by varying the concentration of CTI (sequential) or conjugate (direct). Figure 1 shows the concept schematically.

Biointeractions were investigated by measuring fibrinogen adsorption from buffer and plasma and adsorption from binary solutions of fibrinogen and α-lactalbumin in buffer. FXIIa inhibition, and the clotting time of plasma in contact with the surfaces were also measured.

The present work extends previous studies where PEG and CTI were used together [18] on gold as substrate. Only one surface composition was investigated. These initial studies showed that FXIIa was inhibited, clotting time was prolonged, and nonspecific adsorption was reduced on this surface compared to unmodified controls[19].

MATERIALS AND METHODS

Corn trypsin inhibitor (CTI) was from Haematologic Technologies (Essex Junction, VT) and was dialyzed against phosphate buffered saline-2 mM EDTA (PBS, pH 8) before use. (2,2'-Dithiobisethylhepa(ethylene glycolic) acid)-N-succinimidyl ester (PEG-NHS ester disulfide, MW=1109.3) was from Polypure AS (Oslo, Norway). α-maleimido-ω-amino PEG (MW=2000) was from JenKem Technology USA (Allen, TX). α-hydroxyl-ω-thiol polyethylene glycol (MW=1100) was from Polymer Source (Montreal, Canada). Hydrogen peroxide, ammonium hydroxide, ethanol, 2-iminothiolane-HCl (Traut's reagent) and ethylene diamine tetraacetic acid (EDTA) were from Sigma-Aldrich (Oakville, ON). Human factor XIIa and human fibrinogen (Fg) were from

Enzyme Research Laboratories (South Bend, IN). Fibrinogen was dialyzed against isotonic Tris buffer (TBS, pH 7.4) and stored at −70°C. PD-10 desalting columns were from GE Healthcare (Baie d'Urfe, Quebec, Canada). Silicon wafers sputter-coated with titanium and gold (1000Å) were from Silicon Valley Microelectronics (Santa Clara, CA). They were cut into 0.5 x 0.5 cm squares. Pefachrome XIIa, a FXIIa-directed chromogenic substrate, was from Pentapharm (Basel, Switzerland).

Surface preparation

Gold-coated silicon wafers were cleaned in a solution containing one part (v/v) 30% hydrogen peroxide, one part 30% ammonium hydroxide, and five parts water for 5 min at 85ºC. Surfaces were then rinsed with deionized water three times, five minutes each time.

Primary amino groups of CTI were converted to thiol (thiol-CTI) using Traut's reagent (2-iminothiolane-HCl) [18]. The reaction was carried out for 1 h at room temperature in phosphate buffered saline (PBS)-2 mM EDTA (pH 8) with a 5-fold molar excess of reagent. The product solution was dialyzed against PBS-2mM EDTA (pH 6) for 16 h to remove residual reagent. As reported previously, matrix-assisted laser desorption-ionization, time of flight (MALDI-TOF) mass spectrometry showed that one primary amino group of CTI (most likely the N-terminal) was converted to thiol [18]..

Figure 1 shows a schematic of the surface preparation methods. Sequential surfaces were prepared by first chemisorbing PEG-NHS ester disulfide on gold to give Au-PEG-NHS. These surfaces were incubated with maleimide-PEG-amine to give Au-

PEG-MAL (NHS-NH_2 reaction), and then with thiol-CTI solutions of varying concentration (PBS, pH 7.4) from 2.5 to 20 μM to give surfaces with varying ratios of free to conjugated PEG. Au-PEG-MAL was used as the "100% free PEG" surface for the sequential series.

For the direct surfaces maleimide-PEG-amine was reacted with thiol-CTI to give amine-PEG-CTI conjugate. After removing excess PEG (PD-10 column), amine-PEG-CTI was reacted with PEG-NHS ester disulfide to give thiol-PEG-CTI conjugate. Excess PEG was removed. MALDI-TOF mass spectrometry showed that approximately 33% of the CTI was converted to conjugate [18]. Gold surfaces were incubated with conjugate for 2 h at room temperature and then for 16 h at 4ºC under nitrogen, at concentrations from 2.5 to 20 μM (PBS, pH 7.4). These surfaces were treated with SH-PEG-OH (1 mM, 2 h, room temperature) to cover areas not modified by conjugate. Surfaces modified with SH-PEG-OH only were used as the "100% free PEG" surface for the direct series.

CTI density measurements

CTI density was measured using thiol-CTI and PEG-CTI conjugate radiolabeled with ^{125}I using the Iodo-gen method (Iodination Reagent, Pierce Biotechnology, Rockford, IL)[20]. Sequential and direct surfaces were prepared as described above using the radiolabeled protein and the radiolabeled conjugate, respectively.

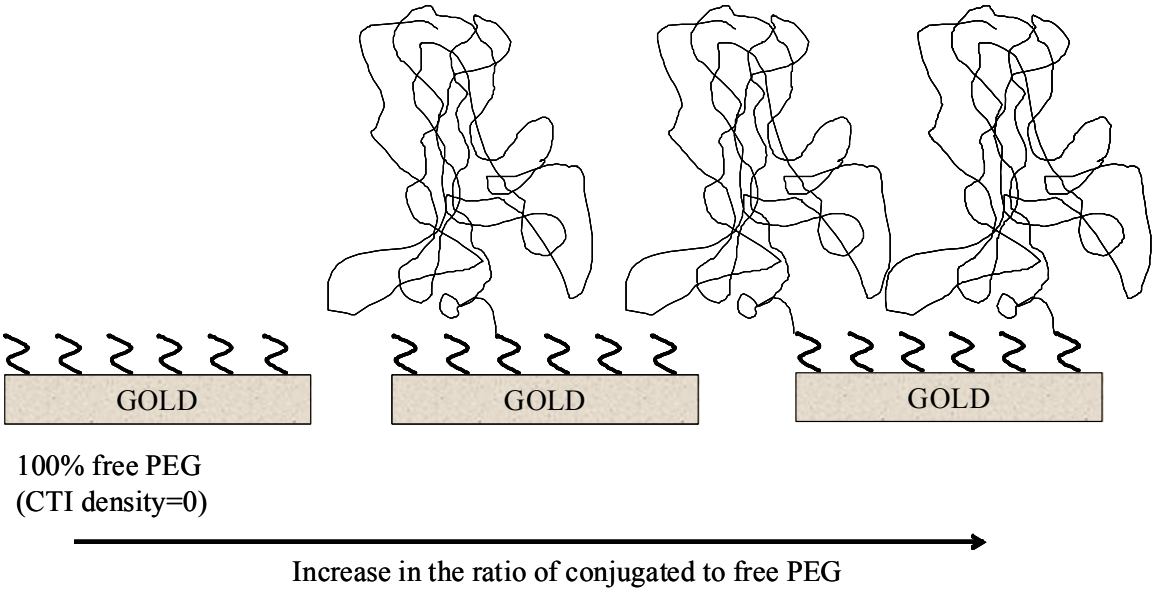

Fig 1. Schematic showing concept of surfaces modified with free PEG and CTI-conjugated PEG and varying free:conjugated ratio.

Surface characterization

Advancing water contact angles were measured with a Ramé-Hart NRL goniometer (Mountain Lakes, NJ) using the sessile drop method.

Modifying layer thicknesses were measured by ellipsometry at a wavelength of 6328 Å and incident angle 70º (Exacta 2000, Waterloo Digital Electronics, Waterloo, ON). The refractive index and extinction coefficient for gold were taken as 0.2 and 3.5, respectively. The refractive indices for PEG-modified surfaces and PEG-CTI modified surfaces were taken as 1.475 and 1.465 respectively[21,22].

Biointeractions

Fibrinogen adsorption from buffer and plasma was measured by ^{125}I labeling (iodine monochloride method)[23]. Labeled fibrinogen was added as a tracer to phosphate

buffered saline-NaI (PBS-NaI, C_{NaI}=0.218 g/L) or plasma. Cold NaI was included to suppress free radioactive iodide adsorption to gold[24]. For the buffer experiments the total fibrinogen concentration was 1 mg/mL (10% ^{125}I-labeled).

For the plasma experiments, blood was collected from a minimum of 10 healthy volunteers. The volunteers were aspirin-free and antihistamine-free for a minimum of 10 days prior to donating. Blood (43 mL) was collected into polypropylene (PP) centrifuge tubes containing 7 mL of acid citrate dextrose (ACD, 1 part ACD in 6 parts whole blood) and mixed gently. It was centrifuged for 5 min at 2500 x g to give platelet rich plasma (PRP). The supernatant was centrifuged again for 5 min at 2500 x g to give platelet poor plasma (PPP). The plasma was stored at -70ºC. The plasma was diluted 1:1 with PBS-NaI. ^{125}I-labeled fibrinogen was added at 10% of the endogenous level.

In the binary adsorption experiments the molar ratio fibrinogen:α-lactalbumin (Lac) was 1:1 and the fibrinogen concentration was 1 mg/ml. Fibrinogen was labeled with ^{131}I and Lac with ^{125}I using the ICl method. For fibrinogen 10% of the protein in the adsorption solutions was labeled; for Lac 100% was labeled.

All adsorption experiments were carried out for 3 h at room temperature (23ºC). After adsorption surfaces were rinsed three times (five minutes each time) with PBS to remove loosely adherent protein. Adsorbed quantities were determined by comparing the surface radioactivity with that of a solution of known concentration and are reported as mass density (μg/cm^2).

FXIIa inhibition was measured using a chromogenic substrate assay. Surfaces were incubated with 100 μL of 50 nM FXIIa solution (TBS, pH 7.4, 2 mM $CaCl_2$, 12.5

μM $ZnCl_2$, 15.4 μM BSA) at room temperature in a 96-well plate format. After 1 h, 50 μL of a 1.6 mM solution of chromogenic substrate was added to the wells. Optical density was measured over time (15 s intervals, 1 h period) at 405 nm.

Coagulation response was evaluated by clotting time measurements. Surfaces were incubated with 100 μL of pooled normal citrated human plasma (PNP) for 15 min at 37˚C in a 96-well plate format. 100 μL of 0.025 M $CaCl_2$ was added and absorbance at 405 nm was recorded at 15 s intervals over a 1 h period. The time to reach half maximum absorbance was taken as a measure of clotting time.

RESULTS

Surface characterization

CTI density

^{125}I-labeled thiol-CTI and ^{125}I-labeled PEG-CTI conjugate were used, respectively, to prepare sequential and direct surfaces for measurement of CTI density. The data are shown in Fig 2. As the concentration of CTI increased, the density increased on both surface types, ranging from 0.004 to 0.03 molecules/nm^2 on the sequential and from 0.006 to 0.07 molecules/nm^2 on the direct surfaces. At a given concentration the density on the direct surfaces was higher than on the sequential ones. Assuming the dimensions of CTI to be similar to those of lysozyme (viz. 45x30x30Å [25]) given their similar molecular weights (lysozyme ~14.6 kDa, CTI ~13 kDa), a close packed monolayer of normal CTI will have a surface concentration in the range of 0.07-0.12 molecules/nm^2 depending on orientation. On the direct surface at a CTI concentration of

20 μM, the CTI density was in this range. On this surface, therefore, very little free PEG should be presented to a contacting fluid. For the sequential series, the highest CTI density was below that of a close packed monolayer. Thus, for this series a significant fraction of the PEG would have remained "free" after reaction with CTI (Fig 2).

The lower CTI density on the sequential surfaces may be due to the protein resistance of the initial PEG layer, i.e. PEG immobilized in the first step may act as a protein resistant layer that inhibits the binding of CTI in the second step.

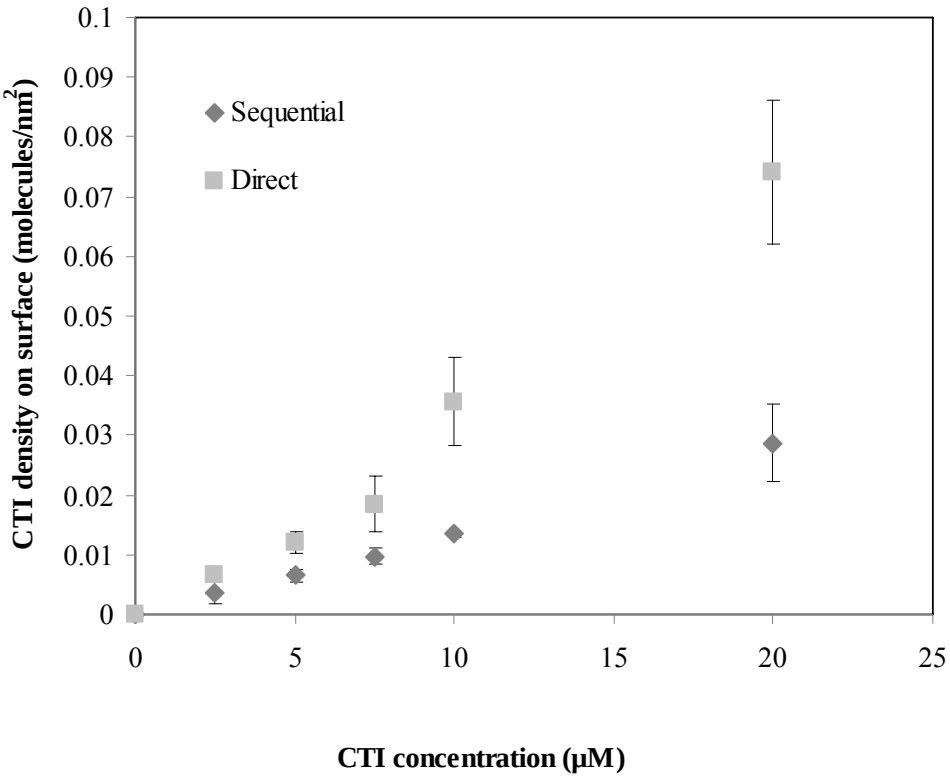

Fig 2. CTI density on sequential and direct surfaces. Data are mean ± SD, n=6.

Water contact angles

Advancing contact angles were measured on the direct surfaces after modification with PEG-CTI conjugate and again after subsequent incubation with PEG (Fig 3). The

contact angle decreased from 56° to 26° after PEG modification of gold (0 μM, Fig3) as observed previously[16]. Upon treatment of gold with CTI-PEG conjugate the contact angle decreased from 56° to about 37° and did not vary greatly with CTI concentration. After subsequent PEG treatment of the CTI surfaces the contact angle decreased further, indicating that attachment of PEG occurred. This decrease became smaller as the CTI concentration (and corresponding density, Fig 2) increased, presumably because there was less bare gold for PEG attachment.

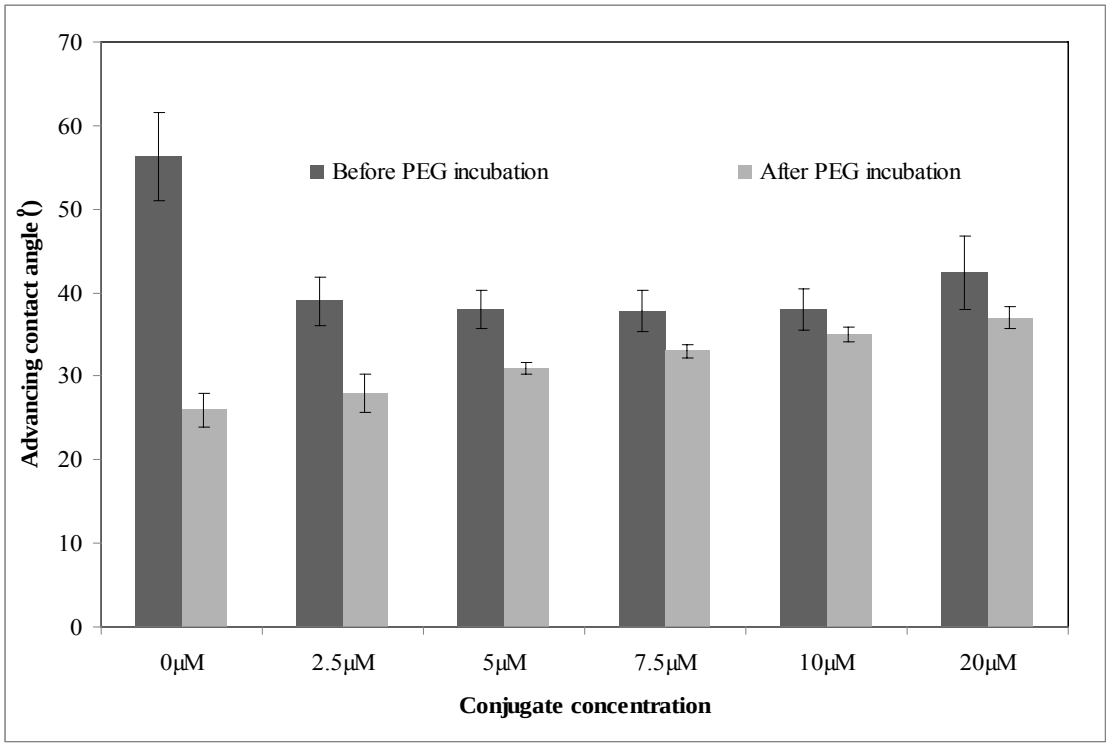

Fig 3. Water contact angles on "direct" surfaces prepared with varying concentrations of conjugate (x-axis). Data are shown after modification with conjugate, and again after incubation of the conjugate-modified surfaces with SH-PEG-OH . Data are mean ± SD, n>6.

Fig 4 shows advancing contact angle versus CTI density for both sequential and direct surfaces, the latter after subsequent PEG treatment. As CTI density increased

(increase in the ratio of conjugated to free PEG) the contact angle increased on both surface types, with values in the range of 24° to 37°. At the same CTI density, the contact angles were similar on the sequential and direct surfaces suggesting similar compositions.

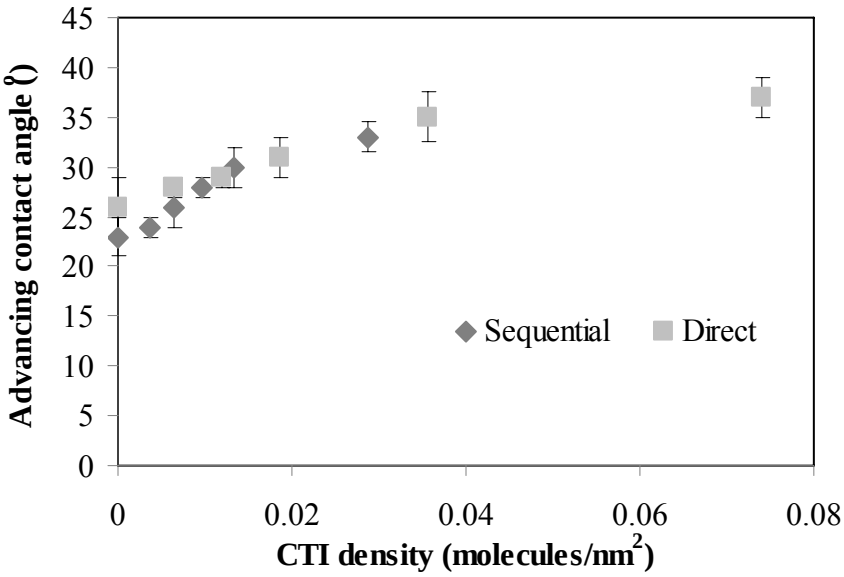

Fig 4. Advancing water contact angles versus CTI density for sequential and direct surfaces. Zero CTI density indicates the surface modified with PEG only. Data are mean ± SD, n>6.

Film thickness

Fig 5 shows layer thickness versus CTI density as determined by ellipsometry. The values ranged from 11 to 26 Å. At zero CTI density the thickness was 11±4 Å on Au-PEG-MAL (sequential) and 13±5 Å on Au-PEG-OH (direct). The PEG density on these surfaces can be estimated as:

$$\sigma = \frac{d\rho_{dry}N_A}{M}$$

where σ is density in chains/nm^2, d is thickness as determined by ellipsometry, ρ_{dry} is density of dry polymer layer (assumed to be 1 g/cm^3), N_A is Avogadro's number and M is the polymer molecular weight[26,27]. The molecular weights used were: PEG-NHS = 554 g/mole, PEG-MAL = 2554 g/mole and PEG-OH = 1100 g/mole.

PEG density on the 100% free PEG surfaces (zero CTI density) was estimated as 1.2±0.5 chains/nm^2 on Au-PEG-NHS, 0.3±0.1 chains/nm^2 on Au-PEG-MAL and 0.66±0.3 chains/nm^2 on Au-PEG-OH. These densities are inversely related to the PEG MW and fall within the expected range for brush-type PEG layers[22]; they indicate high PEG coverage. For the sequential series it is important to note that PEG coverage was high prior to reaction with CTI. The film thickness on both sequential and direct surfaces increased as the CTI density increased. At the same CTI density the layer thickness was similar on both surface types.

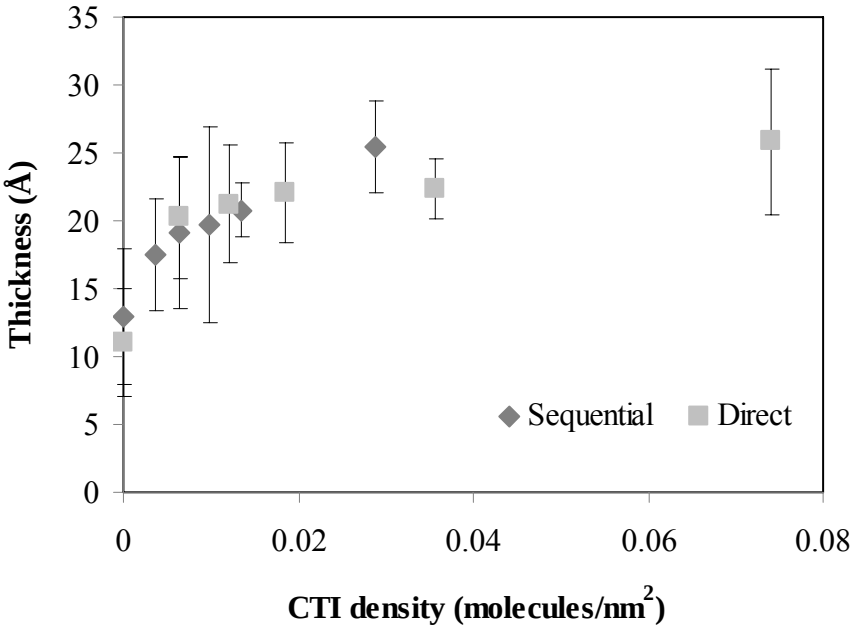

Fig 5. Layer thickness versus CTI density for sequential and direct surfaces. Zero CTI density indicates the surface modified with PEG only. Data are mean ± SD, n>6.

Protein interactions

Protein adsorption from buffer and plasma

To investigate the effect of the conjugated-to-free PEG ratio on protein resistance, single and binary protein adsorption experiments were carried out. Fig 6 shows fibrinogen adsorption from buffer. As CTI density (conjugated-to-free PEG ratio) increased fibrinogen adsorption increased on both surface types. The differences between the 100% free PEG surfaces (zero CTI density) and the highest CTI density surfaces (lowest number of free PEGs) were statistically significant ($p<0.05$). The adsorbed quantities at the higher densities were in the close packed monolayer range (0.14-0.7 $\mu g/cm^2$). At a given CTI density, the direct surfaces adsorbed more fibrinogen than the sequential ones possibly due to the way the PEG is oriented/deployed.

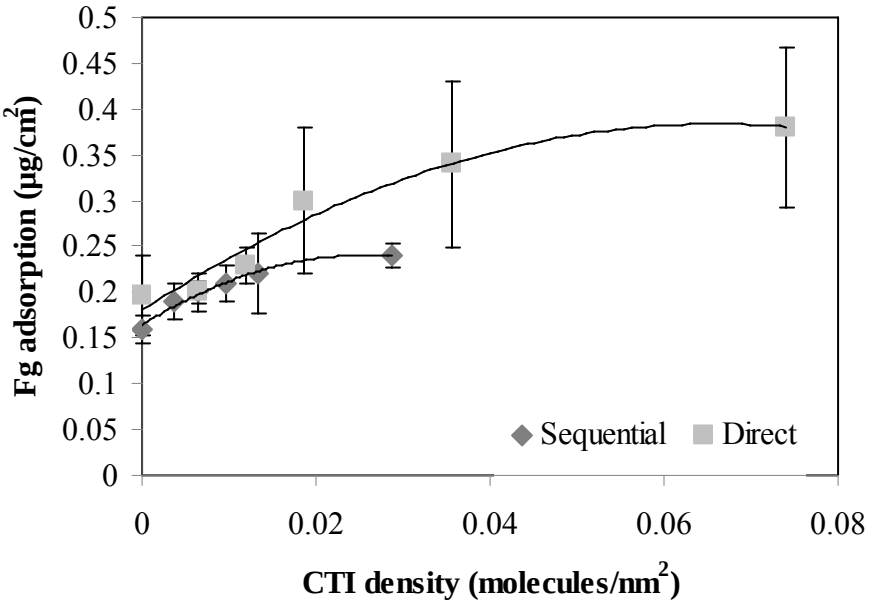

Fig 6. Fibrinogen adsorption from buffer versus CTI density for sequential and direct surfaces. Adsorption time, 3 h. Zero CTI density indicates the surface modified with PEG only. Data are mean ± SD, n=3.

Fig 7 shows fibrinogen adsorption from plasma. Adsorption increased slightly, but not significantly, as the CTI density increased. On both sequential and direct surfaces adsorption ranged from about 0.026 μg/cm^2 for the "pure" PEG surface (zero CTI density) to about 0.035 μg/cm^2 on the surfaces of highest CTI density. The higher CTI densities on the direct surfaces are at the monolayer level. Hence, it is likely that the free PEG content on these surfaces was close to zero, i.e. all of the PEG was conjugated to CTI. Since fibrinogen adsorption on these surfaces was not significantly higher than on the free PEG surface (zero CTI density), it appears that the conjugated PEG on the direct surfaces retained its protein resistant properties.

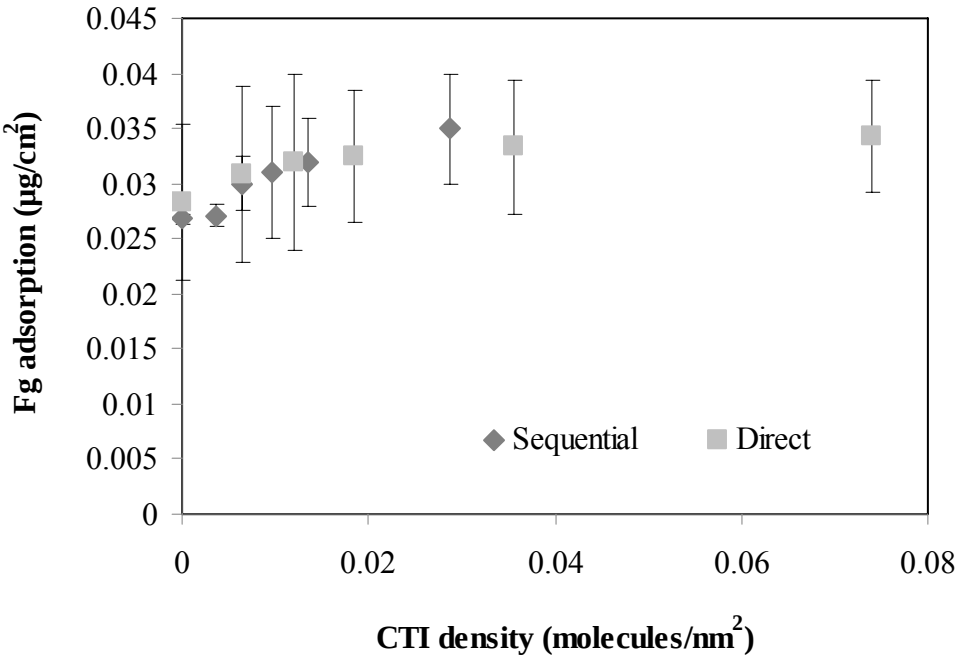

Fig 7. Fibrinogen adsorption from 50% plasma versus CTI density for sequential and direct surfaces. Adsorption time, 3 h. Zero CTI density indicates the surface modified with PEG only. Data are mean ± SD, n=3.

Fibrinogen and α-lactalbumin (Lac) were used in binary adsorption experiments. Fibrinogen has MW 340 kDa, dimensions of 450 x 90 x 90 Å, and isoelectric point 4.5. α-lactalbumin has MW 14.2 kDa, dimensions of 37 x 32 x 25 Å and isoelectric point 4.3[28]. Both proteins will have similar charge at neutral pH thus allowing study of the effect of protein size, independent of charge, on interactions with the modified surfaces. Table 1 shows data from the binary adsorption experiments. The fibrinogen concentration was the same as in the single protein experiments (1 mg/mL) and the molar ratio of the proteins in the solution was 1:1.

Table 1. Adsorption from binary fibrinogen-lactalbumin solutions, molar ratio 1:1.

Sequential surfaces			
CTI density (molecules/nm^2)	Fg adsorption (μg/cm^2)	Lac adsorption (μg/cm^2)	Lac : Fg (molar ratio)
0	0.12±0.01	0.006±0.002	1.21
0.004±0.002	0.16±0.05	0.004±0.0005	0.61
0.006±0.001	0.18±0.02	0.0068±0.0007	0.92
0.010±0.001	0.28±0.01	0.0068±0.001	0.59
0.013±0.0004	0.29±0.02	0.007±0.001	0.59
0.029±0.006	0.31±0.05	0.0073±0.0003	0.57
Direct surfaces			
CTI density (molecules/nm^2)	Fg adsorption (μg/cm^2)	Lac adsorption (μg/cm^2)	Lac : Fg (molar ratio)
0	0.13±0.03	0.008±0.004	1.49
0.006±0.0004	0.21±0.04	0.005±0.002	0.58
0.012±0.001	0.28±0.06	0.008±0.002	0.69
0.019±0.005	0.29±0.01	0.011±0.004	0.92
0.036±0.007	0.33±0.07	0.013±0.002	0.96
0.074±0.012	0.36±0.08	0.013±0.0009	0.88

Data are mean ± SD, n=3.

Fibrinogen adsorption on both the direct and sequential surfaces was similar to that in the single protein experiments, indicating that the presence of the smaller protein

did not affect adsorption of the bigger one. Similar to the single protein experiments, adsorption to the high-density CTI surfaces was in the monolayer range.

α-lactalbumin adsorption was very low (0.004-0.007 μg/cm^2 sequential, 0.008-0.013 μg/cm^2 direct) and increased as CTI density increased. In the direct series, adsorption on the surface of highest CTI density was significantly greater than on the one of lowest density ($p<0.05$).

The molar ratios of adsorbed α-lactalbumin:fibrinogen (Table 1) should be compared with the 1:1 ratio in the solution. Ratios of ~1.2 and 1.5 found on Au-PEG-MAL (sequential, CTI=0) and Au-PEG-OH (direct, CTI=0), respectively, indicate a preference for the smaller protein. This behaviour may reflect the nature of the barrier to adsorption presented by the PEG. On the CTI surfaces, the ratio was lower and ranged from ~0.6 to ~1.0. For the sequential surfaces the ratio did not trend clearly with CTI density and was fairly constant at ~0.6, i.e. inverted compared to the ratio on the zero CTI surface. For the direct surfaces the ratio was ~0.6 at the lowest CTI density; it trended upwards close to 1.0 as the density increased. It is possible that as CTI increased on the surface the effect of the PEG was diminished, and the relative affinities of the proteins competing for CTI sites determined the final layer composition.

FXIIa inhibition

The free PEG controls and the direct and sequential surfaces with the highest and lowest CTI densities were studied for their ability to inhibit FXIIa as described above. The data are shown in Fig 8. For the 100% free PEG surfaces 25-27% inhibition of FXIIa

was observed. Since there was no CTI on these surfaces, inhibition was likely caused by removal of FXIIa from the solution by physical adsorption such that the active site was "hidden" and unavailable to react with substrate.

For the CTI-modified surfaces, FXIIa inhibition increased as CTI density increased. The sequential surfaces with the lowest and highest CTI densities gave 35±1 and 41±2 % inhibition, respectively. On the direct surfaces the corresponding values were 32±1 and 37±2 %. The CTI surfaces thus reacted more extensively than the PEG alone surfaces. On the CTI surfaces it is not possible to distinguish between inhibition due to specific CTI-FXIIa interactions and physical adsorption of FXIIa. It is probable that both are involved. In our previous work [18], we compared the PEG-CTI surface with surfaces modified with PEG-lactalbumin by using FXIIa activity assay, in order to distinguish between the specific CTI-FXIIa interactions and non-specific protein-protein interactions. We observed significantly higher inhibition of FXIIa on PEG-CTI compared with PEG-lactalbumin surfaces. Thus, it can be assumed that most of FXIIa inhibition observed here is due to the specific interactions of CTI with FXIIa.

At a given CTI density the sequential surfaces inhibited FXIIa more effectively than the direct ones. This may be due to the more favorable orientation of CTI on the sequential surfaces, and/or to the effect of PEG conjugation in reducing the activity of CTI on the direct surfaces.

It appears that if CTI density on the sequential surfaces could be increased to a higher level, e.g. a close packed monolayer, a higher degree of FXIIa inhibition would be

achieved. Formation of CTI monolayers by the sequential method, however, may be difficult due to the presence of the pre-formed protein resistant PEG layer.

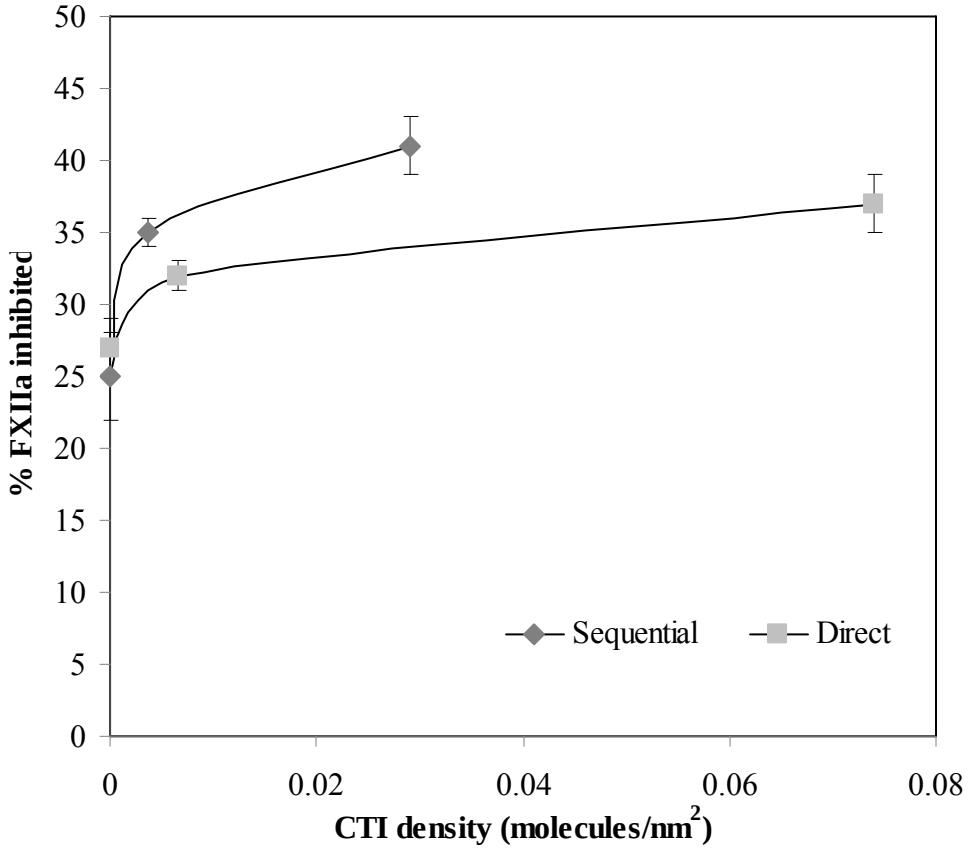

Fig 8. Activity of FXIIa solutions after incubation with sequential and direct surfaces versus CTI density. Zero CTI density indicates the surface modified with PEG only. Data are mean ± SD, n=3.

Clotting time assay

The anticoagulant effect of the materials was evaluated by incubating with citrated human plasma and recording turbidity versus time after re-calcification (Fig 9). On the 100% free PEG surfaces, the clotting time (time to half maximum absorbance) was 510±40 s (average of sequential and direct). The time increased as the ratio of PEG-CTI

conjugate to free PEG increased. For the sequential surface with the highest CTI density, the clotting time was 788±53 s, significantly higher than for the corresponding free PEG surface ($p<0.05$). On the direct surfaces, the maximum clotting time was 675±42s, again significantly higher than for the free PEG surface ($p<0.05$). These data indicate that protein resistance alone, as conferred by PEG, does not prolong the clotting time; the presence of the FXIIa inhibitor CTI does give an anticoagulant effect.

At a given CTI density, the clotting time was significantly longer on the sequential surfaces than on the direct. For example, at 0.01 CTI molecules/nm2, the clotting time was 688±23 s on the sequential surface and 570±42 s on the direct. This result parallels the FXIIa inhibition data and shows, as found previously for the anticoagulant hirudin [16], that the CTI-PEG combination is more effective when the surface is prepared by the sequential method.

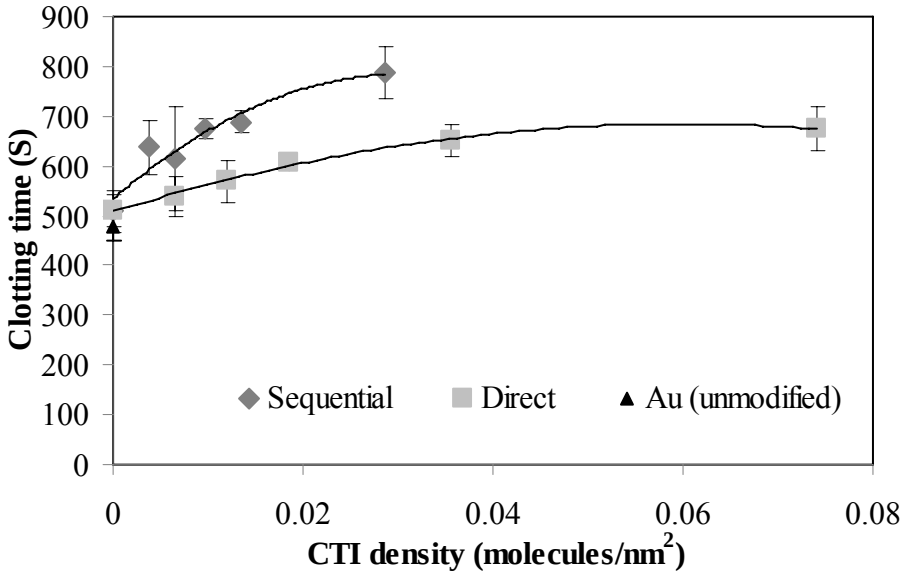

Fig 9. Plasma clotting times versus CTI density on direct and sequential surfaces. Zero CTI density indicates the surface modified with PEG only. Data are mean ± SD, n=3.

DISCUSSION

In recent work [16,18] we used PEG-protein combinations to create dual functioning surfaces, PEG for protein resistance and CTI or hirudin for anticoagulant properties. We used direct and sequential methods to prepare the surfaces as described above. Other PEG-bioactive molecule combinations have been investigated[14,15], mostly using sequential methods where it is unlikely that all of the free PEG is converted to PEG-bioactive molecule, leaving unknown areas covered with free PEG.

It is of interest to consider the effect of the free-to-conjugated PEG ratio on bio-interactions. On the sequential surfaces, while adsorption did increase with increasing CTI density (Figs 6 and 7, Table 1), the levels remained low compared to unmodified gold (~0.5 μg/cm^2 fibrinogen from a 1 mg/mL solution[18]). It thus appears that attachment of CTI to the PEG layer did not seriously compromise its protein resistance. Since the highest FXIIa inhibition and longest clotting times were observed on the surfaces with the highest ratios of conjugated to free PEG, it appears that the maximum possible density of CTI on these surfaces is optimal.

On the direct surfaces CTI density reached the monolayer level at the higher CTI concentrations and very little free PEG appeared to be taken up subsequently (Fig 3). Hence, it is likely that the free PEG content on the high CTI density surfaces was close to zero. Since fibrinogen adsorption on these surfaces was not significantly higher than on the 100% free PEG surface (zero CTI density), it appears that the conjugated PEG on the direct surfaces retained its protein resistant properties in plasma. Again the best biological performance was seen for the surfaces of highest CTI density. Hence, we

conclude that on these dual functioning surfaces the optimal composition is the one with the highest density of the bioactive component.

It is of interest also to consider whether the protein resistance of the PEG component affects the behavior of the CTI. In this as well as in previous work and work of others [9,18], clotting time was not prolonged on the PEG-alone surfaces despite their protein resistance. At first glance, it might seem that the bioactive component alone would be optimal to achieve its effect. In recent work CTI was immobilized on gold and polyurethane substrates without PEG and with PEG (single PEG-CTI ratio) [18,29]. However, FXIIa inhibition on the CTI-alone surface was significantly lower than on the PEG-CTI surface, suggesting that PEG improves the function of the CTI. As the data presented here demonstrate, PEG contributes to the protein resistant properties of the "dual" surfaces but probably more importantly, it may act as a "spacer-presenter" to facilitate the interactions of the bioactive molecule with its target protein.

Finally it is of note that the surfaces remained protein resistant even when the PEG was effectively covered with CTI. This result may be seen as support for the "water barrier", as opposed to the "steric exclusion" hypothesis for PEG protein resistance[30]. The contact angles remained low at all CTI densities (Figs 3 and 4) suggesting that the surfaces were extensively hydrated in aqueous contact, so that water interactions with the PEG would not be significantly diminished.

Summary and conclusions

Gold surfaces modified with free PEG and PEG-CTI in varying ratios were prepared using sequential and direct methods. Protein adsorption from buffer increased as

the ratio of conjugated to free PEG increased, but less so on the sequential than on the direct surfaces. Fibrinogen adsorption from plasma was essentially independent of the ratio of conjugated to free PEG on both surface types. FXIIa inhibition increased and plasma clotting time was prolonged as the ratio of conjugated to free PEG increased on both types. At the same CTI density, sequential surfaces were more effective than direct ones in terms of FXIIa inhibition and clotting time prolongation. The highest ratio of CTI-conjugated to free PEG was optimal for FXIIa inhibition and prolongation of plasma coagulation.

Acknowledgements

Work supported by the Natural Sciences and Engineering Research Council of Canada (NSERC) and the Canadian Institutes of Health Research (CIHR).

References

1. Labarre D. Improving blood-compatibility of polymeric surfaces. Trends in Biomaterials and Artificial Organs 2001;15(1).
2. Sefton MV, Gemmell CH, Gorbet MB. What really is blood compatibility? Journal of Biomaterials Science-Polymer Edition 2000;11(11):1165-1182.
3. Brash JL, Tenhove P. Protein Adsorption Studies on Standard Polymeric Materials. Journal of Biomaterials Science-Polymer Edition 1993;4(6):591-599.
4. Wu YG, Simonovsky FI, Ratner BD, Horbett TA. The role of adsorbed fibrinogen in platelet adhesion to polyurethane surfaces: A comparison of surface hydrophobicity, protein adsorption, monoclonal antibody binding, and platelet adhesion. Journal of Biomedical Materials Research Part A 2005;74A(4):722-738.
5. Gorbet MB, Sefton MV. Biomaterial-associated thrombosis: roles of coagulation factors, complement, platelets and leukocytes. Biomaterials 2004;25(26):5681-5703.
6. Jin ZL, Brash JL, Zhu SP. ATRP grafting of oligo(ethylene glycol) methacrylates from gold surface - Effect of monomer size on grafted chain and EO unit densities. Canadian Journal of Chemistry-Revue Canadienne De Chimie;88(5):411-417.

7. Brash JL. Exploiting the current paradigm of blood-material interactions for the rational design of blood-compatible materials. Journal of Biomaterials Science-Polymer Edition 2000;11(11):1135-1146.
8. Unsworth LD, Sheardown H, Brash JL. Polyethylene oxide surfaces of variable chain density by chemisorption of PEO-thiol on gold: Adsorption of proteins from plasma studied by radiolabelling and immunoblotting. Biomaterials 2005;26(30):5927-5933.
9. Zhang Z, Zhang M, Chen SF, Horbetta TA, Ratner BD, Jiang SY. Blood compatibility of surfaces with superlow protein adsorption. Biomaterials 2008;29(32):4285-4291.
10. McClung WG, Clapper DL, Hu SP, Brash JL. Adsorption of plasminogen from human plasma to lysine-containing surfaces. Journal of Biomedical Materials Research 2000;49(3):409-414.
11. Martins MCL, Curtin SA, Freitas SC, Salgueiro P, Ratner BD, Barbosa MA. Molecularly designed surfaces for blood deheparinization using an immobilized heparin-binding peptide. Journal of Biomedical Materials Research Part A 2009;88A(1):162-173.
12. Yang Z, Wang J, Luo R, Maitz MF, Jing F, Sun H, Huang N. The covalent immobilization of heparin to pulsed-plasma polymeric allylamine films on 316L stainless steel and the resulting effects on hemocompatibility. Biomaterials 2010;31(8):2072-2083.
13. Murugesan S, Xie J, Linhardt RJ. Immobilization of heparin: Approaches and applications. Current Topics in Medicinal Chemistry 2008;8(2):80-100.
14. Li D, Chen H, McClung WG, Brash JL. Lysine-PEG-modified polyurethane as a fibrinolytic surface: Effect of PEG chain length on protein interactions, platelet interactions and clot lysis. Acta Biomaterialia 2009;5(6):1864-1871.
15. Sask KN, Zhitomirsky I, Berry LR, Chan AKC, Brash JL. Surface modification with an antithrombin-heparin complex for anticoagulation: Studies on a model surface with gold as substrate. Acta Biomaterialia 2010;6(8):2911-2919.
16. Alibeik S, Zhu S, Brash JL. Surface modification with PEG and hirudin for protein resistance and thrombin neutralization in blood contact. Colloids and Surfaces B: Biointerfaces 2010;81(2):389-396.
17. Pedersen LC, Yee VC, Vondassow G, Hazeghazam M, Reeck GR, Stenkamp RE, Teller DC. The Corn Inhibitor of Blood-Coagulation Factor Xiia - Crystallization and Preliminary Crystallographic Analysis. Journal of Molecular Biology 1994;236(1):385-387.
18. Alibeik S, Zhu S, Yau JW, Weitz JI, Brash JL. Surface modification with polyethylene glycol-corn trypsin inhibitor conjugate for inhibition of contact factor pathway on blood-contacting surfaces. Acta Biomaterialia 2011;In Press, Accepted Manuscript.
19. Tokumitsu S, Liebich A, Herrwerth S, Eck W, Himmelhaus M, Grunze M. Grafting of alkanethiol-terminated poly(ethylene glycol) on gold. Langmuir 2002;18(23):8862-8870.

20. Knight LC, Budzynski AZ, Olexa SA. Radiolabeling of Fibrinogen Using the Lodogen Technique. Thrombosis and Haemostasis 1981;46(3):593-596.
21. Tosatti S, De Paul SM, Askendal A, VandeVondele S, Hubbell JA, Tengvall P, Textor M. Peptide functionalized poly(L-lysine)-g-poly(ethylene glycol) on titanium: resistance to protein adsorption in full heparinized human blood plasma. Biomaterials 2003;24(27):4949-4958.
22. Unsworth LD, Tun Z, Sheardown H, Brash JL. Chemisorption of thiolated poly(ethylene oxide) to gold: surface chain densities measured by ellipsometry and neutron reflectometry. Journal of Colloid and Interface Science 2005;281(1):112-121.
23. Price ME, Cornelius RM, Brash JL. Protein adsorption to polyethylene glycol modified liposomes from fibrinogen solution and from plasma. Biochimica Et Biophysica Acta-Biomembranes 2001;1512(2):191-205.
24. Du YJ, Cornelius RM, Brash JL. Measurement of protein adsorption to gold surface by radioiodination methods: suppression of free iodide sorption. Colloids and Surfaces B-Biointerfaces 2000;17(1):59-67.
25. Jin ZL, Feng W, Beisser K, Zhu SP, Sheardown H, Brash JL. Protein-resistant polyurethane prepared by surface-initiated atom transfer radical graft polymerization (ATRgP) of water-soluble polymers: Effects of main chain and side chain lengths of grafts. Colloids and Surfaces B-Biointerfaces 2009;70(1):53-59.
26. Unsworth LD, Sheardown H, Brash JL. Protein resistance of surfaces prepared by sorption of end-thiolated poly(ethylene glycol) to gold: Effect of surface chain density. Langmuir 2005;21(3):1036-1041.
27. Feng W, Brash JL, Zhu SP. Non-biofouling materials prepared by atom transfer radical polymerization grafting of 2-methacryloloxyethyl phosphorylcholine: Separate effects of graft density and chain length on protein repulsion. Biomaterials 2006;27(6):847-855.
28. Jin ZL, Feng W, Zhu SP, Sheardown H, Brash JL. Protein-resistant polyurethane by sequential grafting of poly(2-hydroxyethyl methacrylate) and poly(oligo(ethylene glycol) methacrylate) via surface-initiated ATRP. Journal of Biomedical Materials Research Part A 2010;95A(4):1223-1232.
29. Alibeik S, Zhu S, Yau JW, Weitz JI, Brash JL. Immobilization of polyethylene glycol-corn trypsin inhibitor on polyurethane for inhibition of contact factor activation upon blood contact. . 2011.
30. Lee JH, Lee HB, Andrade JD. Blood Compatibility of Polyethylene Oxide Surfaces. Progress in Polymer Science 1995;20(6):1043-1079.

CHAPTER 6. MODIFICATION OF POLYURETHANE WITH POLYETHYLENE GLYCOL-CORN TRYPSIN INHIBITOR FOR INHIBITION OF FACTOR XIIA IN BLOOD CONTACT

Authors: **Sara Alibeik**, Shiping Zhu, Jonathan W. Yau, Jeffrey I. Weitz, John L. Brash

Publication Information: Accepted for Publication in Journal of Biomaterials Science, Polymer Edition

Acceptance Date: September 16, 2011

Working Hypothesis:

Improved blood compatibility of polyurethane may be obtained by the sequential attachment of PEG and corn trypsin inhibitor. Such surfaces may be more effective for inhibition of coagulation and protein resistance compared with PEG-only or CTI-only modified polyurethanes.

Modification of polyurethane with polyethylene glycol-corn trypsin inhibitor for inhibition of factor XIIa in blood contact

Sara Alibeik[a], Shiping Zhu[a,b], Jonathan W. Yau[a], Jeffrey I. Weitz[a,c] and John L. Brash[a,b*]

[a] School of Biomedical Engineering, McMaster University, 1280 Main St. West, Hamilton, ON, Canada, L8S 4K1

[b] Department of Chemical Engineering, McMaster University, 1280 Main St. West, Hamilton, ON, Canada, L8S 4L7

[c] Department of Medicine and Department of Biochemistry and Biomedical Sciences, McMaster University, 1280 Main St. West, Hamilton, ON, Canada, L8S 4L8

Short title: PEG-CTI on PU for inhibition of factor XIIa

Corresponding author: JL Brash,
School of Biomedical Engineering
McMaster University
Hamilton, ON
Canada L8S 4L8
Ph: 905 525 9140 x 24946
Fax: 905 528 1054

Email: brashjl@mcmaster.ca

Abstract

In previous work using gold as a model substrate, we showed that modification of surfaces with polyethylene glycol (PEG) and corn trypsin inhibitor (CTI) rendered them protein resistant and inhibitory against activated factor XII. Sequential attachment of PEG followed by CTI gave superior performance compared to direct attachment of a preformed PEG-CTI conjugate. In the present work, a sequential method was used to attach PEG and CTI to a polyurethane (PU) substrate to develop a material with applicability for blood-contacting medical devices. Controls included surfaces modified only with PEG and only with CTI. Surfaces were characterized by water contact angle and x-ray photoelectron spectroscopy (XPS). The surface density of CTI was in the range of a monolayer and was higher on the PU substrate than on gold reported previously. Biointeractions were investigated by measuring fibrinogen adsorption from buffer and plasma, factor XIIa inhibition and plasma clotting time. Both the PU-PEG surfaces and the PU-PEG-CTI surfaces showed low fibrinogen adsorption from buffer and plasma, indicating that PEG retained its protein resistance when conjugated to CTI. Although the CTI density was lower on PU-PEG-CTI than on PU modified only with CTI, PU-PEG-CTI exhibited greater factor XIIa inhibition and a longer plasma clotting time, suggesting that PEG facilitates the interaction of CTI with factor XIIa. Thus sequential attachment of PEG and CTI may be a useful approach to improve the thromboresistance of polyurethane surfaces.

Key words: Polyethylene glycol, corn trypsin inhibitor, polyurethane, surface modification, blood compatibility, blood coagulation, protein resistance.

1. Introduction

Failure of blood contacting devices due to thrombosis and clotting is initiated by rapid non-specific protein adsorption.[1-3] Two main approaches have been used for the modification of biomaterials to overcome these problems: (1) attachment of protein resistant polymers such as polyethylene glycol (PEG) to reduce non-specific protein adsorption[4-7], and (2) incorporation of bioactive molecules which either inhibit fibrin formation[8,9] (e.g heparin, which acts as an anticoagulant by activating antithrombin [10-12]) or promote fibrin degradation (e.g. lysine, which binds plasminogen and t-PA[13,14]). Combinations of both approaches have also been investigated.[15-17]

In this work, we modified a polyurethane surface with PEG and corn trypsin inhibitor (CTI), the former for protein resistance and the latter as an inhibitor of factor XIIa.[18] The PEG serves also as a tether for CTI. When blood contacts a material, factor XII binds to the surface and undergoes so-called autoactivation. The resultant factor XIIa then initiates clotting via the intrinsic coagulation pathway.[19] Thus active CTI on a surface may be expected to inhibit any factor XIIa generated and thus inhibit clot formation.

In previous work[20] we used gold as a model substrate to investigate the PEG-CTI combination. First, the N-terminal amino group of CTI was converted to a thiol group to allow site specific attachment of this protein. Two methods of surface preparation were then used: (a) a sequential method in which PEG was first immobilized and CTI was then attached to the PEG, (b) a direct method involving initial preparation of a PEG-CTI conjugate and subsequent surface immobilization of the conjugate. It was

shown that PEG retained its protein resistant properties with both methods of surface preparation, but there was greater CTI inhibition of factor XIIa and prolongation of clotting time for the "sequential' than the "direct" surfaces.

Polyurethanes (PU) have been used extensively for medical devices such as catheters and cardiac assist devices.[21-23] The main attributes of PUs for such applications are that they are mechanically well suited and are available over a range of properties from flexible to stiff. However, like other biomaterials, contact of PU with blood induces clot formation. Surface modification is therefore required to improve blood compatibility.[24-27]

In the present work PU was modified with PEG and CTI using a sequential method. First, isocyanate groups were introduced into the surface. PEG was then attached by reaction with the NCO groups; finally CTI was attached covalently via the PEG distal chain end. Protein resistance was investigated by measuring fibrinogen adsorption from buffer and plasma. CTI activity was evaluated by assessing factor XIIa inhibition and plasma clotting time. The PU-PEG-CTI surfaces were compared with several control surfaces including surfaces modified only with CTI and only with PEG.

2. Materials and Methods

Tecothane® polyurethane (PU) (TT-1095A) was from Thermedics Inc. (Wilmington, MA). Dimethyl formamide (DMF) was from Caledon Laboratories (Georgetown, ON, Canada). Toluene and acetonitrile were from EMD Chemicals (Gibbstown, NJ). Triethylamine (TEA, 99%) was from Alfa Aesar (Ward Hill, MA). 2-

iminothiolane-HCl (Traut's reagent), ethylene diamine tetraacetic acid (EDTA) and 4,4′-methylenebis(phenyl isocyanate) (MDI) were from Sigma-Aldrich (Oakville, ON). Maleimide PEG amine (MW, 2000) was from JenKem Technology USA (Allen, TX). Methoxy PEG amine (MW 2000) was from Shearwater Polymers Inc. (Huntsville, AL). It was dried at 60ºC under vacuum for 4 h before use. Corn trypsin inhibitor (CTI) was from Haematologic Technologies (Essex Junction, VT) and was dialyzed against phosphate-buffered saline (PBS, pH 8) before use. Human factor XIIa was from Enzyme Research Laboratories (South Bend, IN). Pefachrome XIIa, a factor XIIa-directed chromogenic substrate, was from Pentapharm (Basel, Switzerland). Human fibrinogen was from Enzyme Research Laboratories (South Bend, IN); it was dialyzed against isotonic Tris-buffered saline (TBS pH 7.4) and stored at -70°C.

2.1. Surface Preparation

Tecothane® polyurethane (PU) was treated with methanol to remove impurities and dried in a vacuum oven at 50ºC for 48 h. It was then dissolved in DMF (5% wt./vol.) at 60°C. Polymer films were cast in a petri dish and dried at 65°C for 48 h. Discs 6 mm in diameter and ~0.5 mm in thickness were cut from the films, washed with ethanol to remove impurities and dried at 50ºC.

CTI was treated with 2-iminothiolane-HCl (Traut's reagent) to introduce thiol groups as described previously[20]. A 5-fold molar excess of Traut's reagent in PBS-2 mM EDTA (pH 8) was used and the reaction allowed to proceed for 1 h at room temperature. The product was dialyzed against PBS-2 mM EDTA (pH 6) to remove

residual Traut's reagent. In previous work[20], we confirmed that the modification was successful using mass spectrometry to determine the product molecular weights. It was shown that the N-terminal amino group of CTI was converted to thiol.

Fig 1 shows the surface modification steps. Surface functionalization with MDI (reaction 1) was carried out as described previously [16,25,27]. Briefly, PU discs were incubated with a toluene solution containing 7.5% (wt./vol.) MDI and 2.5% (wt./vol.) triethylamine under nitrogen purge for 2 h at 50°C (PU-NCO surface). The discs were then rinsed three times with toluene, five minutes each time, and dried in a vacuum oven at 40ºC. PU-NCO surface was incubated with an acetonitrile solution containing 0.01 g/mL of maleimide-PEG-amine (MW 2000) under nitrogen purge for 16 h at 40°C to give PU-PEG-MAL surface (reaction 2 upper, Fig 1). The surfaces were rinsed three times with acetonitrile, five minutes each time, and dried in a vacuum oven at 40ºC.

The PU-PEG-MAL surface was incubated with a 7.5 μM solution of thiol-CTI in PBS for 2 h at room temperature, then for 16 h at 4°C to give PU-PEG-CTI surface (reaction 3c, Fig 1). This surface was rinsed three times with PBS, five minutes each time. The PU and PU-NCO surfaces were modified by treatment with 7.5 μM thiol-CTI to give PU-CTI and PU-NCO-CTI surfaces, respectively (reactions 3a and 3b, Fig 1). These were used as controls in the biointeraction experiments.

Surfaces modified with methoxy-PEG-amine, MW 2000 (PU-PEG-OCH_3), were also prepared for use as controls. PU-NCO surfaces were incubated with 0.05 g/mL methoxy-PEG-amine in toluene for 16 h at 40°C under nitrogen purge (reaction 2 lower, Fig 1). They were rinsed three times with toluene, five minutes each time, then with

water, and dried in a vacuum oven at 40ºC. These surfaces were exposed to 7.5 μM thiol-CTI to give surfaces designated PU-PEG-OCH_3-CTI.

2.2. Surface Characterization

The sessile drop method was used to determine advancing and receding water contact angles (Ramé-Hart goniometer, Mountain Lakes, NJ). Angles were measured at multiple points on both sides of the surfaces. Surface chemical composition was determined by X-ray photoelectron spectrometry (XPS, Thermo Scientific Theta probe). Low resolution scans were taken at 70º, 50º and 30º take off angles (measured from the perpendicular: smaller angle, greater sampling depth) to provide composition information as a function of depth.

2.2.1. Determination of CTI Surface Density

CTI density was measured using ^{125}I-labeled CTI. The Iodogen method (Iodogen Iodination Reagent, Pierce Biotechnology, Rockford, IL) was used to label thiol-CTI.[28] The labeled thiol-CTI was then used to prepare PU-CTI, PU-NCO-CTI, PU-PEG-OCH_3-CTI and PU-PEG-CTI surfaces. The radioactivity of the surfaces was measured and compared with that of a labeled CTI solution of known concentration.[29]

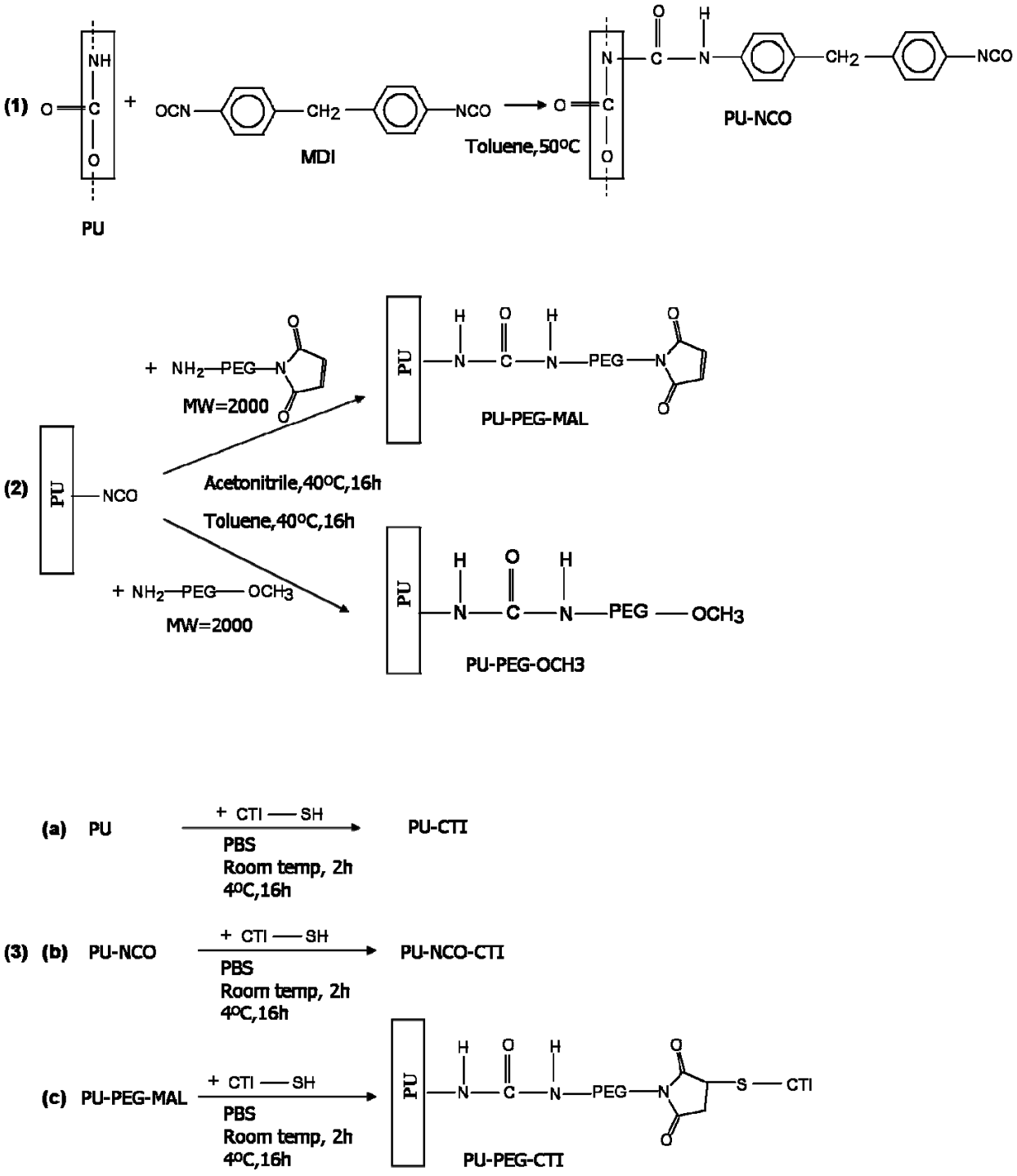

Fig 1. Surface modification. (1) Introduction of NCO groups, (2) Modification with PEG, (3) Modification with CTI

2.3. Biointeractions

Fibrinogen was labeled with ^{125}I (ICN Pharmaceuticals, Irvine, CA) using the iodine monochloride (ICl) method[30] and added as a tracer to a solution of cold fibrinogen in buffer or to plasma to investigate fibrinogen adsorption. The fibrinogen concentration in the buffer experiments was 1 mg/mL (10% labeled). Human citrated platelet poor plasma prepared from blood collected from multiple donors was used in the plasma experiments[20]. The quantity of labeled fibrinogen added to the plasma was equivalent to 10% of the endogenous amount.

To determine the activity of surface-immobilized CTI, surfaces were incubated with a factor XIIa solution, and the residual activity was measured. A chromogenic substrate assay in 96-well plate format was used for this purpose. 100 μL of a 200 nM solution of factor XIIa in TBS (pH 7.4) containing 2 mM $CaCl_2$, 12.5 μM $ZnCl_2$ and 15.4 μM BSA was added to wells containing the surfaces (area, 0.565 cm^2) and incubated for 1 h at room temperature. 100 μL of a 1.6 mM solution of factor XIIa-directed chromogenic substrate (Pefachrome XIIa) was then added to the wells and the plate was immediately placed in a UV-visible plate reader; optical density was recorded at 405 nm over a 1 h period. A factor XIIa standard curve was constructed using solutions of known factor XIIa concentration. Solutions were incubated for 1 h at room temperature in a 96-well plate. Chromogenic substrate was then added, the plate was placed in the plate reader and absorbance determined over a 1 h period.

To determine the effect of the surfaces on plasma clotting time, samples were incubated with 100 μL of pooled human platelet poor plasma for 15 min at 37˚C in a 96-

well plate. 100 μL of 0.025 M $CaCl_2$ was then added to each well to initiate clotting and the optical density at 405 nm was recorded. The time to reach half maximum optical density, as determined using the instrument software, was taken as a measure of the clotting time.

3. Results

3.1. Surface Characterization

Advancing and receding water contact angles are shown in Fig 2. The contact angles decreased upon modification of PU with MDI (PU-NCO surface). The advancing angle decreased from 94° on PU and 85° on PU-NCO to about 45° on the PEG-only surfaces (PU-PEG-OCH_3 and PU-PEG-MAL) confirming the presence of hydrophilic PEG on these surfaces. Upon treatment of PU-PEG-MAL with CTI (PU-PEG-CTI surface), the advancing angle increased to 55°, significantly higher than for the PEG-alone surfaces and significantly lower than for the other CTI modified surfaces (PU-CTI and PU-NCO-CTI). The contact angles on PU-CTI and PU-NCO-CTI were only slightly lower than those on their respective precursors PU and PU-NCO.

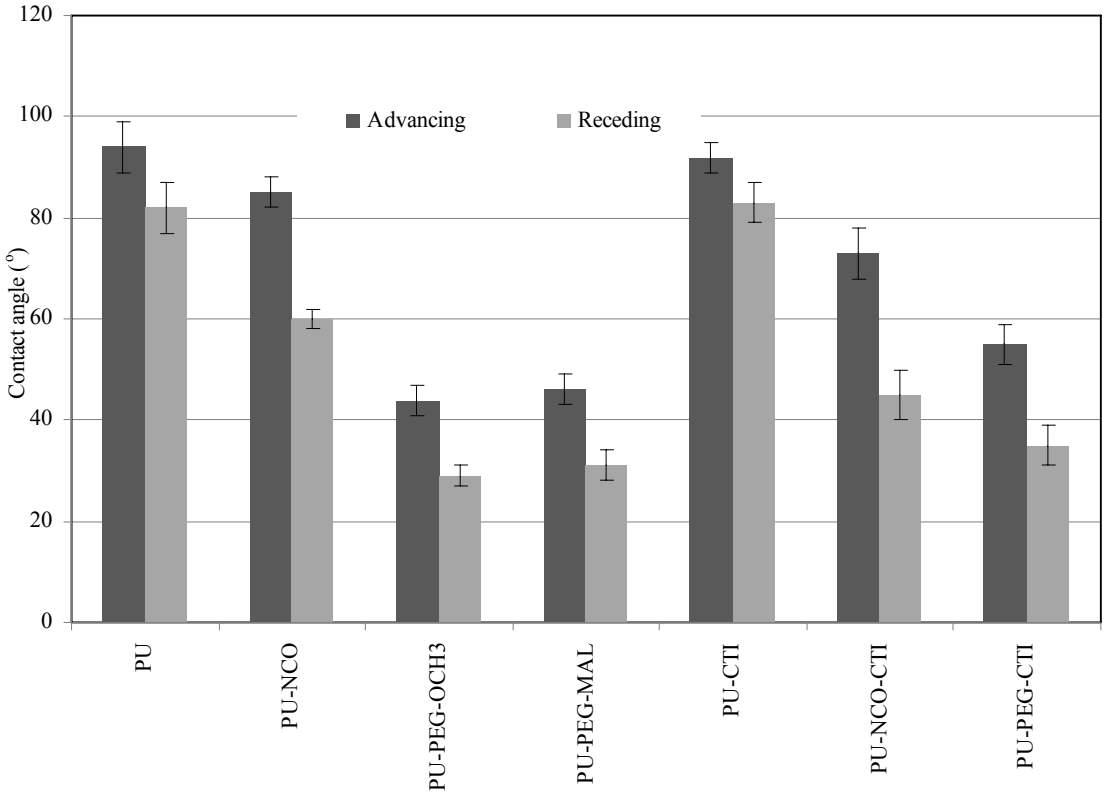

Fig 2. Water contact angles. Data are mean ± SD, n>9.

CTI surface density data are shown in Fig 3. Following exposure to CTI and determination of the density, the surfaces were incubated with 2% SDS solution for 3 h to remove CTI that was relatively loosely bound and the density determined again. As can be seen, the CTI was retained on the PU-NCO-CTI and PU-PEG-MAL-CTI surfaces but was largely released from the PU-CTI and PU-PEG-OCH_3–CTI surfaces. These results suggest that the CTI was more tightly bound (possibly covalently) on the former two surfaces. Specific binding (covalent or other) of CTI to the PU and PU-PEG-OCH_3 substrates is not expected; rather the interactions are presumably physical as suggested by the SDS-induced release. Since NCO groups react with amino and hydroxyl groups, the

PU-NCO substrate is expected to show high uptake of proteins. In thiol-CTI, the N-terminal amino group of CTI is converted to thiol, but the primary amino group of the lysine residue and the hydroxyl groups of serine residues remain available and may react with NCO. The PU-PEG-MAL-CTI and PU-PEG-OCH_3-CTI surfaces showed lower CTI density presumably because of the protein resistance of the PEG. CTI density on PU-PEG-MAL-CTI was significantly higher than on PU-PEG-OCH_3-CTI presumably due to the reaction of the maleimide groups with thiol groups of CTI. A close packed monolayer of CTI should have a density in the range of 0.15-0.25 $\mu g/cm^2$ assuming that the dimensions of CTI are similar to those of lysozyme (MW 14 kDa; 46Å x 30Å x 20Å). Thus all of the surfaces showed CTI density in the monolayer range. For protein adsorption experiments CTI surfaces were used after standard buffer rinsing (not exposed to SDS).

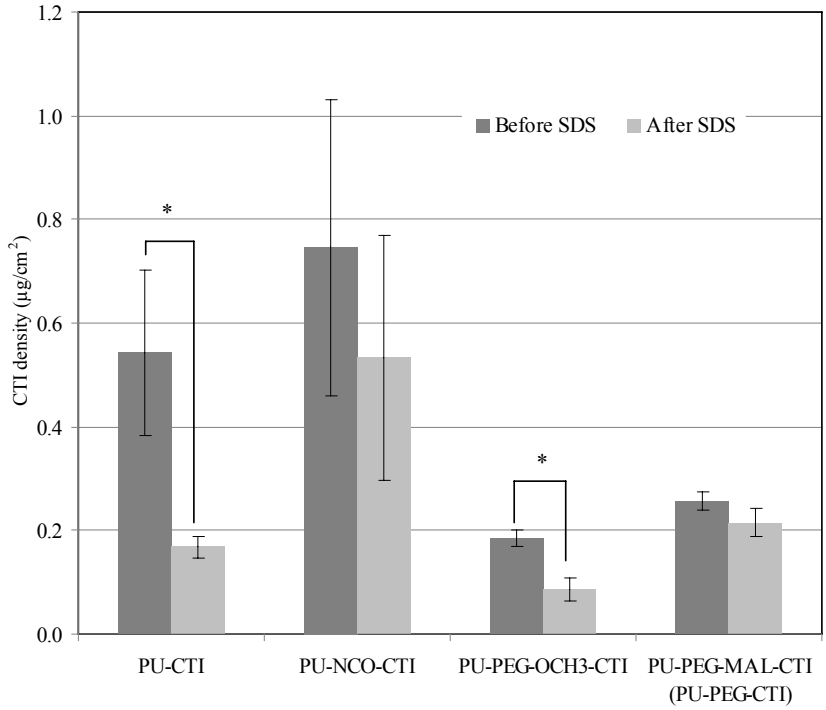

Fig 3. Surface density of CTI. Data are mean ± SD, n=9. * indicates significant difference ($p<0.05$, Student's t-test).

Low resolution XPS data are shown in Table 1. At all three take off angles, a significant increase in nitrogen concentration (from ~4 to ~10 atom%) was observed on PU-NCO compared with PU, indicating modification of PU with MDI. After reaction with PEG, the nitrogen and carbon concentrations decreased while the oxygen concentration increased. As the take-off angle increased (sampling closer to the surface), the oxygen content increased slightly on the surfaces that contained PEG segments but no CTI, confirming that the increase in the oxygen content was due to the presence of PEG. Furthermore, as expected, the C:O ratio decreased upon PEG attachment. Based on the C:O ratio and oxygen concentration, it appears that slightly higher densities of PEG were obtained on the PEG-MAL surface compared with the PEG-OCH3 surface. Upon CTI

reaction with PU-PEG-MAL, the nitrogen and sulfur concentrations increased indicating attachment of the protein.

Table 1. Composition of surfaces from XPS data (mean of two determinations, different samples). Take off angles are relative to the vertical: smaller value, greater sampling depth.

30º angle (greatest depth)	C	N	O	S	C/N ratio	C/O ratio
PU	90.1	4.4	5.4		20.3	16.7
PU-NCO	77.6	10.0	12.4		7.8	6.2
PU-PEG-OCH3	74.2	3.4	22.4		22.0	3.3
PU-PEG-MAL	69.5	4.1	26.4		17.0	2.6
PU-PEG-CTI	70.9	4.7	24.4	0.1	15.2	2.9
50º angle	C	N	O	S	C/N ratio	C/O ratio
PU	91.4	3.9	4.6		23.2	19.7
PU-NCO	75.3	9.1	12.6		8.3	6.0
PU-PEG-OCH3	75.1	2.6	22.3		29.3	3.4
PU-PEG-MAL	70.8	3.5	25.7		20.5	2.8
PU-PEG-CTI	72.0	3.8	24.2	0.1	19.0	3.0
70º angle (nearest surface)	C	N	O	S	C/N ratio	C/O ratio
PU	92.4	3.8	3.7		24.2	24.7
PU-NCO	76.8	9.3	13.9		8.3	5.5
PU-PEG-OCH3	73.4	2.1	24.5		34	3.0
PU-PEG-MAL	69.5	2.8	27.7		24.7	2.5
PU-PEG-CTI	69.1	3.4	27.5	0.03	20.3	2.5

Data precision ~5%

3.2. Blood Protein Interactions

3.2.1 Fibrinogen Adsorption from Buffer and Plasma

Data on fibrinogen adsorption from buffer and plasma are shown in Figures 4a and 4b respectively. Adsorption from buffer (Fig 4a) was slightly lower on PU-CTI than on unmodified PU. The higher adsorption seen on PU-NCO may be related to reaction of the NCO groups with amino and hydroxyl groups of fibrinogen. Adsorption was significantly lower on the PEGylated surfaces PU-PEG-OCH_3, PU-PEG-MAL and PU-PEG-CTI. These results indicate successful modification with protein resistant PEG.

Reaction of PU-PEG-MAL with CTI did not compromise protein resistance: the PU-PEG-CTI surface showed significantly lower fibrinogen adsorption compared with the non-PEG CTI surfaces (PU-CTI and PU-NCO-CTI).

Adsorption from plasma (Fig 4b) was lower than from buffer, and showed similar trends with respect to the different surfaces to those seen in the buffer experiments. Adsorption was relatively high on the non-PEG surfaces and low on PU-PEG-OCH_3, PU-PEG-MAL and PU-PEG-CTI. Again, PEG retained its protein resistance on the PU-PEG-CTI surface.

3.2.2. Factor XIIa Inhibition by Surfaces

Fig 5 shows data on factor XIIa inhibition by the surfaces. Surfaces were incubated with factor XIIa solution for 1 h. The chromogenic substrate was then added and the residual factor XIIa determined. It can be seen that the PU-PEG-CTI surface inhibited about 72% of the factor XIIa, a significantly greater proportion than any other surface. We assume that inhibition on these surfaces is due simply to non-specific interactions of XIIa with the surface such that it is unavailable to react with the substrate. Interestingly, although the CTI density on PU-NCO-CTI was higher than that on PU-PEG-CTI, the factor XIIa inhibition was lower. This result suggests that the "presentation" of CTI on PU-PEG-CTI may be more effective than on PU-NCO-CTI. Two factors may contribute to this improvement. First, the orientation of CTI may be more optimal when attached to PEG via the thiol group, and second the spacer effect of the PEG may increase CTI accessibility for reaction with factor XIIa.

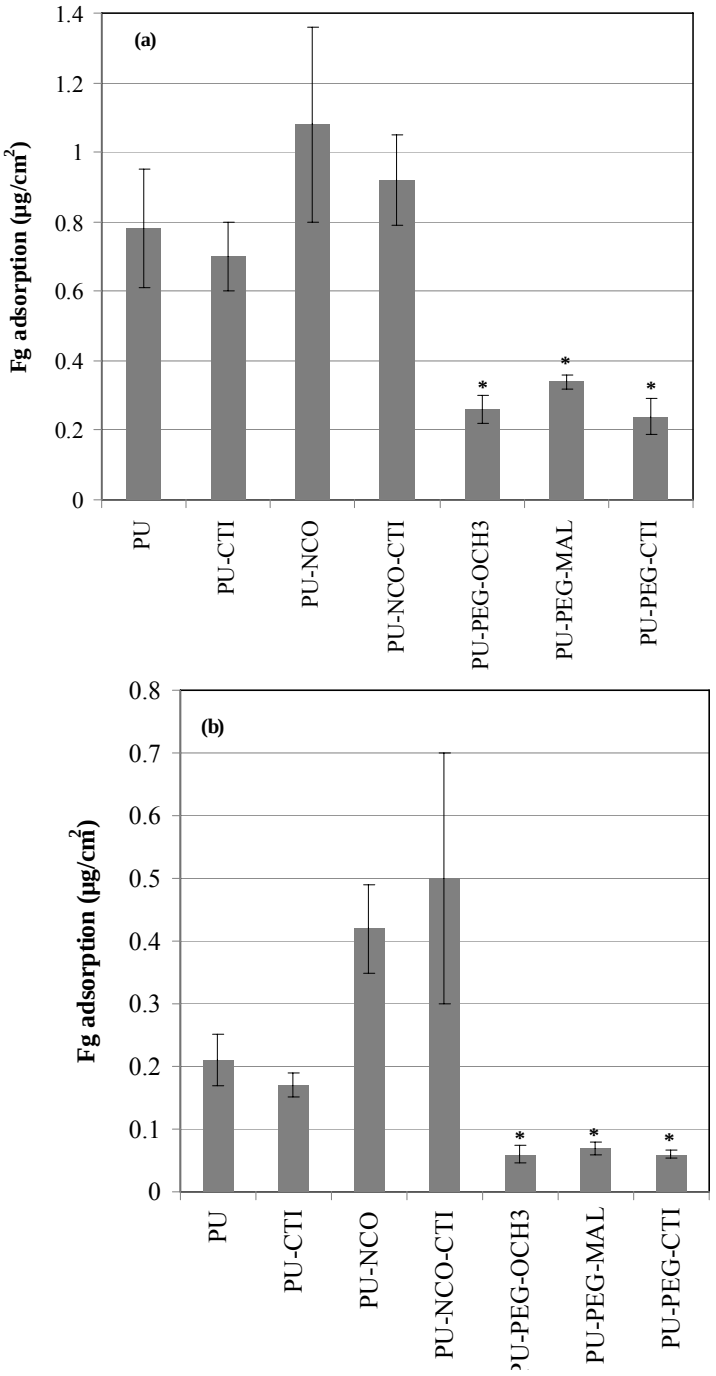

Fig 4. Fibrinogen adsorption from: (a) buffer, (b) plasma. Adsorption time, 3 h. Data are mean ± SD, n=3. * indicates significant difference for PEG-containing surfaces vs. other surfaces ($p<0.05$, Student's t-test).

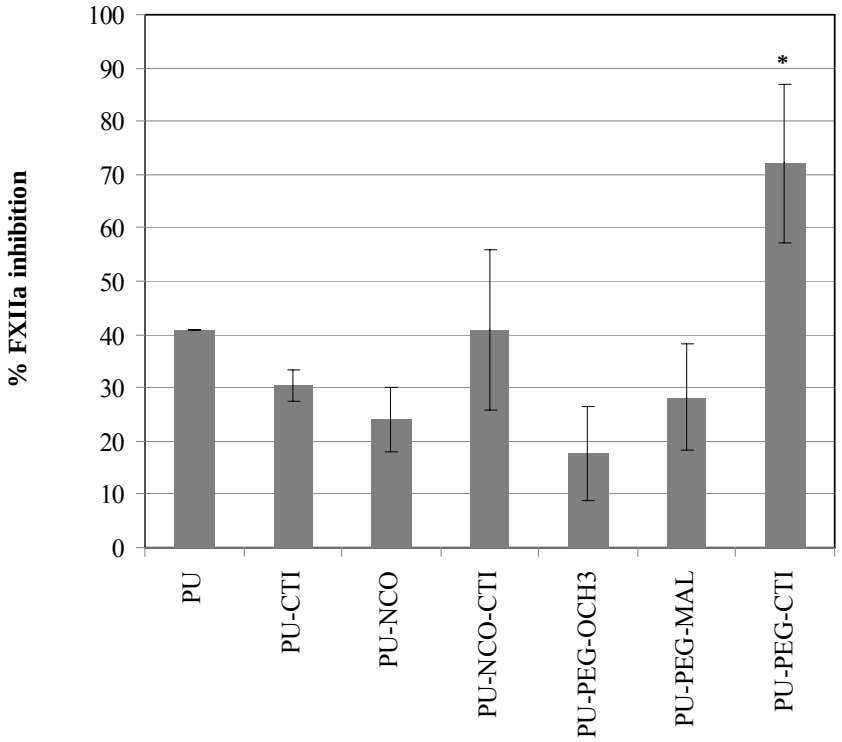

Fig 5. Activity of FXIIa solutions after incubation with surfaces. Data are mean ± SD, n=3. * indicates significant difference ($p<0.05$, Student's t-test).

3.2.3. Plasma clotting times

Clotting time data are shown in Fig 6. Attachment of PEG to the PU surface had only a slight effect on clotting time (PU-PEG-OCH_3). This is consistent with previous results using gold as a model substrate [20]. Since the PU-PEG surfaces showed relatively low fibrinogen adsorption from buffer and plasma but did not prolong the clotting time, it appears that fibrinogen adsorption is not directly related to coagulation, at least as indicated by clotting time. Attachment of CTI increased clotting times on the CTI surfaces relative to controls: PU-CTI vs PU, PU-NCO-CTI vs PU-NCO, and PU-PEG-CTI vs PU-PEG-MAL. Presumably this effect is due to inhibition of factor XIIa. PU-

PEG-CTI was the most effective surface, showing a significantly longer clotting time than PU, PU-NCO, PU-PEG, and PU-CTI ($p<0.05$).

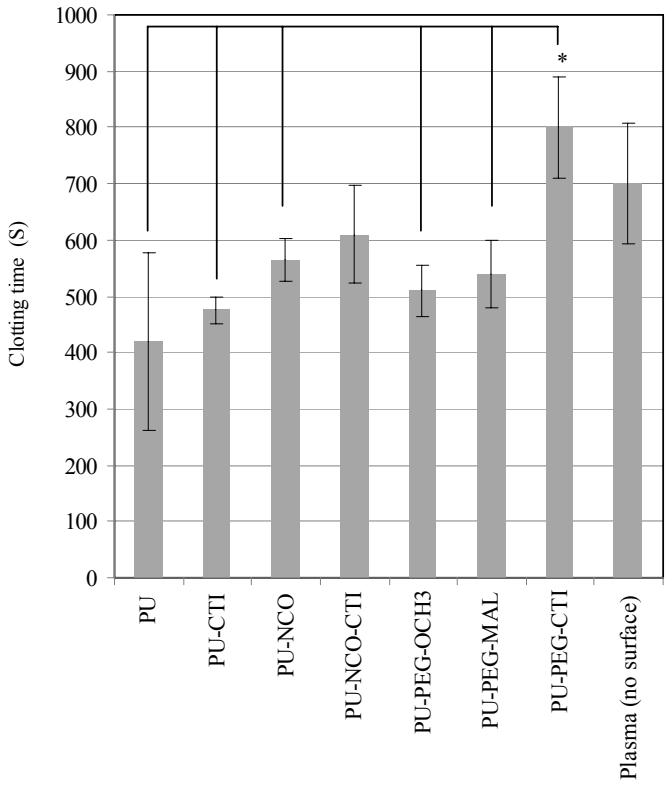

Fig 6. Plasma clotting times. Data are mean ± SD, n=3. * indicates significant difference ($p<0.05$, Student's t-test).

4. Discussion

The guiding hypothesis on which the work is based is that the presence of PEG to provide protein resistance and CTI for anticoagulant activity should improve blood compatibility. Our previous work on PEG-CTI modified surfaces showed that immobilizing PEG first and then attaching CTI (sequential method) was more effective than immobilizing a preformed PEG-CTI conjugate (direct method) [20]. Therefore in this study we used a sequential method to modify the polyurethane substrate.

CTI densities on the polyurethane surfaces in this work were significantly higher than on the gold model substrate surfaces used previously [20]. The higher densities on PU were probably due to the different modification chemistry. For the gold substrate, PEG-NHS disulfide was attached first, followed by maleimide-PEG-amine and finally CTI. In the present work, PU was first reacted with MDI to introduce NCO groups. From the increase in nitrogen content (Table 1), it is clear that a high density of NCO groups was present on the PU-NCO surface, which in turn led to high densities of PEG and CTI. On PU-PEG-CTI, we assume that thiol-CTI was attached via the maleimide groups of PEG and not via unreacted underlying NCO groups. This assumption is supported by the observation of low fibrinogen adsorption on PU-PEG-MAL. If free NCO groups were present to any significant extent on PU-PEG-MAL, they would be expected to react with contacting proteins, and fibrinogen adsorption on PU-PEG-MAL and PU-PEG-OCH3 surfaces would be higher.

The PU-CTI and PU-NCO-CTI control surfaces performed poorly in terms of protein resistance, showing relatively high fibrinogen adsorption from buffer and plasma. PU-PEG-CTI, on the other hand, showed low fibrinogen adsorption, similar to the other PEG surfaces PU-PEG-MAL and PU-PEG-OCH_3. Furthermore, despite the higher density of CTI on PU-NCO-CTI than on PU-PEG-CTI, the former was less effective in inhibiting factor XIIa and prolonging the plasma clotting time. These differences may be due to the orientation of CTI as dictated by reaction with the thiol group in CTI, making the active site of CTI at Arg-62 more accessible for protein interactions. In the reaction of thiol-CTI with PU-NCO to prepare PU-NCO-CTI, the NCO groups can potentially react

with amino and hydroxyl groups as well as with the thiol group in CTI. The CTI orientation might then be altered such that the active site is less available to interact with and inhibit factor XIIa. Greater factor XIIa inhibition by PU-PEG-CTI may also be due to the action of PEG as a spacer, again increasing the accessibility of factor XIIa to the active site of CTI. Both of these effects may contribute to the superior performance of PU-PEG-CTI.

5. Summary and Conclusions

Polyurethane surfaces were modified with PEG and CTI both individually and together. PU-PEG-CTI showed protein resistance similar to PEG-only surfaces. Of the CTI surfaces investigated, PU-NCO-CTI showed relatively high CTI density but relatively low anti-factor XIIa activity. The PU-PEG-CTI surface exhibited the highest factor XIIa inhibition and protein resistance. It is concluded that combined PEG and CTI modification reduces non-specific protein adsorption while promoting specific adsorption of factor XIIa and that this approach may be useful for the development of thromboresistant polyurethanes.

Acknowledgements

Work supported by the Natural Sciences and Engineering Research Council of Canada (NSERC) and the Canadian Institutes of Health Research (CIHR). Dr. Weitz holds the Canada Research Chair (Tier 1) in Thrombosis and the HSFO/J. F. Mustard Chair in Cardiovascular Research.

References

[1] J. L. Brash, *J. Biomater. Sci. Polym. Ed.*, **11**, 1135 (2000).
[2] H. Chen, L. Yuan, W. Song, Z. K. Wu and D. Li, *Prog. Polym. Sci.*, **33**, 1059 (2008).
[3] M. B. Gorbet and M. V. Sefton, *Biomaterials*, **25**, 5681 (2004).
[4] Z. L. Jin, W. Feng, S. P. Zhu, H. Sheardown and J. L. Brash, *J. Biomed. Mater. Res. A*, **91A**, 1189 (2009).
[5] L.D. Unsworth, H. Sheardown, and JL Brash. *Biomaterials,* **26**, 5927 (2005).
[6] L. D. Unsworth, H. Sheardown and J. L. Brash, *Langmuir*, **24**, 1924 (2008).
[7] Z. Zhang, M. Zhang, S. F. Chen, T. A. Horbett, B. D. Ratner and S. Y. Jiang, *Biomaterials*, **29**, 4285 (2008).
[8] Y. J. Du, P. Klement, L. R. Berry, P. Tressel and A. K. C. Chan, *Thromb. Haemost.*, **94**, 366 (2005).
[9] M. C. L. Martins, S. A. Curtin, S. C. Freitas, P. Salgueiro, B. D. Ratner and M. A. Barbosa, *J. Biomed. Mater. Res. A*, **88A**, 162 (2008).
[10] H. Chen, Y. Chen, H. Sheardown and M. A. Brook, *Biomaterials*, **26**, 7418 (2005).
[11] Z. Yang, J. Wang, R. Luo, M. F. Maitz, F. Jing, H. Sun and N. Huang, *Biomaterials*, **31**, 2072 (2010).
[12] A. D. Baldwin and K. L. Kiick, *Biopolymers*, **94**, 128 (2010).
[13] W. G. McClung, D. L. Clapper, A. B. Anderson, D. E. Babcock and J. L. Brash, *J. Biomed. Mater. Res. A*, **66A**, 795 (2003).
[14] W. McClung, D. E. Babcock and J. L. Brash, *J. Biomed. Mater. Res. A*, **81A**, 644 (2007).
[15] S. Alibeik, S. Zhu and J. L. Brash, *Colloids Surf. B: Biointerfaces* **81**, 389 (2010).
[16] H. Chen, Y. X. Zhang, D. Li, X. Y. Hu, L. Wang, W. G. McClung and J. L. Brash, *J. Biomed. Mater. Res. A*, **90A**, 940 (2009).
[17] K. N. Sask, W. G. McClung, L. R. Berry, A. K. C. Chan and J. L. Brash, *Acta Biomater.*, **7**, 2029 (2011).
[18] W. C. Mahoney, M. A. Hermodson, B. Jones, D. D. Powers, R. S. Corfman and G. R. Reeck, *J. Biol. Chem.*, **259**, 8412 (1984).
[19] E. A. Vogler and C. A. Siedlecki, *Biomaterials*, **30**, 1857 (2009).
[20] S. Alibeik, S. Zhu, J. W. Yau, J. I. Weitz and J. L. Brash, *Acta Biomater.*, in press. DOI: 10.1016/j.actbio.2011.07.022.
[21] R. J. Zdrahala and I. J. Zdrahala, *J. Biomater. Applications*, **14**, 67 (1999).
[22] T. Hentschel and H. Munstedt, *Infection*, **27**, S43 (1999).
[23] R. Adhikari, P. A. Gunatillake, I. Griffiths, L. Tatai, M. Wickramaratna, S. Houshyar, T. Moore, R. T. M. Mayadunne, J. Field, M. McGee and T. Carbone, *Biomaterials*, **29**, 3762 (2008).
[24] M. C. Besteiro, A. J. Guiomar, C. A. Goncalves, V. A. Bairos, M. N. de Pinho and H. Gil, *J. Biomed. Mater. Res. A*, **93A**, 954 (2010).
[25] J. G. Archambault and J. L. Brash, *Colloids Surf B: Biointerfaces*, **33**, 111 (2004).
[26] J. H. Silver, H. B. Lin and S. L. Cooper, *Biomaterials*, **14**, 834 (1993).
[27] J. G. Archambault and J. L. Brash, *Colloids and Surf B: Biointerfaces*, **39**, 9 (2004).

[28] L. C. Knight, A. Z. Budzynski and S. A. Olexa, *Thromb. Haemost.*, **46**, 593 (1981).
[29] W. G. McClung, D. L. Clapper, S. P. Hu and J. L. Brash, *J. Biomed. Mater. Res.*, **49**, 409 (2000).
[30] M. E. Price, R. M. Cornelius and J. L. Brash, *Biochim. Biophys. Acta-Biomembr.*, **1512**, 191 (2001).

CHAPTER 7. SUMMARY AND RECOMMENDATIONS FOR FUTURE WORK

7.1 Summary and Conclusions

It was hypothesized in this research that surface modification with polyethylene glycol (PEG) and appropriate bioactive molecules will improve blood compatibility. The following points indicate the thinking behind this hypothesis. First, PEG-modified biomaterials have been studied extensively on the basis of their protein resistant properties [1-3]. Second, bioactive molecules have been used to create surfaces that promote specific protein-surface interactions that are advantageous for blood compatibility [2, 4]. In the work presented in this thesis, surface modification was explored using combinations of PEG and two bioactive molecules: hirudin and corn trypsin inhibitor (CTI). Two methods, sequential and direct, were employed to immobilize PEG and the bioactive molecules. When PEG was immobilized first and the bioactive molecule was then conjugated to the immobilized PEG, the modification method was referred to as sequential. When a conjugate of PEG and bioactive molecule was first prepared and then immobilized on surface, the method was referred to as direct.

In the first part of this research (Chapter 3), gold-coated silicon was modified with PEG and hirudin using sequential and direct methods. Hirudin is a potent anticoagulant with specific thrombin inhibitory activity. After verifying surface modification using contact angle, ellipsometry, XPS and radiolabeled hirudin adsorption experiments, plasma protein interactions were studied by radiolabeling and immunoblotting. Hirudin inhibitory activity against thrombin using a chromogenic substrate assay was also measured.

Fibrinogen adsorption was found to be similar on the PEG-hirudin and PEG-alone surfaces while thrombin adsorption was significantly higher on the PEG-hirudin surfaces. The sequential surfaces were more effective in terms of thrombin inhibition.

In subsequent work, gold coated silicon was modified with PEG and corn trypsin inhibitor (CTI) using sequential and direct methods (Chapter 4). CTI is a specific inhibitor of FXIIa, and thus can inhibit the first step in the contact phase of the intrinsic coagulation pathway. This is in contrast to hirudin which inhibits thrombin and thus interferes near the end of the cascade. Surface modification was confirmed with contact angle, XPS, ellipsometry and radiolabeled CTI adsorption experiments. Plasma protein interactions were studied by radiolabeling, immunoblotting, CTI activity assay using a chromogenic substrate and clotting time measurements. Fibrinogen adsorption on both the direct and sequential PEG-CTI surfaces was the same as on the PEG-alone surface. The PEG-CTI surfaces showed greater FXIIa inhibitory effect and longer plasma clotting times than PEG-alone surfaces. Sequential surfaces showed greater inhibition than direct ones.

The gold-PEG-CTI system was investigated further (Chapter 5) using surfaces with varying ratio of free PEG to conjugated PEG (PEG-CTI), prepared using both sequential and direct methods. The objective was to ascertain whether a particular surface composition would give optimum performance in terms of both protein resistance and bioactivity. Surfaces were characterized by contact angle, ellipsometry and radiolabeled CTI adsorption. Plasma protein interactions were investigated by measuring: (1) fibrinogen adsorption from buffer and plasma, (2) fibrinogen and α-lactalbumin

adsorption competitively (binary system) from buffer, (3) FXIIa inhibition. Plasma clotting time assays were conducted in the presence of the surfaces. With increasing ratio of conjugated to free PEG it was found that protein resistance was preserved while CTI bioactivity (FXIIa inhibition) increased. It thus appears that the optimum surface would be one in which the PEG:CTI ratio is 1:1.

In the final part of this research (Chapter 6), surface modification of a polyurethane with PEG-CTI was studied. Polyurethanes have been widely used to construct blood contacting devices. A sequential method was used for surface modification. Surfaces were characterized by contact angle, XPS and radiolabeled CTI uptake experiments. Fibrinogen adsorption from buffer and plasma, FXIIa inhibition by chromogenic assay and plasma clotting times were measured. Despite having lower CTI density, PU surfaces modified with both PEG and CTI showed significantly greater protein resistance and greater XIIa inhibition compared with PU surfaces modified with CTI only.

Overall, from the research presented in this thesis, it is concluded that modification of biomaterials with combinations of PEG and bioactive molecules can improve blood compatibility. On PEG-hirudin and PEG-CTI surfaces, PEG retained its protein resistant properties while the hirudin and CTI were inhibitory of thrombin and factor XIIa respectively. For both hirudin and CTI as the bioactive component, the effectiveness of the PEG-bioactive combination was greater when the components were attached sequentially to the surface. PEG seemed to have a positive effect, presumably as

a spacer, on interactions between the bioactive component and its target plasma protein especially in the case of sequential surfaces.

7.2 Recommendations for the Future Work

Several foci can be envisaged for future work on protein resistant, bioactive surfaces.

1. Materials that are more relevant to medical devices, specifically in blood contact situations such as catheters and stents should be further investigated. Most of the work reported in this thesis was on gold surfaces as a model substrate. Although this allowed detailed surface characterization and was an appropriate choice to investigate the modification process including variables such as PEG:bioactive ratio, it would be useful to extend the dual modification approach to other appropriate substrates. The work on polyurethanes initiated here should be extended to polyurethanes more generally and to other polymers. From the present work it was concluded that the sequential attachment of PEG and bioactive molecule is more effective than the direct attachment. Thus, the sequential approach should be investigated for the improvement of various blood contacting devices such as catheters and stents.

2. CTI, as an inhibitor of coagulation which acts on the initial step of the intrinsic pathway, should be investigated in greater depth; for example different chain lengths of PEG as spacer should be used to optimize CTI-plasma protein interactions and CTI density.

3. The protein resistant and bioactive components should be further explored. Other protein resistant molecules such as polyMPC and polyOEGMA should be

investigated. Surfaces should be prepared having two bioactive components: for example CTI to inhibit the early stages of coagulation and hirudin or heparin to inhibit the "downstream" stages.

4. Future work should focus on more detailed studies of the biological interactions of PEG-CTI and PEG-hirudin surfaces. Studies of platelet interactions with the modified surfaces should be conducted since platelets play a major role in clot formation. Longer time frames for blood-material exposure will provide essential information for long-term applications. Furthermore, the host response to blood contacting devices is not limited to thrombosis and clot formation. Other reactions such as inflammation and immunological responses generally occur and can lead to device failure [5]. Investigation of such responses should be carried out for PEG-bioactive-molecule modified surfaces.

7.3 References

[1] Lee JH, Lee HB, Andrade JD. Blood Compatibility of Polyethylene Oxide Surfaces. Prog Polym Sci 1995;20:1043-79.
[2] Chen H, Yuan L, Song W, Wu ZK, Li D. Biocompatible polymer materials: Role of protein-surface interactions. Prog Polym Sci 2008;33:1059-87.
[3] Dong BY, Manolache S, Wong ACL, Denes FS. Antifouling ability of polyethylene glycol of different molecular weights grafted onto polyester surfaces by cold plasma. Polym Bull 2011;66:517-28.
[4] Brash JL. Exploiting the current paradigm of blood-material interactions for the rational design of blood-compatible materials. J Biomater Sci Polym Ed 2000;11:1135-46.
[5] Ratner BD, Bryant SJ. Biomaterials: Where we have been and where we are going. Annu Rev Biomed Eng 2004;6:41-75.

APPENDIX A: Experimental Methods

In this appendix the experimental methods used in this work are explained in detail.

A.1 Surface Analysis Methods

1.1 Water Contact Angle

Water contact angle measurement is a simple method for the determination of surface hydrophilicity/hydrophobicity. A drop of water beads up on a hydrophobic surface giving a high contact angle, while it spreads on a hydrophilic surface giving a low contact angle. Young's equation describes the contact angle on a smooth, homogeneous surface [1].

$$Cos\theta = \frac{\gamma_{SV} - \gamma_{SL}}{\gamma_{LV}}$$

Where θ is the contact angle, γ_{SV} is the solid-vapor surface tension, γ_{SL} is the liquid-solid surface tension and γ_{LV} liquid-vapor surface tension. Surface modification results in changes in γ_{SV} and γ_{SL}. Surface chemical heterogeneity, surface roughness, size and shape of the surface can affect contact angle [2]. Since surfaces are usually heterogeneous and rough, two contact angles are measured: advancing and receding. The advancing angle is measured when the droplet is placed on the surface and the receding angle is measured when the droplet is withdrawn. Hysteresis, the difference between advancing and receding contact angles, is an indication of heterogeneity and roughness.

In this work, the static sessile drop method was used to measure water contact angles. The goniometer used for the measurements was a Ramé-Hart NRL (Mountain

Lakes, NJ) instrument. A 10 μL drop of water was placed on the surface using a syringe. After drop equilibration, the advancing angle was measured. Water was then removed from the drop, using the syringe, to the point where the water contact line started to retract. After drop equilibration, the receding angle was measured.

1.2 Ellipsometry

Ellipsometry is an optical technique, that is used to determine film thickness ranging from a few angstroms to micrometers with a precision of around 2 Å. A light source (He-Ne laser in this work) emits radiation which passes through a polarizer, impinges on the sample and is reflected and analyzed [3]. The change in the polarization of the reflected light is measured by the analyzer to determine the reflection coefficient. Reflection coefficient is defined as the ratio of the amplitude of the reflected light to that of the incident light. The change in polarization of reflected light depends on sample properties such as film thickness, refractive index and extinction coefficient [4]. These properties are estimated by mathematical models. To calculate the film thickness estimates must be used for the refractive index and extinction coefficient. For dry polymer films, the extinction coefficient is usually assumed to be zero indicating that the polymer films are non-absorbing [5].

In this work, a self-nulling, single wave length (6328 Å), Exacta 2000^{TM} (Waterloo Digital Electronics, Waterloo, Ontario) was used to measure the thickness of films on modified surfaces. Gold surfaces were cleaned and stored under nitrogen before the ellipsometry measurements. Analyzer and polarizer angles were measured for gold

substrate and the refractive index and extinction coefficient for gold were measured using the Exacta 2000^{TM} variable theta simplex fit program supplied by the manufacturer. These values for gold were 0.2 and 3.5, respectively. The incident angle was 70º. Analyzer and polarizer values were also measured for the modified surfaces and the thickness of PEO film was determined using the software supplied by the manufacturer.

1.3 X-ray Photoelectron Spectroscopy

X-ray photoelectron spectroscopy (XPS), also known as electron spectroscopy for chemical analysis (ESCA) is a quantitative method for determining the elemental composition of surfaces. Surfaces are exposed to an X-ray source and photoelectrons are emitted from the core levels of the surface atoms. The analyzer determines the binding energy of the photoelectrons. Each element has characteristic electron binding energy values and thus by obtaining the number of detected electrons and their binding energy, the chemical composition of the surface can be obtained [6]. XPS typically measures elements in the top 1-10 nm of the surface.

Two XPS spectrometers were used in this work, the Thermo Scientific K-Alpha and the Thermo Scientific Theta Probe. Both use a monochromated Al Kα X-ray source with a spot area of 400 μm. For K-Alpha, the low resolution spectra were taken at two take-off angles, 90º and 20º (90º is perpendicular to the surface, so bigger angle, greater sampling depth). For the Theta probe, the low resolution spectra were obtained at 70º, 50º and 30º take-off angles (90º is parallel to the surface, so smaller angle, greater sampling depth). On spectra of gold surfaces, the position of the energy scale was adjusted to place

the main Au 4f7/2 peak at 84.0 eV. On the spectra of polyurethane surfaces, position of the energy scale was adjusted to place the main C 1s feature (C-C) at 285.0 eV. As an example, a low resolution spectrum of unmodified polyurethane is shown in Fig A-1.

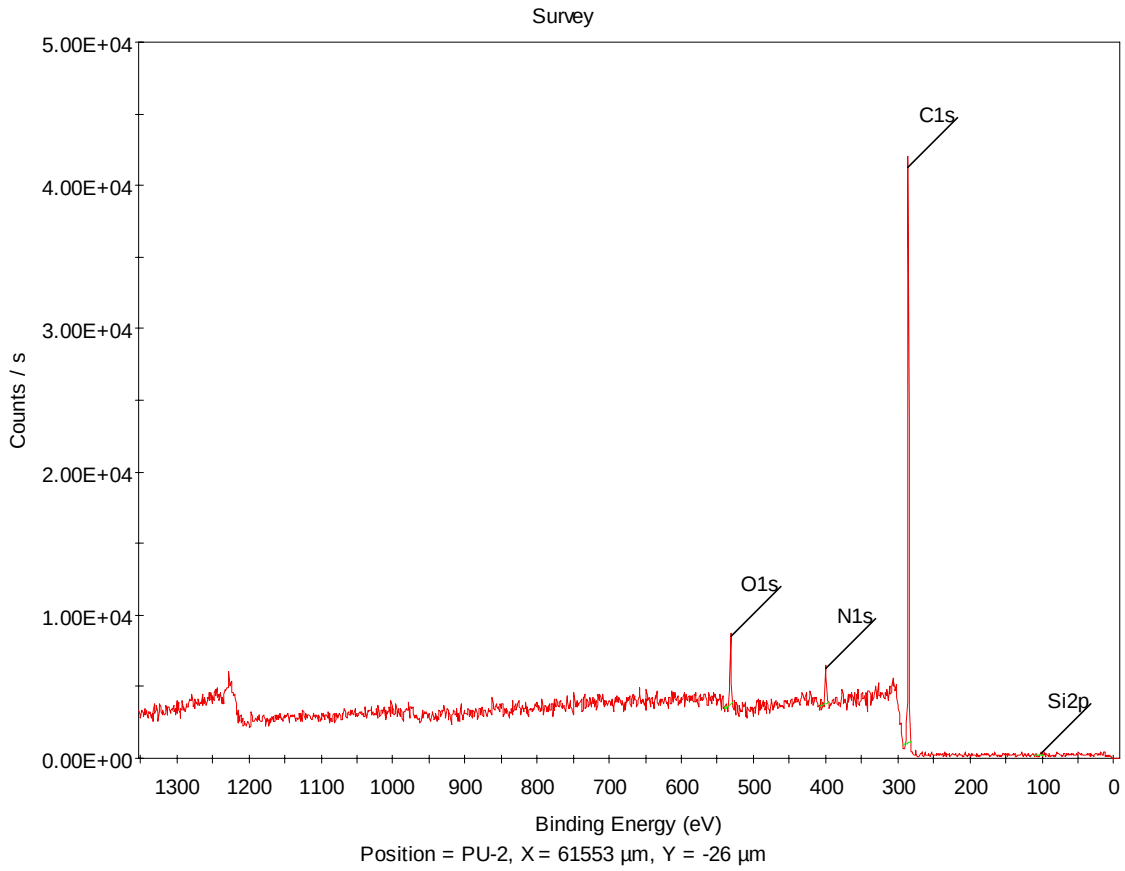

Peaks (P)\Peaks Angle (Ø)	C1s	N1s	O1s	Si2p
	At%	At%	At%	At%
30	89.48	4.09	6.00	0.42
50	90.22	4.01	5.25	0.51
70	91.20	3.90	4.28	0.62

Figure A- 1 Low resolution XPS of unmodified polyurethane

A.2 Matrix-Assisted Laser Desorption/Ionization Mass Spectrometry

Matrix-assisted laser desorption ionization mass spectrometry (MALDI-MS) is a technique that can be used to determine the molecular weights of proteins, peptides and other large biomolecules that cannot tolerate the harsh conditions of conventional ionization methods [7]. The sample is embedded in a matrix material (eg 3,5-dimethoxy-4-hydroxycinnamic acid (sinapinic acid)) which protects it from the laser beam. The ions produced by the action of the laser then travel through a field free region to reach the detector. The detector can identify the ions based on the time to reach the detector and thus can categorize them based on their mass to charge ratio (m/z). Calibration with a known sample is required to create the mass to charge ratio scale.

In this work, MALDI-MS was used to confirm the polymer-protein conjugation reactions (see paper 2). The equipment was a Waters/Micromass MALDI Micro MX with the ability to detect masses ranging between 100 Da to 200 kDa. Samples were de-salted before conducting mass spectrometry. MALDI-MS was carried out at the McMaster Regional Centre for Mass Spectrometry.

A.3 Biological Interactions

3.1 Plasma Preparation

To prepare plasma pool for the plasma experiments, blood was collected from a minimum of 10 healthy volunteers. The volunteers were aspirin-free and antihistamine-free for a minimum of 10 days prior to donating. Blood was added into polypropylene centrifuge tubes containing acid citrate dextrose (ACD, 1 part ACD, 6 parts whole blood) and mixed. It was centrifuged for 5 min at 2500 x g to give platelet rich plasma (PRP).

The supernatant was centrifuged again for 5 min at 2500 x g to give platelet poor plasma (PPP). The plasma was pooled and stored at -70ºC. This procedure has ethics approval from McMaster University (McMaster University ethics protocol #04-046).

Defibrinogenated plasma was prepared by adding Atroxin (snake venom) to platelet poor plasma (PPP) (0.5 μg per mL of plasma). The mixture was incubated for 10 min at 37ºC, followed by 30 min at 4ºC. It was then centrifuged at 1000 x g for 30 min to remove the fibrin clot.

Serum was prepared by mixing 4 mL of 0.25M $CaCl_2$ with 24 mL PPP in a 50 mL conical centrifuge tube. The tube was incubated at 37ºC until the clot was fully formed. It was then centrifuged at 1000 x g for 30 min to remove the clot. The serum was stored at -70°C.

3. 2 Protein Adsorption Experiments

Protein adsorption was measured using ^{125}I-labeled proteins. This method allows quantification of proteins adsorbed on surfaces. In radiolabeling, the protein is chemically modified by introducing radioactive iodine atom(s) [8]. Two radioactive isotopes of iodine, ^{125}I and ^{131}I, were used for labeling in this work. Both of these isotopes are γ emitters. ^{131}I also decays by β emission. Since the half life of ^{131}I is much shorter than that of ^{125}I (8 days vs. 60 days) ^{125}I was used in all experiments except those where two proteins were labeled. In the labeling reactions conducted in aqueous solution, iodine attaches to tyrosine and/or histidine residues of proteins.

A list of proteins used in the radiolabeling experiments is given in table A-1. Two methods were used for radiolabeling using Na ^{125}I: the Iodo-Gen method and the iodine

monochloride (ICl) method. The Iodo-Gen method was used to label CTI and thrombin both of which were available in limited quantities. The ICl method was used to label hirudin, fibrinogen and α-lactalbumin. For both methods, free iodide was removed from the preparations by either ion exchange chromatography (AG 1-x4 analytical grade anion exchange resin, Bio-Rad) or dialysis. Free iodide in the final protein solutions, as determined by trichloroacetic acid precipitation [9], was <3% for all proteins.

In the Iodo-Gen method, 10 μg of Iodo-Gen reagent (Pierce chemical Co, Rockford IL) was dissolved in chloroform and used to coat glass vials. 100-200 μg of protein and 0.5 mCi of Na ^{125}I was added to each vial and the contents mixed for 15 min. The free iodide was then separated. The amount of radiolabeled protein added to buffer or plasma for protein adsorption experiments was 2-10 % of the total protein present.

In the ICl method, 1-10 mg/mL of protein (depending on the type of protein labeled) was mixed with 200 μL of glycine buffer (pH, 8.8). ICl reagent (0.0033 M in 1.8 M NaCl) in a molar ratio of 2.5:1 (reagent:protein) was mixed with 40 μL of glycine buffer (pH, 8.8) and 0.5 mCi of Na ^{125}I for 1 min. This mixture was then added to the protein solution and mixed for 2 min. The free iodide was then separated. The amount of radiolabeled protein added to buffer or plasma for protein adsorption experiments was 2-10 % of total protein concentration. Table A-2 shows the recipe of glycine buffer and ICl reagent.

Surfaces were exposed to the radiolabeled protein solutions in a 96 well plates for a given time (typically 3 h for adsorption experiments from plasma). After exposure to the radiolabeled protein solution, the surfaces were rinsed and their radioactivity was

determined by gamma counter. The quantity of protein adsorbed (μg/cm^2) was calculated using the following equation:

$$\text{Protein adsorbed } (\mu g/cm^2) = \frac{(CPM_{total} - CPM_{background}) * [protein]_A}{A_t * CPM_{solution}} \quad \text{Equation 2.2}$$

Where CPM is counts per minute, $[protein]_A$ is the protein concentration in solution and A_t is the total surface area of the sample.

Table A- 1 Proteins used in radiolabeling experiments

Protein	Molecular weight	Isoelectric point
Fg	340 kDa	5.1-6.3
Hirudin	6.9 kDa	3.9
Thrombin	37 kDa	7-7.6
CTI	13 kDa	4.5
α-lactalbumin	14.2 kDa	4.2-4.5

Table A- 2 ICl reagents

ICl Reagent:

- Dissolve 150 mg NaI in 8 mL of 6N HCl
- Dissolve 108 mg NaIO3.H2O in 2 mL Milli-Q water
- Mix the two solutions above and bring volume up to 40 mL with Milli-Q H2O
- Add 5 mL of CCl4 and shake vigorously. Repeat until there is no longer any pink colour visible in the organic phase.
- Remove residual CCl4 by aerating solution for 1 hour in fumehood.
- Bring solution volume to 45 mL with Milli-Q H2O
- For the labelling procedure, 1 part of the above ICl stock solution is mixed with 9 parts of 2M NaCl ==> 0.0033 M ICl in 1.8M NaCl.

Glycine Buffer (2M Glycine in 2M NaCl):

	500 mL wt., g	formula	mw
Glycine:	75.0	C2-H5-NO2	75.07
Sodium Chloride:	58.5	NaCl	58.44
pH to 8.8 with 2N NaOH:	(8 g of solid NaOH in 100 mL Milli-Q H2O ==> 2N NaOH)		

3.3 Western Blotting

SDS-PAGE and immunoblotting were used to identify proteins adsorbed to the surfaces from plasma. SDS-PAGE allows the separation of the proteins in a mixture based on size. Immunoblotting can then be used to identify specific proteins using antibodies directed against the proteins of interest.

In Summary, surfaces were incubated with platelet-poor plasma or serum for 3 h. They were then rinsed 3 times, 5 minutes each time with water. Adsorbed proteins were eluted by incubation overnight in 2% SDS. The protein eluates were then run on SDS-PAGE and the gels. The gels were transferred to polyvinylidene fluoride (PVDF) membrane for immunoblotting. The membrane was cut into 3 mm strips and each strip was exposed to an antibody directed against a specific protein of interest. The strips were then exposed to a secondary antibody (conjugated to alkaline phosphate) directed against the primary antibody. A chromogenic substrate for alkaline phosphatase was then used to detect the protein on the blot. The following describes the detailed Western blot procedure and recipe for the reagents. Table A-3 shows the list of antibodies used and their sources.

Gel preparation (12% separating gel, 4% stacking gel):
(ref: Mini Protean II Dual Slab Cell Instruction Manual)

12% SeparatingGel:	Distilled water	3.35 mL
	1.5M Tris-HCl, pH 8.8	2.5 mL
	10% (w/v) SDS stock (room temp)	100 µL
	Acrylamide/Bis (30% stock)	4.0 mL
	Degas above 4 reagents for 15 min @ room temperature.	
	Add: 10 % ammonium persulfate (fresh)	50 µL
	TEMED	5 µL

Fill gel plates with polymer solution, leaving enough space to add stacking gel later. Layer a small amount of water over gel. (Instead of water, some people overlay with saturated isobut./water.) Allow the separating gel to polymerize for 1 hour before adding stacking gel.

4% Stacking Gel:	Distilled water	3 mL
	0.5M Tris-HCl, pH 6.8	1.2 mL
	10% (w/v) SDS stock (room temp)	100 µL
	Acrylamide/Bis (30% stock)	0.65 mL
	Degas above 4 reagents for 10 min @ room temperature.	
	Add: 10 % ammonium persulfate (fresh)	25 µL
	TEMED	5 µL

Fill remainder of gel plates with stacking (4%) polymer solution. Add comb. Allow to polymerize for 1 hour before use.

Prepare samples by adding the appropriate amount to the Sample Buffer (SDS reducing buffer).

Sample Buffer: (also referred to as tracking dye, TD)

Distilled water	4 mL
0.5M Tris HCl, pH 6.8	1.0 mL
Glycerol	0.8 mL
10 % (w/v) SDS	1.6 mL

Mix the above 4 reagents, and aliquot into 225 µL volumes, and store in fridge until needed.

Add: (to 225 uL aliquot)

2-Bmercaptoethanol	30 µL
0.05% (w/v) Bromphenol blue	30 µL

Typical loading volumes for 3 well comb.

(Lane 1) 1 μL markers, 10 μL TD
(Lane 2) 150 μL sample, 80 μL TD
(Lane 3) 7.5 μL prestained markers

Typical loading volumes for 10 well comb.

(Lane 1) 1 μL markers, 10 μL TD
(Lanes 2-9) 1 to 20μL sample, 10 μL TD
(Lane 10) 7.5 μL prestained markers

The above samples are placed in 95 °C water for 7.5 minutes. Note that the prestained markers are used to ensure that the gel is running properly, and are not used for molecular weight determination.

Electrophoresis Remove gels from casting stand, and place into clamp assembly. Place clamp assembly into buffer chamber. Fill upper buffer chamber to 3 mm below outer long glass plate with electrophoresis buffer. Fill lower buffer chamber until 1 cm of gel is covered with electrophoresis buffer. Add samples onto gels. Operate power pack at 200 volts for approximately 45 minutes of electrophoresis. Layer a small quantity of Pyronin dye (in sample buffer) into wells just before the tracking dye (TD) reaches the bottom of the separating gel. Continue the electrophoresis until the Pyronin dye has just reached the top of the separating gel. (ref: Mini Protean II Dual Slab Cell Instruction Manual)

Electrophoresis Buffer: (5X stock solution, pH 8.3)

Tris Base	15 g
Glycine	72 g
SDS	5 g

Fill to 1 L with water. Check pH. Do not adjust with NaOH or HCl. Just before use dilute to 1X strength.

Gel Equilibration in transfer buffer (25 mM Tris, 192 mM glycine, 15% HPLC grade methanol, pH 8.2-8.3) for 15-20 minutes.

Transfer Buffer:

3.03 g Tris
14.4 g glycine
200 mL methonal
fill to 1 L with water.
pH should be 8.3. Do not adjust with NaOH or HCl.

Electrophoretic Transfer using Immobilon PVDF transfer membrane and iBlot® Gel Transfer Device (Invitrogen) for 7 min.

Molecular Weight Determination. Remove marker lane and small portion of sample lane (which covers the remainder of the blot). Block for 1 hr, Tween-PBS. Rinse with Milli-Q water, 3X. Stain using stabilized gold sol (Protogold, Cedarlane Laboratories, Hornby, Ontario, Canada).

Block Unbound Membrane Sites. Cut remainder of blot into 3 mm wide strips. Wet strips with 100% methanol, rinse with distilled water, and place into culture tubes. Incubate the strips for 1h, with gentle agitation, in 5% w/v nonfat dry milk in TBS, pH 7.4. This procedure blocks the areas of the membrane devoid of bound proteins so that nonspecific binding of antibodies to these areas will not occur. Wash strips 3 times for 5 minutes in 0.1% (w/v) nonfat dry milk in TBS.

Incubate with primary antibody. Incubate for 1h in 1 mL 1% (w/v) nonfat dry milk, 0.05% (v/v) Tween 20 in TBS containing the first antibody to the protein of interest.

We typically use a 1/1000 titre for the majority of first antisera.

Wash away unreacted material. Wash the strips as before, in 0.1% (w/v) nonfat dry milk in TBS.

Incubate with second antibody. Incubate strips for 1h with enzyme-conjugated second antibody. Alkaline phosphatase conjugate diluted 1/1000.

Wash away excess and nonspecific probe. Wash the strips as before, in 0.1% (w/v) nonfat dry milk in TBS

Detect. Incubate with the appropriate substrate to develop the colour reaction. Stop reaction by rinsing with distilled water.

The substrate for alkaline phosphatase is 5-bromo-4-chloro-3-indolyl phosphate (BCIP), and nitroblue tetrazolium (NBT).

TBS

50 mM Tris
150 mM NaCl
Adjust pH to 7.4

Carbonate Buffer

20 mg MgCl2 6H20
840 mg NaHCO3
-fill to 100 mL with ddH20
- pH with NaOH to 9.8

NBT & BCIP

dissolve 30 mg NBT in 300 μL H20, 700 μL DMF

dissolve 15 mg BCIP in 1000 μL DMF

-add above reagents to 100 mL of carbonate buffer just before use.

Note: these reagents are light sensitive with a maximum working time of 1 hour.

Please note that the water used in the preparation of all reagents is Milli-Q Plus water (18 megohm-cm resistivity). It meets or exceeds all ASTM, CAP, ACS, and NCCLS standards for purity.

Resistivity	18 megohm-cm
Total Organic Carbon	< 10 ppb
Particle Free	< 0.22 μm
Total dissolved solids	< 20 ppb
Silicates	< 0.1 ppb
heavy metals	< 1 ppb
Microorganisms	< 1 cfu/mL

Table A- 3 List of antibodies and their sources

Protein	**HOST (anti-human)**	**AP-conj. second Ab**	**Supplier**
Factor XI	GAH	anti-Goat	Cedarlane
Factor XII	GAH	anti-Goat	Cedarlane
HMWK	GAH	anti-Goat	Cedarlane
Fibrinogen	GAH	anti-Goat	Cedarlane
Plasminogen	GAH	anti-Goat	Sigma
ATIII	SAH	anti-Sheep	Cedarlane
C3	GAH	anti-Goat	Calbiochem
Albumin	GAH	anti-Goat	Cedarlane
IgG	GAH	anti-Goat	Sigma
Vitronectin	SAH	anti-sheep	Cedarlane
Protein C	SAH	anti-sheep	Cedarlane
Protein C	GAH	anti-Goat	American Diag. Inc.
Thrombin	SAH	anti-sheep	Cedarlane
Apolipoprotein A1	GAH	anti-goat	ESBE

3.4 Activity Assays

Chromogenic substrate assays were employed to measure the activity of factor XIIa and thrombin on surfaces. Chromogenic substrates are synthetic peptides that selectively bind to and react with enzymes giving products that can be measured colorimetrically. The rate of color generation is proportional to the enzyme activity. The color generation is usually due to release of p-nitroaniline (pNA) from the substrate and is measured at 405 nm. Two substrates were used in this work: one to measure thrombin activity and the other to measure factor XIIa activity.

The substrate used for thrombin was S-2238 from DiPharma group (West Chester, Ohio). S-2238 was a tripeptide H-D-Phe-Pip-Arg-pNA·2HCl (MW, 625.6). The substrate used for FXIIa was H-D-HHT-Gly-Arg-pNA.2AcOH from Pentapharm Ltd. (Basel, Switzerland) (MW, 640.7). In both cases the peptide-pNA bond of the substrate was hydrolyzed and release of pNA generated color measured at 405 nm.

For thrombin activity experiments, surfaces were incubated with 100 µL of 0.01 mg/mL thrombin solution in PBS for 1 h in a 96-well plate format. 100 µL of 500 nM chromogenic substrate (S-2238) solution was then added to the wells. For FXIIa activity assay on gold surfaces, surfaces were incubated with 100 µL of 25 nM FXIIa solution in TBS (pH 7.4) containing 2 mM CaCl2, 12.5 µM ZnCl2 and 15.4 µM BSA in a 96-well plate format for 1 h at room temperature. 50 µL of a 1.6 mM solution of chromogenic substrate (Pefachrome) solution was then added to the wells. For FXIIa activity assay on polyurethane, 100 µL of 200 nM FXIIa in TBS (pH 7.4) containing 2 mM CaCl2, 12.5 µM ZnCl2 and 15.4 µM BSA was added to the wells containing the surfaces (total

surface area, 0.565 cm2) and incubated for 1 h at room temperature. 100 μL of a 1.6 mM solution of chromogenic substrate (Pefachrome) was then added to the wells.

Plate reader was used to measure the change in the absorbance of light over time. This change was proportional to enzyme activity and thus by comparing that with a standard curve of known concentration of enzyme, the activity of enzyme could be measured in both cases.

References

[1] Chau TT. A review of techniques for measurement of contact angles and their applicability on mineral surfaces. Miner Eng 2009;22:213-9.
[2] Chau TT, Bruckard WJ, Koh PTL, Nguyen AV. A review of factors that affect contact angle and implications for flotation practice. Adv Colloid Interface Sci 2009;150:106-15.
[3] Azzam RMA. Ellipsometry and polarized light North-Holland Pub. Co.,; 1977.
[4] Tengvall P, Lundstrom I, Liedberg B. Protein adsorption studies on model organic surfaces: an ellipsometric and infrared spectroscopic approach. Biomaterials 1998;19:407-22.
[5] Sofia SJ, Premnath V, Merrill EW. Poly(ethylene oxide) grafted to silicon surfaces: Grafting density and protein adsorption. Macromolecules 1998;31:5059-70.
[6] Briggs D. Surface analysis by Auger and X-ray photoelectron spectroscopy SurfaceSpectra 1948.
[7] Cole RB. Electrospray and MALDI Mass Spectrometry : Fundamentals, Instrumentation, Practicalities, and Biological Applications John Wiley & Sons, Inc.,; 2010.
[8] Hermanson GT. Bioconjugate Techniques. 2nd ed: Burlington : Elsevier; 2008.
[9] Regoezi E. Iodine-Labelled Plasma Proteins: CRC Press, Boca Raton, FL; 1984.

APPENDIX B: List of Publications

PUBLICATIONS

Refereed Journal Articles

S. Alibeik, S. Zhu, J. Yau, J.I. Weitz, J.L. Brash. Dual surface modification with PEG and corn trypsin inhibitor (CTI): effect of PEG:CTI ratio on protein resistance and anticoagulant properties. Submitted. 2011

S. Alibeik, S. Zhu, J. Yau, J.I. Weitz, J.L. Brash. Immobilization of Polyethylene Glycol-Corn Trypsin Inhibitor on Polyurethane for Inhibition of Contact Factor Activation upon Blood Contact. Journal of Biomaterials Science: Polymer Edition (Accpeted), 2011

S. Alibeik, S. Zhu, J. Yau, J.I. Weitz, J.L. Brash. Surface modification with polyethylene glycol-corn trypsin inhibitor conjugate for inhibition of the contact factor pathway on blood-contacting surfaces. Acta Biomaterialia (In Press), 2011

S. Alibeik, S. Zhu, J.L. Brash. Surface modification with PEG and hirudin for protein resistance and thrombin neutralization in blood contact. Colloids and Surfaces B: Biointerfaces, 81(2):389-396, 2010

S. Alibeik, H. Sheardown, A. Rizkalla, K. Mequanint. Protein adsorption and platelet adhesion onto ion-containing polyurethane biomaterials. J. Biomaterials Science: Polymer Ed, 18:1195–1210, 2007

S. Alibeik, A. Rizkalla, K. Mequanint. The effect of thiolation on the mechanical and protein adsorption properties of polyurethanes. European Polymer J. 43(4):1415-1427, 2007

Refereed Conference Proceedings

S. Alibeik, S. Zhu, J. Yau, J.I. Weitz, J.L. Brash. “Immobilization of polyethylene glycol-corn trypsin inhibitor on polyurethane for inhibition of contact factor activation upon blood contact." Annual Meeting of the Society for Biomaterials, Orlando, FL, 2011

S. Alibeik, S. Zhu, J. Yau, J.I. Weitz, J.L. Brash. "Surface modification with polyethylene glycol-corn trypsin inhibitor for inhibition of the contact factor pathway in blood-contacting devices." 28th Annual Conference of the Canadian Biomaterials Society, Kingston, ON, 2010

Z. Wu, H. Chen, K. Sask, **S. Alibeik**, J.L. Brash. "Tissue plasminogen activator-containing polyurethane surfaces for fibrinolytic activity." 28th Annual Conference of the Canadian Biomaterials Society, Kingston, ON, 2010

S. Alibeik, S. Zhu, J.L. Brash. "Surface modification with PEG and hirudin for protein resistance and thrombin neutralization in blood contact." Annual Meeting of the Society for Biomaterials, Seattle, WA, 2010

S. Alibeik, S. Zhu, J. Yau, J.I. Weitz, J.L. Brash. "Immobilization of corn trypsin inhibitor for inhibition of the contact factor pathway on blood-contacting materials." Annual Meeting of the Society for Biomaterials, Seattle, WA, 2010

S. Alibeik, S. Zhu, J.L. Brash. "Surface immobilization of PEG-Hirudin for improved blood compatibility." 27th Annual Conference of the Canadian Biomaterials Society, Quebec City, QC, 2009

S. Alibeik, S. Zhu, J. L. Brash. "Immobilization of PEGylated proteins on gold surface for blood compatibility." Annual Meeting of the Society for Biomaterials, San Antonio, TX, 2009

S. Alibeik, A. Rizkalla, K. Mequanint. "Synthesis and characterization of ion-containing polyurethane for biomedical applications." 25th Annual Conference of the Canadian Biomaterials Society, Calgary, AB, 2006

Other Conference Presentations

"Surface modification with polyethylene glycol-protein conjugates for improved blood compatibility." PolyMac Meeting, McMaster University, 2010

"Surface modification with polyethylene glycol-corn trypsin inhibitor for improved blood compatibility of blood contacting devices." Women in Science and Engineering (WISE) Initiative International Women's Day Conference, McMaster University, 2010

"Surface immobilization of PEG-Hirudin for improved blood compatibility." PolyMac Meeting, McMaster University, 2009

AWARDS AND SCHOLARSHIPS

Graduate Student Association Travel Grant ($500) 2011
McMaster University

McMaster Internal Prestige: Clifton W. Sherman Scholarship ($11,000) 2010-2011
McMaster University

Yates Scholarship Fund ($500) 2009
Travel Award, McMaster University

Natural Sciences and Engineering Research Council of Canada Scholarship (NSERC) ($63,000) 2007-2010

Ontario Graduate Scholarship (OGS) ($15,000) 2007-2008
(received and declined)

Western Graduate Research Scholarship ($5,950) 2005-2006
The University of Western Ontario
The Graduate Program in Biomedical Engineering

Special University Scholarship ($5,950) 2004-2005
The University of Western Ontario
The Graduate Program in Biomedical Engineering